The American Mineralogist

Journal of the Mineralogical Society of America

Vol. 40 JANUARY–FEBRUARY, 1955 Nos. 1 and 2

Contents

Published bi-monthly by the Society

Mineralogical Society of America

ASSOCIATED WITH THE GEOLOGICAL SOCIETY OF AMERICA

President: **Harry H. Hess,** Princeton University, Princeton, New Jersey.
Vice-President: **Clifford Frondel,** Harvard University, Cambridge 38, Massachusetts.
Secretary: **C. S. Hurlbut, Jr.,** Harvard University, Cambridge 38, Massachusetts.
Treasurer: **Earl Ingerson,** U. S. Geological Survey, Washington 25, D. C.
Editor: **Walter F. Hunt,** University of Michigan, Ann Arbor, Michigan.
Councillors: **Victor T. Allen,** Institute of Geophysical Technology, St. Louis, Missouri.
C. Osborne Hutton, Stanford University, Palo Alto, California.
Felix Chayes, Geophysical Laboratory, Washington, D. C.
Leonard G. Berry, Queen's University, Kingston, Ontario, Canada.
Sterling B. Hendricks, U. S. Department of Agriculture, Beltsville, Maryland.

The enlarged issues of this journal for 1955 are made possible by a grant from the Penrose Fund of the Geological Society of America.

The American Mineralogist—Journal of the Mineralogical Society of America

A journal containing articles on mineralogy, crystallography, petrography, and allied sciences, is issued every two months. Contributions are invited from everyone.

Office of Publication, Mineralogical Laboratory, Ann Arbor, Michigan.

The general conduct of the journal is in the hands of the editor, **Walter F. Hunt,** Ann Arbor, Michigan, to whom all manuscripts should be submitted. To assist the editor the council of the Mineralogical Society has appointed **Lewis S. Ramsdell,** Ann Arbor, Michigan, assistant editor, and the following board of associate editors:

William F. Bradley, Illinois State Geological Survey, Urbana, Illinois.
Ian Campbell, California Institute of Technology, Pasadena 4, California.
Brian H. Mason, American Museum of Natural History, New York, N. Y.
Elburt F. Osborn, Pennsylvania State College, State College, Pennsylvania.
Adolf Pabst, University of California, Berkeley 4, California.
Francis J. Turner, University of California, Berkeley 4, California.

It will expedite publication if two copies of each manuscript are submitted to the editor.

Contributors of leading articles are given without charge 100 reprints (without covers) of their article. If additional reprints are desired these can be purchased at the following rates:

Pages	*1–4*	*5–8*	*9–12*	*13–16*	*17–20*	*21–24*	*25–28*	*29–32*	*Covers*
Copies									
25	$3.50	$5.00	$ 8.00	$ 9.50	$11.00	$13.00	$15.00	$16.00	$4.90
50	3.80	5.55	8.80	10.40	12.10	14.20	16.40	17.50	5.50
75	4.10	6.10	9.60	11.30	13.20	15.40	17.80	19.00	6.10
100	4.40	6.65	10.40	12.20	14.30	16.60	19.20	20.50	6.70
Addl. C's	1.20	2.20	3.20	3.60	4.40	4.80	5.60	6.00	2.40

Cover Composition $1.55.

Sent to all members and fellows of the Mineralogical Society of America. Membership dues $4.00 annually, fellowship dues $5.00 annually. Subscriptions for libraries, colleges, institutions, companies and similar organizations $6.00 annually.

Entered as second class matter at the post office at Menasha, Wis., under Act of March 3, 1879. Acceptance for mailing at the special rate of postage provided for in section 1103, Act of Oct. 3, 1917, paragraph 4 section 429 P. L. & R. authorized March 13, 1922.

Notice of change of address, orders, and remittances should be sent to Dr. Earl Ingerson, U. S. Geological Survey, Washington 25, D. C.

Printed by the George Banta Publishing Company, Menasha, Wisconsin
Printed in the United States of America

THE AMERICAN MINERALOGIST

JOURNAL OF THE MINERALOGICAL SOCIETY OF AMERICA

Vol. 40 JANUARY-FEBRUARY, 1955 Nos. 1 and 2

MOSAIC STRUCTURE IN QUARTZ*

A. F. FREDERICKSON, *Washington University, St. Louis, Missouri.*

ABSTRACT

Natural quartz crystals have a pronounced mosaic structure. The smallest mosaic units are tiny rods approximately 0.0009 mm. in diameter by 0.009 to 0.05 mm. long. The rods are laid side by side to form sheets. Several sheets produce the "shingle" appearance seen when the quartz is etched with distilled water under elevated temperatures (up to 360° C.) and pressures (up to 300 bars).

The anomalous solubility of quartz surfaces produced by grinding is attributed to a mechanical loosening of the rods and sheets to produce a relatively large surface easily attacked by solvents. The existence of an amorphous layer to account for the anomalous solubility is questioned.

The nature of the forces or cementing holding the rods together is of considerable geological interest.

INTRODUCTION

A mosaic crystal is simply a large one made up of many discrete smaller crystals. A brick wall might be an example of a mosaic crystal in which the individual bricks would be the crystallites. This is a good example because many natural crystals are much like brick walls. The individual bricks may all be more or less perfectly aligned. However, slight departures from perfect alignment are quite common, especially where the bricks can be physically disturbed.

Grinding the surface of crystals disturbs the alignment of the building bricks or crystallites. The manner in which the intensity of x-ray reflections are increased by grinding and subsequently decreased by further polishing or etching furnishes a method of classifying crystals according to the degree to which the crystallites or mosaic units are perfectly aligned (Sakisaka, 1930). Measurements of this kind also enable one to calculate the approximate size of the individual blocks and their angular departure from perfect alignment (Armstrong, 1946).

The sizes of the mosaic blocks have been calculated by several methods. The blocks are said by many authors to be about 10^{-4} cm. on an edge for

* Contribution number 172 of the Department of Geology, Washington University, St. Louis, Missouri.

many metals and salts. Work designed to yield information on residual stresses in metals has usually been based on a crystal model consisting of a mosaic of small regions within which the lattice is essentially perfect. The size of these blocks exceeds 10^{-5} cm. (1000 Å) on an edge. The literature on this topic is reviewed by Barrett (1943, pp. 219–223). If the mosaic units are no smaller than this, it should be possible to see them directly under an ordinary microscope.

Resolution of a Microscope

The smallest distance d two spots must be separated to be recognized as two distinct spots is expressed by

$$d = \frac{1.22\lambda}{2\mu \sin \alpha}$$

where λ is the wave length of light used, μ is the index of refraction of the media (usually air) between the objects being observed and the objective of the microscope, and α is half the angular distance between the spots and the edge of the objective lens. If an oil immersion lens is used, μ is commonly taken as 1.52. The maximum value for α is 67°. Since sin

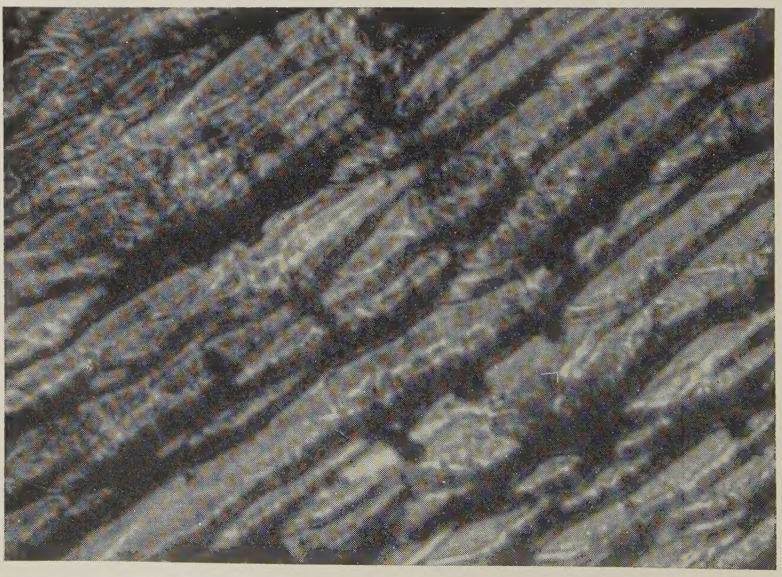

Fig. 1. Mag. 100×. Ordinary photomicrograph of the surface of a water-etched quartz crystal. Highly inclined transmitted illumination was used. The surface has the general appearance of a stack of shingles. By adjusting the illumination so that light enters the "rear" part of the shingles, the size of the individual layers can be clearly seen. The most interesting detail is that the layers seem to be made up of individual rods. The shingles are made up of layers and each layer consists of a series of rods laid side by side.

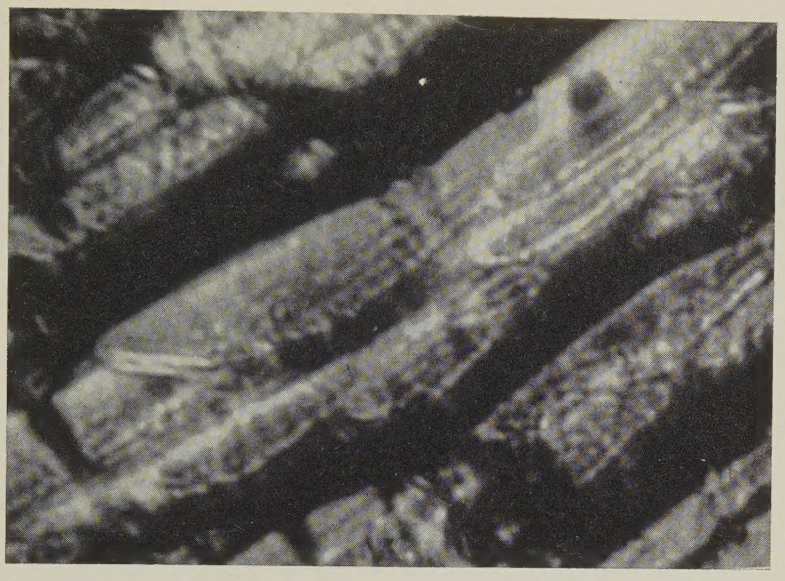

FIG. 2. An enlargement (200×) of the same area shown in Fig. 1. Here the regularity of the layers and the individual rods can be clearly seen. An isolated rod in a layer can be seen in the upper left part of the photomicrograph.

67° equals 0.92, substitution of these figures in the above formula shows that it should be possible to resolve detail separated by as little as $\lambda/2$. Inasmuch as the arbitrary figure of 1.22 is considerably too high and that a higher index oil may be used, it is theoretically possibly to resolve objects separated by as little as 0.3 (Meyer, 1933 p. 208). With the use of highly inclined illumination (Frederickson, 1953) twice this resolution should be possible. If light of $\lambda = 5 \times 10^{-5}$ cm. is used, the predicted mosaic blocks should be clearly visible.

The study of the size and regularity of etch pits and Widmanstätten figures indicates that mosaic blocks of this size exist. Work of this kind however, has been severely criticized by Buerger (1934) and others who believe that the apparent regularity in both etch pits and Widmanstätten figures is illusory. Although etch-pit and Widmanstätten-figure evidence may not be conclusive, modified etching techniques applied to quartz reveals a highly regular mosaic structure (Fig. 1) made up of units of approximately the same size as predicted by earlier workers.

MOSAIC STRUCTURES OBSERVED IN QUARTZ

Small quartz crystals, $\frac{1}{2}$ to 1 inch in length, were etched by suspending them in a bomb partially filled with distilled water. The system was heated to 300° C. for various lengths of time ranging up to 48 hours. The pressure in the bomb was 300 bars.

Prism faces consist of a series of overlapping plates giving the crystal a shingle-like appearance. By arranging the light so that it appears to enter the ends of the plates, individual layers within the shingles can be clearly seen (Figs. 1 and 2). Each little plate lights up much like a plastic rod held on the end of a flashlight. The thickness of these layers can be measured directly: each layer is approximately 0.0009 mm. thick.

Some layers are better illuminated and appear much brighter than others. Slight movement of the stage on which the crystal is mounted causes different layers to be more intensely illuminated. This indicates that all of the layers are not in perfect alignment. Armstrong (1946) has studied the disorientation of mosaic blocks in quartz by x-ray rocking-crystal techniques. She showed that large "blocks" may be disoriented as much as 4°. "Blocks" disoriented by more than three degrees were thought to be broken loose from the parent crystal. She estimated that

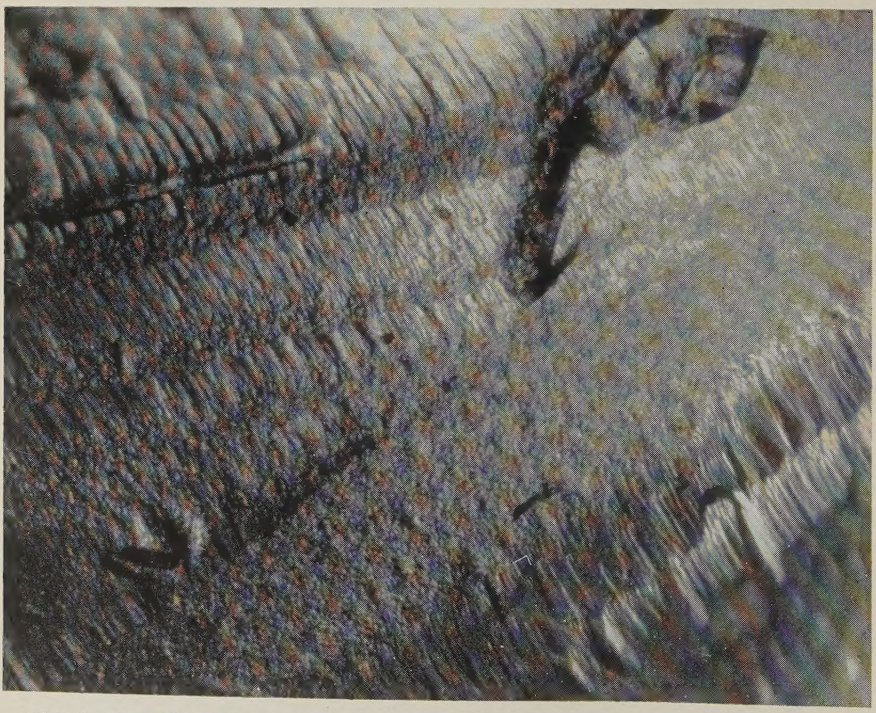

FIG. 3. Mag. 21×. This is the beveled intersection of two prism faces of a quartz crystal naturally etched during weathering. Here we see the individual rods stacked up like piles of cord wood. The length to width ratio of individual rods varies within wide limits; the width of the rods is highly uniform. The rods are not all straight. Maybe the reason why a crystal grows faster in one direction than another is related to whether the material must be added onto the end of a rod or if more rods must be formed and stacked onto the parent crystal.

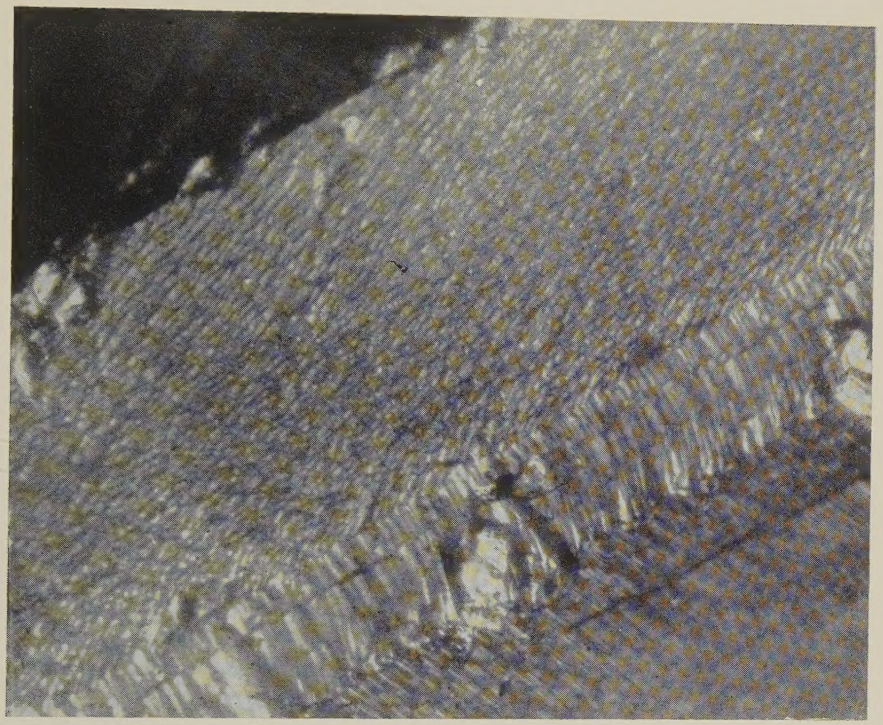

FIG. 4. Mag. 30×. Here we see a small *s*-face on a water-etched quartz crystal. The edges of the shingles appear as tiny rods on the *r*-face in the foreground. The shingles are quite irregular and apparently quite brittle. The very ragged appearance of the beveled edge between the *r* and *s* faces must have been due to its rapid solution in the hydrothermal solution of the bomb. The shingles upended into the *r*-face are almost of the same length. They seem to be separated from the crystal by an irregular crack. At present, no satisfactory answer can be given concerning the parallelism of the irregular line with the intersection of the two faces.

for 3° of disorientation, the "blocks" would have to possess a length to width ratio of 26:1 to keep from breaking. She concluded that there was no experimental evidence for the existence of such rods.

Careful observation of the individual layers in Fig. 2 reveals that they consist of a series of bright spots which are very close together. These spots look like the ends of tiny rods. Figure 3 shows that the basic units making up the individual layers actually are tiny rods.[1] The diameter of a rod in a "shingle" is approximately 0.0009 mm. whereas the length ranges from 0.005 up to 0.09 mm. The length to width ratio is as high as

[1] The diameter of the rods shown in Fig. 3 is about 10 times as large as those in the shingles. This is the only exception to the 0.0009 mm. diameter figure we have observed. At present no satisfactory explanation can be offered as to why these are so much larger than all of the others studied.

100:1 for some of the rods although most of them have a ratio closer to 40 or 50:1. Armstrong's conclusion that "blocks" misoriented by more than 3° must be broken from the bulk crystal is therefore not correct. The crystals were buffed on rough canvas cloth and rephotographed. The same area can be found by use of an odd-shaped ridge or channel as a guide. Careful comparison of the two photomicrographs did not indicate any differences. Even tiny, thin, quartz platelets (Fig. 4) were not removed by this treatment; hence, it appears that both the thin plates and the narrow rods are quite firmly fixed onto the parent crystal.

Crystallinity of Crystal Faces and Interfaces

A large literature exists which deals with the physical nature of polished surfaces and interfaces of many types of crystals. The classic Beilby layer (1921) is supposed to be an amorphous layer occurring on surfaces and interfaces. It is usually reserved for metallic systems but is also thought to exist on quartz (Demster and Ritchie, 1952). The basic experimental fact supporting the idea that an amorphous layer develops from grinding or otherwise "working" the surface is that the thin surface "layer" is often much more soluble in various solvents than the bulk of the crystal.

Metals are not reduced to the amorphous state by cold work (Barrett, 1942, p. 229). Only under severe shearing strains and high compressive stress can crystalline fragments be reduced to the state where they give typical amorphous x-ray patterns (Bridgman, 1937, p. 328). If metals cannot be reduced to an amorphous state by ordinary cold working, it is almost certain that much less ductile materials like silicates cannot develop amorphous layers when ground.

Electron diffraction photographs (Armstrong, 1946, p. 153) of freshly ground quartz surfaces show a series of rings analogous to those produced by powders. Even though of small particle size, this material must be well crystallized to give such a pattern. After the crystal surface was scrubbed with water and a toothbrush, the rings are replaced by Laue spots. Apparently the first, very loose material resulting from grinding can be easily removed leaving a surface which produces a single-crystal pattern. These experiments clearly contradict the opinion of Dempster and Ritchie (1952):

"The evidence suggests that there exists on powdered quartz particles a vitreous skin, produced by surface-flow during grinding, and blending via a transitional layer into the truly crystalline core."

Grinding apparently fractures the crystal surface and loosens the piles of rods (Figs. 3 and 5) which, because of their greater surface area, are much more soluble in acids or other solvents than the undisturbed por-

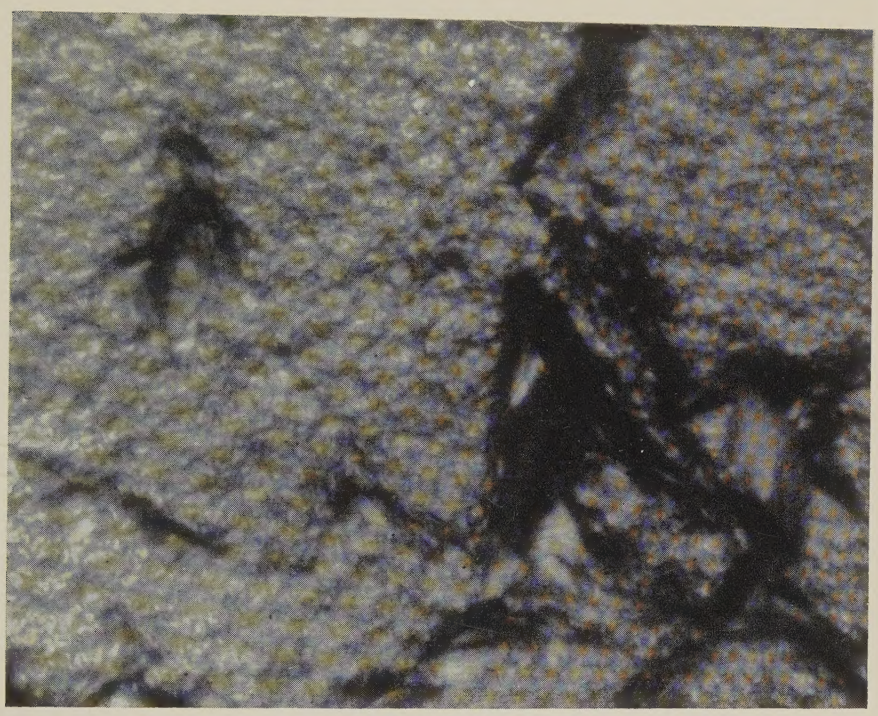

FIG. 5. Mag. 98×. A quartz wafer suitable for piezoelectric purposes was etched in the bomb. The wafer was first acid etched (in HF) and then placed in the bomb to reveal surface detail. The hydrofluoric acid etched deep pits and left irregular ridges that made focussing difficult. The wafer was then polished and again put in the bomb. The surface produced is shown here. The deep pits are remnants of the acid etch. The rest of the surface consists of a mass of rod-shaped aggregates. Some of the shingles can be seen on the sides of the acid etch pits.

tions of the crystal. In unground crystals, the quartz along the "pore-spaces" between the rods and the plates is first removed to produce the relief features shown in the photomicrographs. This material is removed first for the simple reason that it forms the external surface of the crystallites which the etchant first encounters.

Unetched surfaces look as if tiny chips had been gouged from them by a curved chisel (Fig. 6). Although these concave hollows vary considerably in size, they are of the same order of magnitude as the length of the rods. These surfaces are relatively smooth. Some sort of cementing material must bind the rods together and fill up the irregularities between them. Because the rods are not perfectly aligned, the cementing material must have a lower degree of order and consequently slightly different properties from the rods; the solubility of the cement, for example, should

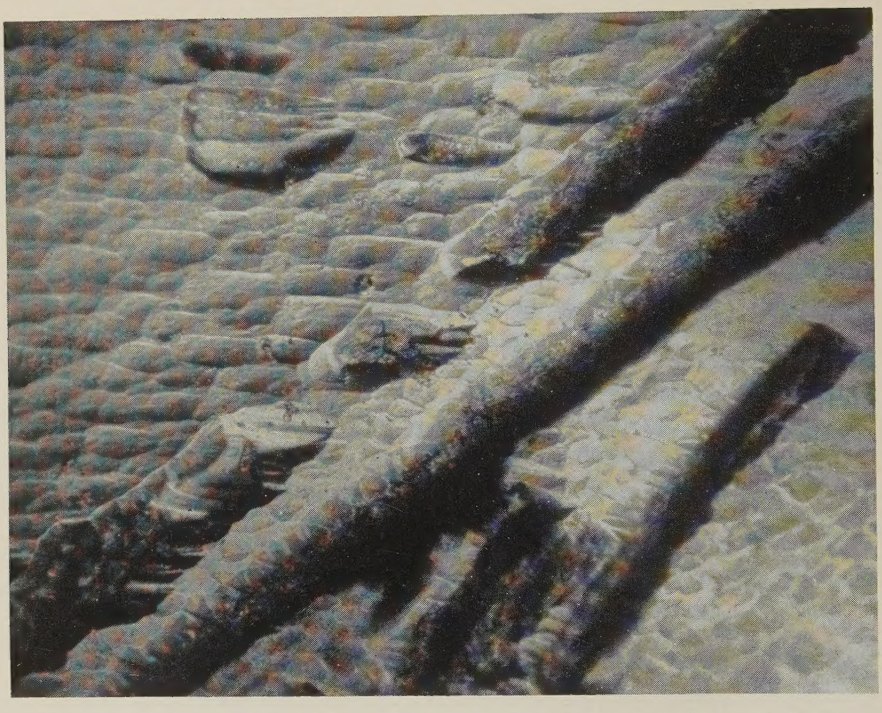

FIG. 6. Mag. 22×. This crystal was water-etched in a bomb for a short period of time. The dark rectangular-shaped zones actually are etch pits or channels. Notice the septa across the large channel. These channels are thought to be molecular sieve zones from which much of the silica was removed from around some of the rods by natural solutions before it was placed in the bomb. Channels of this kind are common in many metamorphic rocks, but this is the first time it has been seen on a single crystal.

Irrespective of interpretation as to their origin, the quartz that was differentially etched from the channels must have had a greater apparent "solubility" than the bulk of the crystal.

Unetched faces of quartz look as if a chisel had grooved small flakes from the quartz surface as shown here. The long dimension of these grooves is about the same as the length of the rods shown in Fig. 3. These surfaces look as if they were formed by piling up a stack of rods and cementing them together much like concrete is poured into a suitable mold containing a bundle of reinforcing rods.

be different than that of the rods. Are these the "pore spaces" through or along which hydrothermal solutions, ions or ichors migrate?

ACKNOWLEDGMENTS

This work is part of a U. S. Army Signal Corps Contract (*DA 36–039–sc–5513*) concerned with the mechanism of crystal growth and synthesis of certain minerals. Their courteous assistance and material help is gratefully acknowledged.

References

Armstrong, E. J. (1946), *X*-ray studies on the surface layers of crystals: *Bell System Tech. Jour.*, **25,** 136–155.

Barrett, C. S. (1943), Structure of Metals. McGraw-Hill Book Co., New York, N. Y.

Beilby, G. (1921), Aggregation and Flow of Solids. McMillan, London.

Bridgeman, P. W. (1937), Flow phenomena in heavily stressed metals: *Jour. Applied Physics,* **8,** 328–336.

Buerger, M. J. (1934), The lineage structure of crystals: *Zeit. Krist.*, **89,** 195–220; and The nonexistence of a regular secondary structure in crystals: *Zeit. Krist.*, **89,** 242–267.

Demster, P. B., and Ritchie, P. D. (1952), Surface of finely ground silica: *Nature,* **169,** 538–539.

Frederickson, A. F. (1953), A method of effectively increasing the resolving power of a microscope: *Am. Mineral.*, **38,** 815–826.

Meyer, C. F. (1934), The Diffraction of Light, *X*-Rays, and Material Particles. Univ. Chicago Press, Chicago, Ill.

Sakisaka, Y. (1930), Reflexion of monochromatic *x*-rays from some crystals: *Proc. Physico-Math. Soc. Japan, 3rd ser.*, **12,** 189–202. See also: The effects of the surface conditions on the intensity of reflexion of *x*-rays by quartz: *Japanese Jour. Phys.*, **4,** 171–181 (1927).

Manuscript received Sept. 14, 1953

SYNTHETIC MICA INVESTIGATIONS, VI: *X*-RAY AND OPTICAL DATA ON SYNTHETIC FLUOR-PHLOGOPITE*

J. A. Kohn and R. A. Hatch, *Electrotechnical Laboratory, U. S. Bureau of Mines, Norris, Tennessee.*

Abstract

Isomorphism studies in the synthetic fluor-mica group have shown the need for standard basic information on synthetic fluor-phlogopite ($KMg_3AlSi_3O_{10}F_2$).

Relatively large (up to 25 mm.), well-formed, single-crystal plates of synthetic fluor-phlogopite were obtained from one particular internal resistance melting experiment (method of synthesis described). Selected crystals were petrographically analyzed and found to be 99% pure. A chemical analysis was made.

Optical determinations gave the following values:

$\alpha = 1.522 \pm 0.001$	$2V = 14 \pm 0.5°$
$\beta = 1.548_5 \pm .0005$ (calculated)	Biaxial negative
$\gamma = 1.549 \pm .001$	

The following monoclinic unit cell constants were determined using a Geiger diffractometer:

$a_0 = 5.299 \pm 0.004$ Å	Space Group $= Cm$ (C_s^3)
$b_0 = 9.188 \pm .002$ Å	$Z = 2$
$c_0 = 10.135 \pm .002$ Å	$D_x = 2.879 \pm 0.004$ g/cm^3
$\beta = 99° 55' \pm 3'$	

Using these values, all resolved maxima or significant doublets on an *x*-ray powder-diffraction pattern were indexed up to 77° 2θ, and an observed-calculated 2θ comparison showed good agreement. Single-crystal rotation and Weissenberg exposures were made. Optical goniometric measurements gave values in excellent agreement with those calculated from the unit cell data. The chemical and optical data were compared with literature values for both natural and/or synthetic material.

Introduction

The primary objective of the synthetic mica program at the Electrotechnical Laboratory† has been development of commercially practicable methods for manufacturing synthetic mica and fabricating mica products. Necessarily, the solution of engineering problems has received major emphasis; nevertheless, extensive investigations of a more fundamental character have also been made, of which this article represents one aspect.

One of the important requirements of a comprehensive mineral study is to identify precisely the compound chemically, optically, and struc-

* A contribution from the Synthetic Minerals Section, Industrial Minerals Branch, U. S. Bureau of Mines, Norris, Tennessee.

† This project has been conducted since 1947 in cooperation with the Office of Naval Research, the Bureau of Ships, and the Army Signal Corps.

turally. Precision measurements are presented herein on chemically analyzed, pure, single crystals of fluor-phlogopite which were produced in the internal electric resistance furnace. The data serve as bases of comparison for an extensive series of fluorine-mica isomorphs which have been prepared at this laboratory.

Literature

Since an extensive review of the literature on synthetic mica is already available (1), only a brief sketch is presented here.

According to the older literature (2), synthetic fluorine-micas have been known for nearly 70 years; however the bulk of the work in this field has been done during the last 20 years in Russia, Germany, and Japan, and since the close of World War II, in the United States. The desire to produce synthetic mica as a commercial product, as indicated by early patents (3), has been a major stimulus to progress, although by no means the only incentive.

In the 10-year period 1934–44, Grigoriev, working on petrogenic and crystallochemical problems at the Leningrad School of Mines, published at least 18 papers describing his experiments on the synthesis of fluorine-micas and amphiboles. His work clearly established the equivalence of F^- and $(OH)^-$ in the mica structure and the practicability of crystallizing fluor-phlogopite ($KMg_3AlSi_3O_{10}F_2$) at atmospheric pressure from fluorosilicate melts. Although his early mica product (4) was a high-lime (6.43%) fluor-phlogopite (fluoride introduced as CaF_2), its x-ray diffraction pattern was very similar to that of natural phlogopite (5, 6). The refractive indices of a reasonably pure fluor-phlogopite made ten years later (7) were given as $\alpha = 1.518$, $\gamma = 1.554$.

Grigoriev's work probably was largely responsible for the renewed interest in the commercial development of synthetic mica. At any rate, in the mid 1930's, Siemens & Schuckert began an extensive engineering development to grow fluor-phlogopite in sheet form. By 1943 a pilot plant had been established, and a few crystals several inches in diameter were obtained by the slow crystallization of 100-kg. melts (8) contained in high-silica (82%) pots (9). Although these crystals were reported to be of high quality, no chemical, optical, or x-ray data on them are known to be available.

Concurrent with the Siemens development, an extensive crystallochemical investigation of fluor-phlogopite synthesis and isomorphism was conducted by Dietzel and Eitel (10, 11) at the Kaiser Wilhelm Institute for Silicate Research. Mica melts weighing about 150 g. were crystallized in carbon crucibles; the fluor-phlogopite crystals obtained were biaxial negative, with the principal optic plane parallel to (010);

$\gamma = 1.545$, $2E = 10°$ to $20°$. The similarity of their x-ray pattern to that of natural muscovite was noted but no data were given. Their attempts to synthesize fluor-muscovite ($KAl_2AlSi_3O_{10}F_2$) from melts of different kinds failed.*

Since about 1940, Japanese investigators (12) have contributed substantially to the literature on fluorine-micas, especially Noda and associates at the University of Nagoya (13), who have published at least 20 papers. Optical data were presented on fluor-phlogopite crystals from three representative experiments, as follows:

$\alpha = 1.522$	1.544	1.513
$\beta = 1.553$	1.564	1.539
$\gamma = 1.554$	1.566	1.540
$2V = 11°$	13°	14°
$c \wedge X = 1.5°$	1.5°	0.5°

In another report (15), it was remarked that the refractive indices of fluor-phlogopite decreased as the amount of fluoride in the melt was increased beyond its theoretical content in the mica structure. However, no evidence was presented to show any change of fluoride content in the crystals.

The German development of synthetic mica terminated in 1945, but their accomplishments quickly became known to the world and prompted a series of similar mica investigations in the United States. First of these was a $1\frac{1}{2}$-year project (16) initiated in November 1945 at the Corning Glass Works in cooperation with Owens-Corning Fiberglas Corp., to check on the feasibility of producing synthetic mica commercially. The Bureau of Mines, Army-Navy cooperative engineering development program was an outgrowth of the Corning work. In 1946, an engineering program for the development of synthetic mica, sponsored by the Army Signal Corps, was started at the Colorado School of Mines (17). In the same year, exploratory experiments were started at the National Bureau of Standards (18), later to be continued as a basic research program sponsored by the Office of Naval Research. The Bureau of Standards measurements on fluor-phlogopite crystals probably are the most self-consistent and accurate presented to date (see Tables 1 and 2).

Experimental Data

Synthesis of the Mica

The fluor-phlogopite crystals used in this study were prepared in a pilot-plant type of operation in which about 3 tons of mica batch were

* Fluor-muscovite has been synthesized at the Electrotechnical Laboratory by solid state reaction of K_2SiF_6 with calcined kaolinite at temperatures of 500° to 700° C. It is unstable at higher temperatures.

melted and crystallized. The batch materials (technical grades) were compounded according to the following formula (27):

$$K_2SiF_6+6MgO+Al_2O_3+5SiO_2 \text{ (quartz)}$$
$$\text{Wt. } \%=25.5+28.0+11.8+34.7=100.0.$$

The major impurities were 1.5% CaO in the MgO and 0.7% Na_2O in the Al_2O_3, for which no compensations were made. It should be noted that the batch formula contains a 50 mol per cent excess of fluoride above the amount required in the theoretical fluor-phlogopite formula (F_6 instead of F_4).

About 15 tons of this batch were dry-mixed and loaded into a 12-foot high internal-electric-resistance melting furnace. The basic principle of operation of such a furnace (31) is illustrated by the accompanying sketch (Fig. 1). Melting was started at the center of the batch by means of an electrically heated graphite resistor, which was in contact with graphite electrodes. After several hours of operation, the resistor was consumed by oxidation and from then on the electric current was conducted through the melt. At all times the melt was contained, and the fluoride vapors were effectively sealed, by the surrounding mica batch. This particular melt (R-14) cooled under its own inertia at a rate of about 5° C./hour. Smaller melts have been cooled by gradual reduction of the electric power input (see ref. 31 for details).

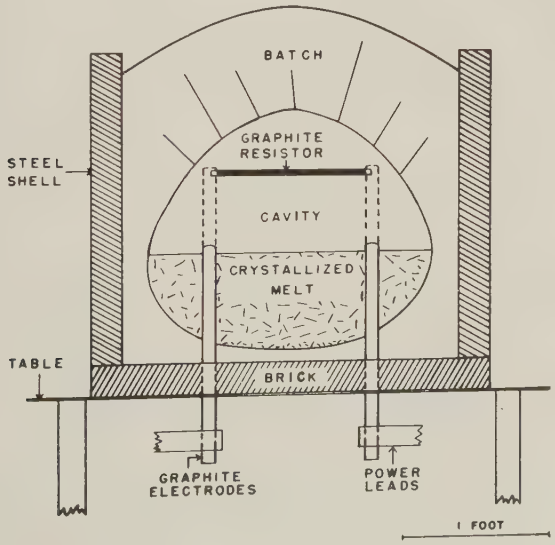

FIG. 1. Sectional view of model internal-electric-resistance melting furnace used for melting and crystallization studies of various synthetic mica batches.

The well-formed single-crystal plates selected for this study ($\frac{1}{4}$ to $\frac{3}{4}$ inch in diameter) came from a porous zone (crust) near the top of the melt. Simultaneous crystallization at the top and fusion at the bottom had resulted in the melt being slowly drained away from its crust, forming the porous stratum. In the massive state this material was slightly gray because microscopic particles of carbon were dispersed throughout the mass. As the carbon content did not exceed 0.013% by actual analysis, its effect on the properties investigated was considered negligible.

Chemical Composition

Several crystals were selected on the basis of freedom from inclusions and clarity. Optical examination of the crushed material showed the presence of 0.5 to 1.0% glass and a minute amount of MgF_2. Thus the sample was judged to be 99% pure. The results of a chemical analysis (No. 3689) are given in Table 1, which also includes an analysis (No. 3691) of selected pure crystals from the coarse zone above the middle of the melt (among the last to crystallize) to demonstrate the chemical uniformity of the fusion product. The table also includes an analysis by the Bureau of Standards (18) on its synthetic fluor-phlogopite.

With virtually no exception, chemical analyses of fluor-micas have consistently given low fluoride contents. In some cases this deficiency has been attributed to a substitution of oxygen for fluorine in the mica structure (4). The authors feel that no convincing evidence has yet been offered for this substitution in synthetic micas and would rather attribute the deficiency to errors in chemical analyses. The analytical procedure

Table 1. Chemical Analyses of Synthetic Fluor-phlogopite

Constituent	Theoretical Composition	No. 3689 Upper Porous Zone*	No. 3691 Coarse Middle Zone*	Bureau of Standards
SiO_2	42.79	42.50	42.70	41.87
Al_2O_3	12.10	12.35	12.21	12.97
Fe_2O_3	.00	.04	.06	—
MgO	28.71	28.36	28.58	28.27
CaO	.00	.14	.00	—
Na_2O	.00	.06	.06	.12
K_2O	11.18	10.88	10.92	10.94
F^-	9.02	9.30	9.20	8.52
O=F	−3.80	−3.92	−3.87	−3.51
Ignition loss (at 640° C.)	.00	.15	.20	—
	100.00	99.86	100.06	99.18

* Analysts: H. R. Shell and R. L. Craig.

developed and used in connection with the mica samples reported herein has recently been described by Shell and Craig (19).

The molecular formulas were calculated for the two analyzed fluor-phlogopites on the basis of 10 oxygen anions in the simplest possible formula weight, as follows:

$$\text{No 3689}—(K_{0.98}Na_{0.01}Ca_{0.01})Mg_{2.99}(Al_{1.03}Si_{3.00})O_{10}F_{2.08}$$

$$\text{No. 3691}—(K_{0.98}Na_{0.01}Ca_{0.00})Mg_{3.00}(Al_{1.01}Si_{3.01})O_{10}F_{2.05}$$

Thus it is evident that these micas closely approach the accepted theoretical composition for fluor-phlogopite, namely $KMg_3AlSi_3O_{10}F_2$.

Optical Properties

Refractive indices of the selected crystals were determined both with a petrographic microscope and an Abbe refractometer (method of grazing incidence) at 25° C., using sodium (D) light. Although the crystals measured had well-formed side pinacoids, they were not thick enough perpendicular to the basal face to give sharp lines as seen in the refractometer. Thus the accuracy of the refractometric determinations was reduced and judged to be about the same as that of the oil-immersion technique. α and γ were determined by both methods, and the values by each were found to be identical within the experimental error. Several relatively thick crystals from a previous experiment (R-7) were examined on the refractometer; their sharper field lines permitted greater accuracy, and values in agreement with those determined on crystals from the later experiment were obtained. The optical constants are listed in Table 2 and compared with those of a natural phlogopite (20) and with one synthesized at the Bureau of Standards (18). The table also includes the

Table 2. Phlogopite Optical Constants

	Authors' F-phlogopite*	West's Measurements	Bur. Standards F-phlogopite	Winchells' Phlogopite (20)
α	1.522±0.001	1.5224±0.0002	1.519 calc.	1.535
β	1.548_5±.0005 calc.†	1.5489 calc.§	1.545	1.564
γ	1.549±.001	1.5494±.0002	1.547	1.565
2V	14±.5°‡	14.4°	About 9°	About 10°
Optical Character	(−)	(−)	(−)	(−)

* M. V. Denny assisted in the optical determinations.

† The value for β was so close to that of γ that a calculation of the former was considered advisable.

‡ 2V was derived from measurements made on a 5-axis universal stage, using sodium (D) light.

§ West calculated $\gamma-\beta$ as 0.0005.

results of optical measurements made by West of Polaroid Corp.* on crystals synthesized at the Electrotechnical Laboratory in an earlier experiment (also R-7).

The substitution of fluoride for hydroxyl in the phlogopite structure obviously lowers the indices of refraction, as is the case with fluor-tremolite (21). The latter compound, however, shows virtually no change in 2V upon substitution, while the optic angle of fluor-phlogopite is noticeably larger.

X-ray Data

The powder-diffraction data for synthetic fluor-phlogopite were recorded, using a chart operation with the Philips high-angle x-ray diffractometer. The instrumental setting used was as follows: Scale factor, 16; multiplier, 1.0 (thus giving a counting rate of 800 counts per second, full scale); time constant, 4 seconds; Geiger overvoltage, 300 volts; divergence slit, 1°; receiving slit, 0.003 inch; scatter slit, 1°; scanning speed, $\frac{1}{4}$° per minute; chart scale, $\frac{1}{2}$ inch per degree; radiation, unfiltered Cu.

The sample subjected to x-ray analysis was obtained by mechanically shearing the previously-selected crystals. A minus 325-mesh portion was packed in the normal rectangular aluminum holder supplied with the high-angle diffractometer. The recorded maxima were read to 0.005° 2θ (0.0025 inch on the chart) by using a low-power binocular microscope; readings were " . . . taken at the midpoint of the peak at approximately two-thirds of the peak height . . . " (22). Instrumental corrections were applied from a smooth $\Delta\ 2\theta$ curve obtained by exposing a silicon standard compact (also supplied with the instrument) both before and after the fluor-phlogopite analysis. Corrections ranged from +0.030° at 77° 2θ to +0.070° in the low-angle region.

Since the monoclinic unit cell is defined by four parameters, it was necessary to establish accurately the positions of at least four clearly resolved and properly indexed peaks to solve the quadratic form (23). Such peaks were sought in the 2θ range above approximately 50°. Since mica usually gives an excellent $(00l)$ series, it was a fairly simple matter to determine the d_{001} dimension. The latter was derived from $(007)\alpha_1$† and $(008)\alpha_1$, both giving identical values of 9.983_6 Å. It remained to locate three additional maxima not included in the $(00l)$ series. The $(33\bar{1})\alpha_1$ maximum was determined at 60.450° by scanning the same region four times and averaging the resultant readings. A similar technique gave $(136)\alpha_1$ at 69.205°. No additional satisfactory peaks were available above 50° 2θ in the front-reflection region. It had previously been decided that

* Section of status report No. 11 to the Office of Naval Research.

† CuKα_1 taken as 1.54050 Å.

the back-reflection region was unsuitable owing to uncertainty in indexing. However, a back-reflection pattern* obtained from a relatively coarse sample (−100+200) was examined in the hope that preferred orientation might lend certainty to the indexing of an otherwise suitable peak. It was found that $(139)\alpha_1$ could be indexed and, furthermore, that the nearby $(0\cdot0\cdot10)\alpha_1$ peak could be used to determine the correction $\Delta\ 2\theta$. $(139)\alpha_1$ was thus located at 101.825°, and enough data were available for solution of the quadratic form. These data are summarized in Table 3, along with the unit cell parameters derived therefrom.

Table 3. Monoclinic Cell Dimensions of Synthetic Fluor-phlogopite

Peak	2θ	Cell Dimensions (Angstroms)
$(33\bar{1})\alpha_1$	60.450°	$d_{100}=5.220\pm0.002$; $a_0=5.299\pm0.004$
$(136)\alpha_1$	69.205°	$d_{010}=9.188\pm .002$; $b_0=9.188\pm .002$
$(139)\alpha_1$	101.825°	$\beta=99°55'\pm3'=99.92°\pm.05°$
$(007)\alpha_1$	65.330°	$d_{001}=9.984\pm .001$; $c_0=10.135\pm.002$
$(008)\alpha_1$	76.225°	

Using the calculated cell dimensions and the space group symmetry, Cm (C_s^3), obtained from Weissenberg exposures, the positions of all permissible maxima in the 2θ range up to 77° (152 peaks) were calculated. Each resolved peak in this range was indexed; Table 4 compares the observed positions with those calculated from the cell dimensions. Only one maximum, $(001)\alpha$ ($\Delta\ 2\theta=-0.025°$), shows a deviation greater than 0.02°. The total of the positive deviations virtually cancels that of the negative differences, the actual unweighted average deviation being 2×10^{-4}°. The latter speaks favorably for the accuracy of the unit cell dimensions.

The literature was searched for accurate unit cell dimensions on either natural or synthetic phlogopite for comparison with the results of the present invesigation; however, no such data could be found.

The calculated density of synthetic fluor-phlogopite, on the basis of a bimolecular unit cell (Z=2), is 2.879 ± 0.004 g/cm.^{3} This compares favorably with the observed value of 2.88_2 g/cm.^{3}, determined† on a 77-mg. crystal with a Roller-Smith torsion microbalance (using toluene‡) at 25° C.

Rotation and Weissenberg (zero through third-level) exposures were made with rotation about the a axis, using unfiltered Cu radiation. The

* Time constant, 8 seconds; divergence and scatter slits, 4°; receiving slit, 0.006 inch.

† Density determination by M. V. Denny.

‡ The crystal was soaked overnight in toluene, preparatory to the liquid weighing.

TABLE 4. X-RAY DIFFRACTION DATA (POWDER) FOR SYNTHETIC FLUOR-PHLOGOPITE

(SPACE GROUP Cm)

hkl	2θ obs.	2θ calc.*	$\Delta\ 2\theta$	Meas. Int.	d calc.
001	8.88°	8.855°	−0.025°	≫100	9.984 Å
002	17.765	17.77	+ .005	18	4.992
022	26.335	26.34	+ .005	7	3.380
003	26.765	26.765	0	≫100	3.328
112	28.48	28.465	− .015	9	3.133
$11\bar{3}$	30.80	30.82	+ .02	8	2.898
023	33.215	33.21	− .005	5	2.695
130	33.89	33.905	+ .015	4	2.642
$13\bar{1}$	34.315	34.32	+ .005	2	2.611
004	35.96	35.95	− .01	21	2.496
201 $13\bar{2}$	37.05	37.04 37.06	—	2	2.425 2.424
202	41.67	41.68	+ .01	2	2.165
$13\bar{3}$	41.72	41.725	+ .005	2	2.163
005	45.39	45.38	− .01	73	1.9967
134	52.535	52.545	+ .01	1	1.7402
$31\bar{1}$	52.73	52.725	− .005	1	1.7345
$13\bar{5}$ 006	55.155	55.145 55.15	—	9	1.6641 1.6693
$33\bar{1}$	60.445	60.45	+ .005	6	1.5301
116	62.19	62.17	− .02	1	1.4918
205	63.265	63.265	0	1	1.4687
007	65.37	65.375	+ .005	6	1.4262
$11\bar{7}$	65.54	65.55	− .01	4	1.4229
027	68.86	68.87	+ .01	2	1.3621
136	69.24	69.245	+ .005	6	1.3557
$20\bar{7}$	69.385	69.38	− .005	4	1.3533
117	72.30	72.285	− .015	2	1.3059
206	72.34	72.345	+ .005	2	1.3050
008	76.225	76.225	0	7	1.2480

* Using λ CuKα (=1.5418 Å) below 25° 2θ and λ CuKα_1 (=1.54050 Å) above 25° 2θ.

rotation film led to a d_{100} value of 5.2 Å, whereas the zero-level Weissenberg gave d_{010} and d_{001} directly as 9.2 Å and 10.0 Å, respectively. None of the crystals x-rayed by single-crystal methods showed a structure other than Hendricks and Jefferson's (24), "single layer structure of the micas (monoclinic hemihedral)," the space group symmetry of which is Cm

(C_s^3). The single-crystal films also made possible several unambiguous indexings, on the basis of intensities, where two or more possibilities arose for a particular resolved maximum on the powder pattern.

Several selected crystals were measured on an optical goniometer. All of the crystals measured showed good to excellent basal pinacoids, side pinacoids, and hemi-prisms. Indications were seen of possible tetarto-bipyramid and hemi-side-dome faces. The goniometric data are summarized in Table 5.

Table 5. Synthetic Fluor-phlogopite Goniometric Data

Angle	No. Times Observed	Range	Average	Calculated
(100)∧(110)	5	29° 35′–29° 37′	29° 36′	29° 36′
(001)∧(110)	6	81° 11′–81° 19′	81° 16′	81° 16′

Acknowledgments

The authors wish to express their appreciation to H. R. Shell and R. L. Craig for the chemical analyses and to M. V. Denny for the density measurement and assistance in the optical determinations. Thanks are also due to Wilhelm Eitel, Alton Gabriel, and B. H. Clemmons for their critical review of the manuscript.

References

1. Roy, Rustum (1952), Synthetic mica, a critical examination of the literature: *School of Mineral Industries, The Pennsylvania State College, State College, Pa.: prepared for the Office of Naval Research, October 15.*
2. Doelter, C. (1917), Handbuch der Mineralchemie: Steinkopf, Dresden and Leipzig, vol. II, pt. 2, 438.
   Clarke, F. W. (1924), Data of Geochemistry: *U. S. Geol. Survey, Bull.* **770,** 395–399.
3. Machalske, F. J. (1908), Method of making artificial micas: *U. S. Patent No.* **885,934,** *April 28.*
   Siemens and Halske Company (1923), Procedure for the preparation of synthetic mica: *German Patent No.* **367,537,** *January 22.*
   Stuckhardt, K., and Reichmann, R. (1940), Method of producing an inorganic insulating material: Assigned to Siemens and Schuckert Company and Westinghouse Electric and Manufacturing Company, *U. S. Patent No.* **2,185,280,** *January 2.*
4. Grigoriev, D. P. (1934*A*), The preparation of artificial magnesian mica: *Centr. Mineral. Geol.*, 219–223.
5. Alexejewa, E. F., and Boldyrew, A. K. (1935), *X*-ray study of artificial phlogopite: *Neues Jahrb. Mineral. Geol., Beil.-Bd.* **70A,** 219–233; *Mém. soc. russe mineral.*, **64,** 80–106.
6. Machatschki, F. (1936*A*), On Grigoriev's synthetic phlogopite, a correction: *Centr. Mineral. Geol.*, 55–58.
7. Grigoriev, D. P. (1944), Synthesis and study of phlogopite: *Compt. rend. acad. sci. (USSR),* **43,** 63–65.

8. Reichmann, R., and Middel, V. (1938–1943), Siemens and Schuckert microfilmed internal reports; obtainable as *P. B. reports Nos.* **70369** *and* **70371**.
Curtis, H. A. (1946), German pilot-plant production of synthetic mica: *Chem. Met. Eng.*, **53,** No. 3, 109.
9. Ellefson, B. S. (1947), Crucibles for synthetic mica development: *Fiat Final Report No.* **1050**, *P. B.* **63552**.
10. Eitel, W., et al. (1946), The synthesis of fluorine-mica of the phlogopite group: *Fiat Final Report No.* **747,** *P. B.* **20530**.
11. Eitel, W., and Dietzel, A. (1946), Crystallochemical and microscopic investigations of synthetic phlogopites: *Fiat Final Report No.* **748,** *P. B.* **20531**.
12. Nagai, S., and Murakami, K. (1941), Synthesis of mica, I: *J. Japan. Ceram. Assoc.*, **49,** 419–421.
13. Noda, T. (1950), Synthetic mica research: *Bull. Chem. Soc. Japan*, **23,** No. 2, 40–43 [excellent English summary].
14. Noda, T., and Sugiyama, S. (1943), Chemical compositions and optical properties of synthetic micas: *J. Soc. Chem. Ind. Japan*, **46,** 760–762.
15. Noda, T., and Sugiyama, S. (1943), The temperature of crystallization of synthetic mica from silicate melts: II—The temperature of crystallization of mica from the melts of different mica concentrations and a constant glass composition: *J. Soc. Chem. Ind. Japan*, **46,** 1082–1085.
16. Hatch, R. A., and Humphrey, R. A. (1947), Final report of investigations on the production and properties of synthetic (phlogopite) mica: Unpublished internal report, Corning Glass Works and Owens-Corning Fiberglas Corporation, June.
17. Aitkenhead, W. C. (1950), Colorado School of Mines makes "cool hearth" synthetic mica: *Mining World*, **12,** 33–35.
18. Van Valkenburg, A., and Pike, R. G. (1952), Synthesis of mica: *J. Research Nat. Bur. Standards*, **48,** 360–369, *R. P.* 2323.
19. Shell, H. R., and Craig, R. L. (1954), Determination of silica and fluoride in fluorosilicates: *Anal. Chem.* **26,** 996–1001.
20. Winchell, A. N., and Winchell, Horace (1951), Elements of optical mineralogy, Part II: Description of minerals: J. Wiley and Sons, Inc., New York, Chapman and Hall, Ltd., London, 374.
21. Comeforo, J. E., and Kohn, J. A. (1954), Synthetic asbestos investigations, I: Study of synthetic fluor-tremolite: *Am. Mineral.*, **39,** 537–548.
22. Donnay, Gabrielle, and Donnay, J. D. H. (1952), The symmetry change in the high-temperature alkali-feldspar series: *Am. J. Sci., Bowen Vol.* 118.
23. (1944) Internationale Tabellen zur Bestimmung von Kristallstrukturen: Gebrüder Borntraeger, Berlin, vol. II, revised ed., 454.
24. Hendricks, S. B., and Jefferson, M. E. (1939), Polymorphism of the micas: *Am. Mineral.*, **24,** 729–771 (see 734).

Electrotechnical Laboratory Synthetic Mica Contributions

25. Hatch, R. A., Comeforo, J. E., and Pace, N. A. (1952), Transparent, plastic-ball, crystal structure models, illustrated by phlogopite mica: *Am. Mineral.*, **37,** 58–67.
26. Comeforo, J. E., Hatch, R. A., Humphrey, R. A., and Eitel, W. (1953), Synthetic mica investigations, I: A hot-pressed machinable ceramic dielectric: *J. Am. Ceram. Soc.*, **36,** 286–294.
27. Eitel, W., Hatch, R. A., and Denny, M. V. (1953), Synthetic mica investigations, II: The role of fluorides in mica batch reactions: *ibid.*, **36,** 341–348.

28. Humphrey, R. A., and Worden, E. C. (1954), Synthetic mica investigations, III: Precision-controlled electric furnaces for temperatures to 1500° C.: *ibid.*, **37,** 196–202.
29. Comeforo, J. E., and Hatch, R. A. (1954), Synthetic mica investigations, IV: Dielectric properties of hot-pressed synthetic mica and other ceramics up to 400° C.: *ibid.*, **37,** 317–322.
30. Comeforo, J. E. (1954), Synthetic mica investigations, V: A low-shrinkage, machinable ceramic of phosphate-bonded synthetic mica: *ibid.*, **37,** 427–432.
31. Hatch, R. A., Humphrey, R. A., and Worden, E. C. (1955), Synthetic mica investigations, VII: Manufacture of fluor-phlogopite by the internal electric resistance melting process: In preparation as *U. S. Bur. Mines Rep. Invest.*

Manuscript received Nov. 30, 1953

THE LUMINESCENCE AND TENEBRESCENCE OF NATURAL AND SYNTHETIC SODALITE

Russell D. Kirk, *Solid State Division, Naval Research Laboratory, Washington 25, D. C.*

Abstract

Luminescence emission spectra at 20° C. and at −196° C. of hackmanite, other natural sodalites, and certain synthetic, sulfur-containing sodalites are nearly identical. The luminescence of these sodalites is very closely related to that of scapolite and of a sodium polysulfide-sulfate mixture. From this similarity of the emission spectra and from the known occurrence of sulfur in sodalite and scapolite, it is concluded that the orange-yellow luminescence of sodalite and the yellow luminescence of scapolite are due to the presence of sodium polysulfide.

Hackmanite from Bancroft, Ontario, exhibits, on exposure to 1850 Å ultraviolet, a slow-bleaching blue coloration, in addition to the red-purple coloration described in earlier literature.

Introduction

Hackmanite, a variety of sodalite, has long been of special interest to mineralogists. First noticed over one hundred years ago, and later the basis for its being classed as a separate variety of sodalite, is the fact that a freshly fractured piece of the mineral has a pink color which fades rapidly on exposure to daylight. The pink color returns when the mineral is kept in the dark for several weeks. References to the early literature on these findings are given by Miser and Glass (1941). Lee (1936) found that a few minutes exposure to an ultraviolet source produced a deep permanganate color, the latter also being rapidly bleached by visible light.

The orange fluorescence of hackmanite and other specimens of sodalite has been noted by many observers; references are recorded by Iwase (1938) and Déribéré (1937–38).[1] Iwase recorded the luminescence of hackmanite photographically and found broad emission bands with maxima at 5800 and 6400 Å. Medved (1953) reported formation of sodalite which colored under 2537 Å ultraviolet by heating synthetic sodalite in hydrogen at 1060° C.

Sodalite has the general formula $6NaAlSiO_4 \cdot 2NaCl$; Na^+ and Cl^- ions are incorporated in the cavities of the open aluminosilicate framework (Bragg, 1937; Pauling, 1945). In synthetic products sodium is replaceable by other alkali metals, NaCl, by a wide variety of other salts (Doelter, 1917, pp. 276-284) with little change in the crystal structure. In the natural minerals, replacement of 2NaCl by Na_2SO_4 is found in noselite;

[1] Some specimens of sodalite show a blue luminescence; this emission is not treated in this paper.

replacement by other sodium salts and by calcium salts is exemplified by other members of the sodalite and cancrinite groups.

Analyses of hackmanite have shown that it has the crystallographic and chemical constitution of sodalite. The first described analysis (Borgström, 1901) showed the presence of 0.39% sulfur. Haberlandt (1949) found traces of boron, lead, and sulfur. Lee (1936) suspected that the luminescent and photosensitive properties of hackmanite are connected with the presence of manganese, which he found to the extent of 0.001–0.002% in hackmanite from Bancroft, Ontario.

The purpose of the present investigation was to determine, if possible, the nature of the luminescent centers present in hackmanite and other fluorescent sodalites and to synthesize products having the luminescent and coloring properties of hackmanite.

Experimental

Experimental methods employed in the physical measurements and reagents used in the syntheses have been described in an earlier paper (Kirk, 1954).

The first successful synthesis of a substance having the properties of hackmanite involved two steps. The first step was the reduction by hydrogen at 900° C. of all the Na_2SO_4 in a material having the composition $6NaAlSiO_4 \cdot 1.8NaCl \cdot 0.1Na_2SO_4$. The resulting mono-sulfide-containing material was then fired in air at 900° C. for 15 minutes causing a partial oxidation of the sulfur.

The hydrogen-fired product was not luminescent under either 3650 or 2537 Å excitation. It showed strong tenebrescence under a 2537 Å source.[2]

The air-oxidized material had a strong orange-yellow luminescence under a long wave ultraviolet source, colored red-purple within ten seconds on exposure to a 4 watt germicidal lamp (short wave ultraviolet) at a distance of one centimeter, and bleached rapidly on exposure to a tungsten light source. Extended heating of the product in air at 900° C. resulted in a material which exhibited no tenebrescence but which still had a yellow luminescence.

An *x*-ray powder diffraction pattern of this material was identical with that of hackmanite from Bancroft, Ontario, both showing only sodalite lines.

Attempts to duplicate this product showed that the oxidation step is dependent upon such factors as the amount of surface exposed to the air and the amount of air circulation in the furnace. Variation of the firing

[2] Tenebrescence refers to the property of darkening and bleaching which some nearly colorless solids possess. The darkening may be caused by various types of irradiation; the bleaching, by either heat or irradiation.

temperature or the firing time or both may be necessary to produce a product which is both tenebrescent and luminescent.

A method of synthesis involving firing together of $6NaAlSiO_4 \cdot (2-x)NaCl \cdot (0.5x)Na_2SO_4$ and $6NaAlSiO_4 \cdot (2-x)NaCl \cdot (0.5x)Na_2S$ in helium has been described in the above-mentioned earlier paper by the author. This method allows excellent control of the degree of luminescence and tenebrescence. Products with a large Na_2S/Na_2SO_4 ratio have the best tenebrescence; those with a large Na_2SO_4/Na_2S ratio show the brightest luminescence.

A simpler but more empirical method of preparation consists of the following: the component oxides and salts to give the $6NaAlSiO_4 \cdot 1.8NaCl \cdot 0.1Na_2SO_4$ composition are ball-milled together for three hours in acetone. The filtered cake of reactants is dried for one hour at 100° C., packed into a tall-form silica crucible, and fired for 15 minutes at 800° C. The resulting product has luminescent and tenebrescent properties like those of hackmanite, but to a lesser degree than products made by the above two methods. Milling in acetone is an essential part of this preparative procedure. The same composition prepared by dry mixing is not luminescent after firing.

The products more nearly approaching noselite in composition, e.g. $6NaAlSiO_4 \cdot 1.0NaCl \cdot 0.5Na_2SO_4$[3] show brighter fluorescence and color to a darker shade than those with higher NaCl content. Lowering the silica content to 90% of the theoretical value also improves both the luminescence brightness and the colorability of the synthetic sodalites. Synthetic noselite itself, when prepared by milling the components in acetone and firing, shows an orange luminescence but does not tenebresce. Similarly prepared sodalite with no sulfate neither luminesces under 3650 Å excitation nor tenebresces under 2537 Å ultraviolet.

Results

Luminescence

Emission spectra at room temperature of the partially reduced $1.8 NaCl \cdot 0.1 Na_2SO_4$ sodalite composition and of hackmanite from Kola Peninsula, U.S.S.R. under 3650 Å excitation are given in Fig. 1, which shows the near identity of the spectral distribution. Figure 2 compares the emission spectra of sodalites from various sources, all exhibiting emission maxima at about 6150 and 6350 Å. The luminescence color is thus the same for all the specimens studied.

In observations made by eye some apparent differences in emission color appear which are actually brightness differences, with resulting

[3] Starting composition. Formulas given hereafter in this paper denote only the starting composition and are not intended to represent the final chemical constitution.

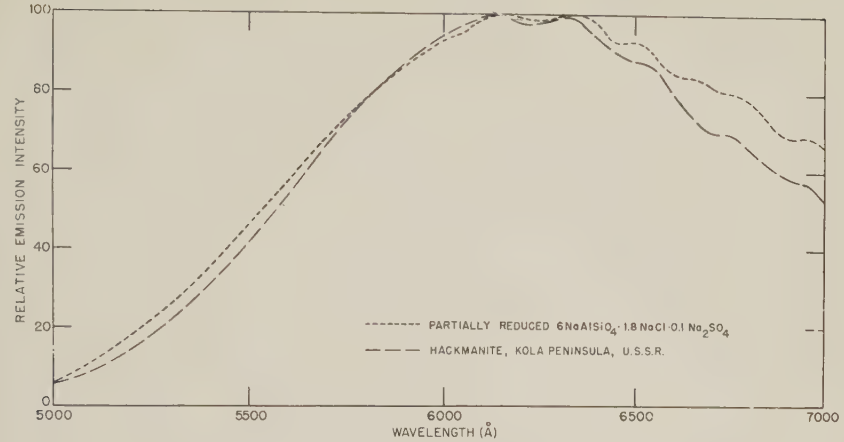

FIG. 1. Luminescence emission of synthetic and natural hackmanite at 20° C. with 3650 Å excitation.

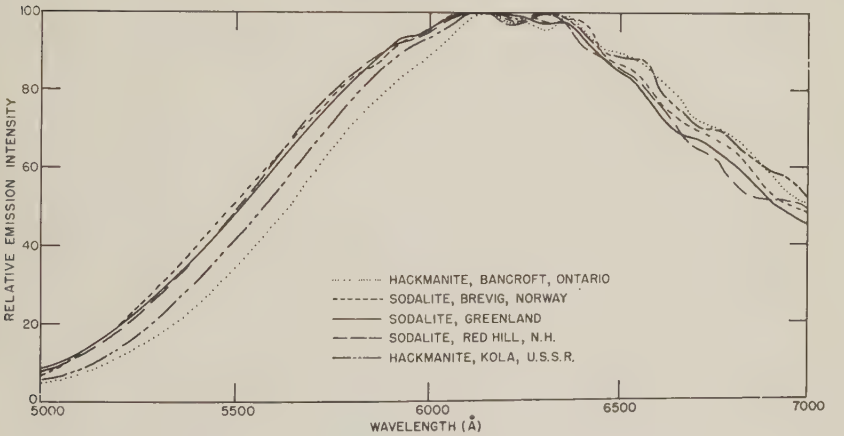

FIG. 2. Luminescence emission of natural sodalite and hackmanite at 20° C. with 3650 Å excitation.

variation in the ratio of luminescence emission to visible light reflected by the specimen; the reflected visible light originates in the ultraviolet source. Insertion of a 5 mm.-thick Corning No. 5860 filter (which passes practically no visible light) between the ultraviolet source and the specimens shows that all the fluorescent sodalites studied luminesce yellow, with a slightly orange tint, rather than red-orange.[4]

[4] This common subjective error was also demonstrated in a different manner by Schulman et al. (1947), who showed that the fluorescence color of calcite from Franklin, N. J., is actually red-orange, rather than rose or pink as it is often stated to be.

Figure 3 shows the luminescence emission spectra of scapolite from Argenteuil, Quebec, and sodalite from Red Hill, N. H., with long wave ultraviolet excitation. Although the spectral positions are different, the similarity of the emission structure is evident.

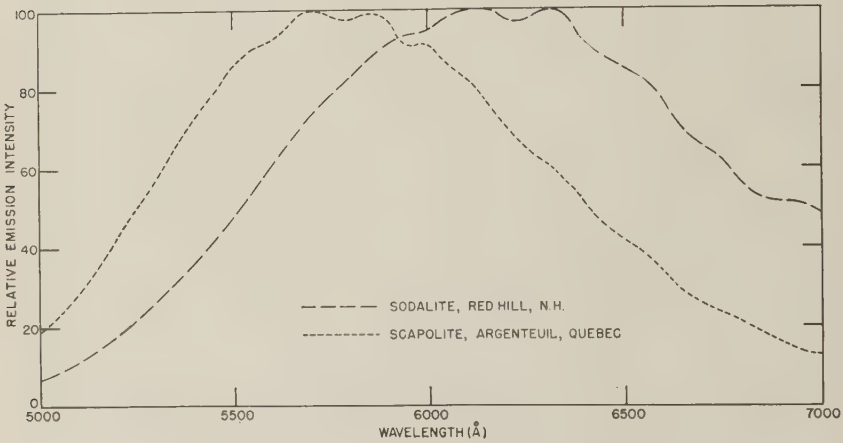

Fig. 3. Luminescence emission spectra of scapolite and sodalite at 20° C. with 3650 Å excitation.

The luminescence emission spectra at −196° C. of hackmanite from Kola, U.S.S.R., scapolite from Argenteuil, Quebec, sodium polysulfide-sulfate mixture prepared by heating thiosulfate as described in the author's earlier paper, and partially reduced $6NaAlSiO_4 \cdot 1.8NaCl \cdot 0.1Na_2SO_4$ are shown in Fig. 4. The near identity of the locations of the

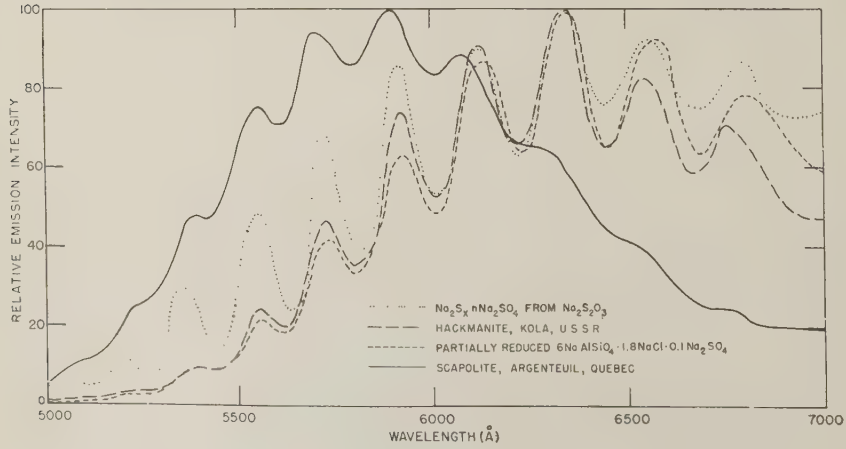

Fig. 4. Luminescence emission at −196° C. with 3650 Å excitation.

emission peaks indicates that the luminescence centers are very likely the same in all the materials given. Exactly the same emission peaks at −196° C. are exhibited by hackmanite from Bancroft, Ontario, and sodalite from Brevig, Norway, Red Hill, N. H., and Greenland, the emission spectra of which are not illustrated.

The excitation spectra of the synthetic sodalite products, of $Na_2S_x \cdot nNa_2SO_4$ prepared by heating $Na_2S_2O_3$, of scapolite from Argenteuil, Quebec, and of sodalite and hackmanite specimens from the localities just mentioned are identical. Maximum emission is produced by an excitation wavelength of 4000 Å, the emission dropping to almost zero under 2500 Å and 5000 Å excitation, as shown for hackmanite from Bancroft, Ontario in Fig. 5.[5]

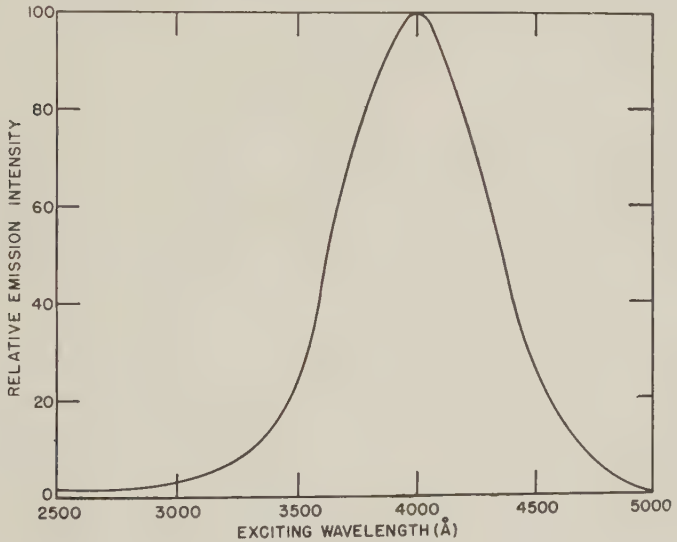

FIG. 5. Excitation spectrum of hackmanite from Bancroft, Ontario.

Tenebrescence

Although the coloration of hackmanite by ultraviolet to a red-purple color is well known, a new tenebrescence color has also been found. Exposure of hackmanite from Bancroft, Ontario, to an unfiltered low-pressure, silica-envelope mercury arc ("Mineralight" Model *R-51*) caused

[5] The very weak luminescence of scapolite, hackmanite and sodalite under a short wave ultraviolet source (e.g., a "Mineralight" lamp) is due almost entirely to the small amount of long wave ultraviolet emitted by the source. This can be readily demonstrated by the interposition of a Pyrex filter, Corning No. 7740, between the source and the sample, whereby the brightness of this fluorescence is not noticeably diminished. This filter in a 2 mm. thickness cuts off 99.5% of the 2537 Å radiation.

the appearance of the usual magenta color within a few seconds. Exposure of the same sample to this source for a period of several hours produces in addition, a blue coloration. The blue color, like the pink-purple, is scattered in patches and streaks throughout the specimen and is sometimes coincident with the purple areas, but often not. The blue coloration, however, fades out very slowly over a period of several weeks, and does not appear to be affected by visible light. Moreover, unlike the purple color, the blue color is not produced when a Corning No. 9863 filter is placed between the source and the specimen. Since this filter cuts off light below 2300 Å, it is likely that the blue color is produced by 1850 Å radiation. Extended x-irradiation also causes formation of the blue color along with the pink-purple. When the specimen is heated at 400° C. for a short period it will no longer color pink but formation of the blue color is not affected. The composition of the mineral at these blue-coloring spots is not known, although it is suspected that it is some variety of sodalite.

Similar extended irradiation of the tenebrescent synthetic products prepared as previously described produces only a deepening of the first-formed magenta color. However, synthetic sodalites with small amounts of Na_2SO_4 (unreduced) replacing NaCl, although not sensitive to 2537 Å, become blue-violet under extended 1850 Å and x-irradiation. This color, like the above blue, is very slow to bleach.

Discussion

Haberlandt (1934, 1935) noted the peculiar luminescence emission structure of sodalite and scapolite at room temperature and at low temperatures and suspected the presence of uranium. Iwase (1937) likewise ascribed the band structure of the emission of scapolite to a content of uranium. Haberlandt later showed that these minerals contain no uranium (1949) and mentioned the possibility that the activator is a sulfur compound.

Thugutt notes in Doelter's handbook (1917, p. 247) that a sulfur content in sodalites is of common occurrence. Miser and Glass (1941) reported the presence of sulfur and SO_3 in hackmanite from Magnet Cove, Arkansas, and noted an evolution of H_2S on addition of the mineral to hot, dilute hydrochloric acid, as did Iwase (1938) with hackmanite from Korea. Walker and Parsons (1925) reported no sulfur in the Bancroft, Ontario, hackmanite; however, qualitative tests with sodium plumbite paper showed sulfide to be present in samples of this material available to the author. Haberlandt (1949) noted the formation of H_2S on powdering fluorescent scapolite from Grenville, Canada.

Summarizing these statements and some of the earlier parts of this paper:

1. Many sodalites contain sulfur, often as a sulfide.

2. Synthetic sodalite compositions containing (*a*) no sulfur, or (*b*) sulfur as Na_2SO_4 only, or (*c*) sulfur as Na_2S only, show no luminescence.

3. Synthetic sodalite products containing sulfur partially reduced from sulfate show emission peaks at $-196°$ C. identical in spectral position with the emission peaks of natural hackmanite and other fluorescent sodalites.

4. A sodium polysulfide-sulfate mixture prepared by heating sodium thiosulfate in air at 900° C. also has these same emission peaks.

It is concluded that the orange-yellow luminescence of hackmanite and other fluorescent varieties of sodalite and the yellow luminescence of scapolite (scapolite is related to sodalite in chemical composition) are due to the presence of the polysulfide ion in an environment similar to that present in a sodium polysulfide-sulfate mixture prepared by heating sodium thiosulfate. The author believes by analogy that the orange luminescence with line structure of the closely related haüynite, which was noted by Haberlandt (1935) in specimens from several localities, is likewise due to polysulfide.

Since the luminescence of the non-tenebrescent sodalites is the same as that of the hackmanite varieties and since synthetic sodalites can be prepared which color violet but are non-fluorescent, or which fluoresce but do not color, it is obvious that the luminescence centers of hackmanite are different from its color centers. The color centers, by analogy to those of synthetic products (Kirk, 1954), are believed to be related to the combined presence of sodium chloride and sodium (mono) sulfide in the sodalite-type lattice. The loss of tenebrescence of the synthetic hydrogen-fired sulfur-containing sodalite on extended heating in air at 900° C. would then be attributable to the oxidation of all the monosulfide sulfur to a polysulfide or higher oxidation state.

Thus, the hackmanite variety of sodalite appears to contain small amounts of both sodium mono- and poly-sulfide.

On a few occasions supposedly pure NaCl-sodalites, after hydrogen firing at 900° C., gave an extremely weak coloration on prolonged exposure to a 2537 Å source. The author ascribes this sensitivity to the presence of traces of sulfur in the starting reagents.

Firing of pure synthetic sodalite in hydrogen at 1060° C., in attempts to duplicate the work of Medved, resulted in losses of more than 50% of the contained NaCl. The resulting products, like those fired in hydrogen at 900° C., were very weakly 2537 Å sensitive. However, like pure sodalite

fired at 1060° C. in air, they colored red-violet under 1850 Å irradiation.

Ultramarines, which have a composition and structure closely related to that of sodalite (Jaeger, 1930) are not luminescent, nor is a mixture of synthetic sodalite and ultramarine fired together in helium. However, the sodalite-ultramarine product after firing in hydrogen and oxidizing by firing in air shows the typical orange-yellow luminescence of sodalite.

It is usually stated that the blue chromophore in ultramarine (and the blue sodalite minerals) consists of Na_2S_x groups; if this is true, the environment of the groups in ultramarine must be widely different from those in hackmanite and fluorescent sodalite. The possibility that the chromophore is not Na_2S_x alone is shown by the fact that the so-called "primary" ultramarine which contains excess water-soluble sodium polysulfide is a weak, dull pigment (Beardsley and Whiting, 1948). Only after a subsequent oxidation step is true, deep-blue ultramarine formed.

Acknowledgments

Thanks are gratefully given to Dr. James H. Schulman and Dr. Clifford C. Klick of this laboratory for their helpful discussions concerning this work.

The writer also wishes to thank Dr. George Switzer of the U. S. National Museum for assistance in obtaining some of the specimens used.

References

1. Beardsley, A. P., and Whiting, S. H. (1948), *U. S. Patents* **2,441,950**; **2,441,951**; **2,441,952**.
2. Borgström, L. H. (1901), Hackmanit ett nytt mineral i sodalitgruppen: *Geol. För. Stockholm*, **23**, 563.
3. Bragg, W. L. (1937), Atomic Structure of Minerals, Cornell Univ. Press, Ithaca, N. Y., pp. 265–268.
4. Déribéré, M. (1937–8), Les mineraux fluorescents; fluorescences dans le group des sodalites et les groupes voisins: *Ann. soc. geol. Belg., Bull.* **61**, 52–55.
5. Doelter, C. (1917), Handbuch der Mineralchemie, Bd. II, 2, Theodor Steinkopff, Dresden and Leipzig.
6. Haberlandt (1934), Fluoreszenzanalyse von Mineralien: *Sitz. Ber. Akad. Wiss. Wien, Abt. IIa*, **143**, 11.
   (1935), Lumineszenzuntersuchungen and Fluoriten and anderen Mineralien, II: *Sitz.-Ber. Akad. Wiss. Wien, Abt. IIa*, **144**, 663–666.
   (1949), Neue Lumineszenzuntersuchungen an Fluoriten und anderen Mineralien, IV: *Sitz.-Ber. Osterr. Akad. Wiss. Wien. I.*, **158**, 609–646.
7. Iwase, E. (1937), Luminescence of scapolite from North Burgess, Canada: *Sci. Pap. Inst. Phys. Chem. Res., No. 734*, **33**, 299.
   (1938), Über die photochemischen Eigenschaften des Sodaliths von Kisshu, Korea: *Z. Krist.*, **99**, 314–325.
8. Jaeger, F. M. (1930), Spacial Arrangements of Atomic Systems and Optical Activity, Part III. The Constitution and Structure of Ultramarines, McGraw Hill Book Company, New York, N. Y.

9. Kirk, R. D. (1954), The role of sulfur in the luminescence and coloration of some aluminosilicates: *Jour. Electrochem. Soc.*, **101,** 461–465.
10. Lee, O. I. (1936), Reversible photosensitivity in hackmanite from Bancroft, Ontario: *Am. Mineral.*, **21,** 764–775.
11. Medved, D. B. (1953), The optical properties of natural and synthetic hackmanite: *J. Chem. Phys.*, **21,** 1309–1310.
12. Miser, H. D., and Glass, J. J. (1941), Fluorescent sodalite and hackmanite from Magnet Cove, Arkansas: *Am. Mineral.*, **26,** 437–445.
13. Pauling, L. (1945), Nature of the Chemical Bond, Cornell University Press, Ithaca, N. Y., p. 387.
14. Schulman, J. H., Evans, L. W., Ginther, R. J., and Murata, K. J. (1947), The sensitized luminescence of manganese activated calcite: *Jour. Applied Physics,* **18,** 732–739.
15. Walker, T. L., and Parsons, A. L. (1925), Evanescent pink sodalite and associated minerals from Dungannon Township, Ontario: *Univ. of Toronto Studies, Geol. Studies, No.* **20,** 5.

Manuscript received Dec. 2, 1953

OCCURRENCE OF PYROPHANITE IN JAPAN

Donald E. Lee, *Stanford University, Stanford, California.*

Abstract

Pyrophanite, previously reported from only three localities, is widely distributed in Japanese manganese ores. The mineral is present in six of eleven scattered mines that were sampled. Paragenetic associations are summarized and physical, optical, spectrographic and x-ray data are given. Some of the pyrophanite described has an abnormal greenish-yellow color which it is suggested might possibly be due to the presence of minor amounts of cerium.

Introduction

Pyrophanite has been previously reported from only three localities. It was originally described by A. Hamberg (1890) who, with G. Flink, found the mineral in drusy cavities in manganese ore at the Harstig mine, Pajsberg, Sweden. The associated minerals are garnet, ganophyllite, "manganophyll," and calcite, the latter having been introduced at a later stage.

Pyrophanite was next reported by A. O. Derby (1901) from the Piquery mine of the Queluz district, Minas Gerais, Brazil, as minute hexagonal grains of a transparent red mineral embedded in garnet and quartz, and he stated; "The crystallographical, optical and chemical characters of this mineral, so far as they can be made out, agree with those of pyrophanite." He describes the quartz as being "abundantly threaded with delicate transparent needles of a white asbestiform mineral."

Later, from the same mine, Derby (1908) reported transparent red grains of a rutile-like mineral which he says gave "strong characteristic reactions for both titanium and mangenese." According to Derby, this mineral is associated with a "carbonate (rhodochrosite?), an olivine-like silicate (tephroite)," spessartite, pyrite, ilmenite and occasional rhodonite.

The other occurrence of pyrophanite is from the Benallt mine, Rhiw, Carvarvonshire, Wales, where W. Campbell Smith (1947) found the mineral associated with pennantite. The identity of this pyrophanite was confirmed by x-ray photographs.

In early 1951 the author, with Dr. C. F. Park, made a reconnaissance survey of a number of small manganese mines in Japan and representative samples were collected from nine mines. In addition the sample and data from the Ajiro mine were furnished by Dr. B. M. Page, and the X-mine specimen studied was supplied by the Department of Mining Engineering, Tokyo University. Pyrophanite was identified in specimens from six mines shown in Fig. 1.

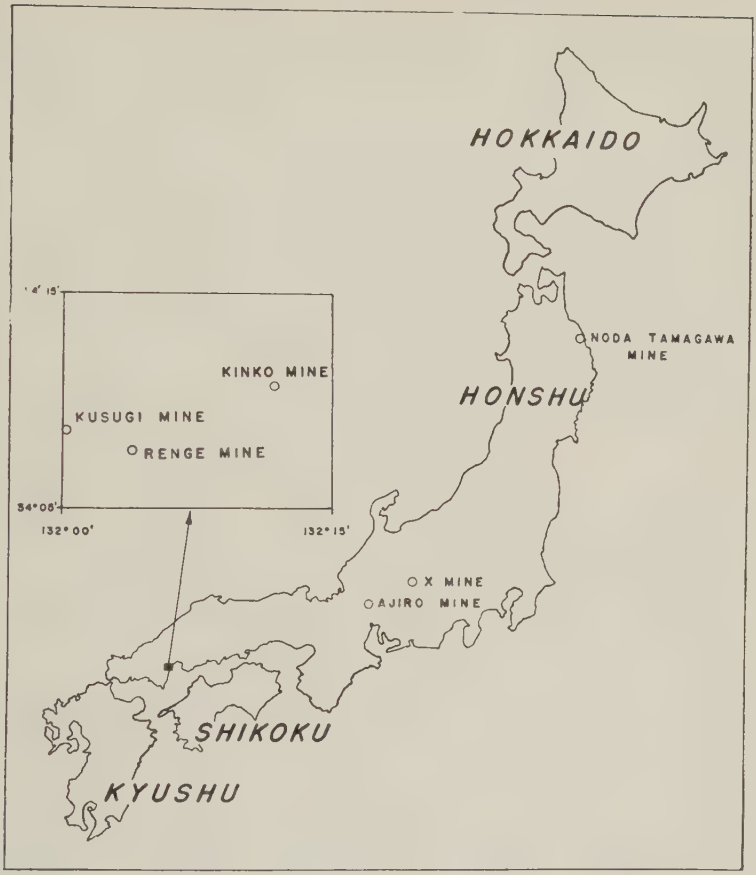

Fig. 1

Acknowledgments

Dr. C. F. Park directed the field work and suggested a laboratory study of the specimens collected. This study was aided by a grant from the Austin Flint Rogers Fellowship in Mineralogy. The author wishes to express particular thanks to Dr. C. O. Hutton for encouragement and advice on principles and techniques throughout this study.

General Field Relations

Although this paper is not concerned with the genesis of the manganese deposits, a brief summary of available field data will provide a general setting for the minerals described.

Two main types of manganese ores are recognized in Japan. Tertiary

mesothermal fissure-filling deposits, mostly confined to the Oshima Peninsula in southwest Hokkaido, are grouped as the first type.

Deposits of the second type are associated with what Japanese geologists call the "Chichibu Complex." This "Complex" includes an unknown thickness of largely undifferentiated chert, slate, dark graywacke, basic volcanic or intrusive rocks, limestone and dolomite. The oldest known rocks in the "Complex" are Silurian whereas the youngest are Permian in age. They were deposited on an unknown basement in a Paleozoic deep off the coast of Asia. Now, more or less metamorphosed, they are distributed in broad areas throughout the four main islands of Japan. The "Complex" contains numerous small manganese deposits which appear to have replaced the chert beds. All specimens described here are from deposits of this kind.

Paragenetic Associations

Pyrophanite was found in rocks from the Ajiro, Kinko, Kusugi, Noda Tamagawa, Renge, and X-mines.

(1) *Ajiro mine.*—A mineralized lens in gray chert was being worked. This lens, about two feet thick and 20 feet long, is parallel to, and about three feet from, a healed fault. Thin sections show rhodochrosite, quartz and twinned euhedral pyroxmangite,* and some evidence points to replacement of the latter by later-introduced carbonate. The small heavy fraction recovered by centrifuging 200-mesh material included grains of alabandite, garnet and greenish-yellow pyrophanite about .03 mm. thick.

(2) *Kinko mine.*—The ore is replacing a chert bed about four feet thick included between beds of graphitic slate, and the workings show clearly an anticlinal structure with limbs dipping about 40°. Minerals seen in thin section are garnet, carbonate, alleghanyite, alabandite, neotocite, pyrophanite and pyroxmangite. The alleghanyite is being replaced, mostly by pyroxmangite, and alabandite exhibits a patchy distribution. Neotocite is characteristically confined to late veinlets. Pyrophanite crystals up to .2 mm. across are often found as inclusions in carbonate or pyroxmangite. Smaller crystals of pyrophanite are concentrated in a few irregular stringers that mark paths of later-introduced material. Pyrophanite ranges in color from blood-red to greenish-yellow, but colors show no relation to crystal size or immediate environment. Rarely does the pyrophanite show any evidence of alteration.

(3) *Kusugi mine*—The most interesting and significant deposit which was extensively sampled consists of a tabular body in chert of undetermined thickness.

* It is planned to present data on this and other minerals from this suite in a later paper.

One specimen consists almost entirely of rhodonite through which are scattered small garnet and pyrophanite crystals and rare allanite. Most of the pyrophanite crystals are crimson-red blebs about .003 mm. long, although a few larger crystals are yellowish in color. Other minerals present are neotocite and a very small amount of carbonate.

A second specimen is mainly fine-grained quartz, almost chert-like in some instances. This material is host to allanite, actinolite crystallites, small garnet, apatite grains, tiny blebs of yellow pyrophanite and an opaque mineral with cubic outline. Veinlets of somewhat more coarsely-crystalline quartz criss-cross the finer-grained material as an irregular network. These veinlets are devoid of inclusions except for one euhedral crystal of zoned allanite. Some of the apatite, garnet and pyrophanite is confined to thread-like zones that appear to outline old fracture systems not related to the later network of quartz veinlets. This occurrence is very similar to that described by Derby (1901).

Intergrown pyroxmangite and carbonate are cut by veinlets of later carbonate in the third specimen, and alabandite is associated with both pyroxmangite and carbonate. Other minerals noted are garnet, neotocite, apatite (commonly as inclusions in pyroxmangite), and tephroite. The sparsely-distributed tephroite appears to have been partially replaced by carbonate and pyroxmangite. Garnet and pyrophanite are concentrated in, but not confined to, subparallel bands which may reflect original bedding. Pyrophanite, mostly subhedral, ranges in color from reddish-orange to greenish-yellow and rarely exceeds 0.1 mm. in size. Allanite and monazite were found in crushed material.

Pyroxmangite is the dominant constituent in the fourth specimen with huebnerite, pyrophanite, quartz and an unidentified non-magnetic opaque mineral, all distributed at random in the pyroxmangite. Allanite and barite are rare. Pyrophanite is usually subhedral and, except in one case, is crimson-red in color; the exception occurred as an inclusion in allanite and exhibited a yellowish tint.

(4) *Noda Tamagawa mine*—A deposit about four feet thick is bedded in chert and folded into an overturned syncline. Rhodonite is dominant here and contains stringers of garnet clouded with tiny red pyrophanite blebs. However, larger pyrophanite blebs, up to .003 mm. in diameter, were detected throughout the rhodonite, and exhibit a range of color from crimson-red to yellowish-green. The rhodonite also contains pyrophanite veinlets, the edges of which are yellowish, whereas the central parts are red to orange. Larger veinlets contain later-introduced carbonate, neotocite and bementite (?). Barite, allanite and ilmenite, though present, are not seen in thin section.

(5) *Renge mine*—Chert is the host rock of the deposit and the ore is

concentrated in aligned potato-shaped pods, each up to four yards long. Twinned pyroxmangite makes up most of the sample. Other minerals are garnet, carbonate, neotocite, tephroite, pyrophanite and a ferromagnetic constituent, probably jacobsite, in small discontinuous fractures in pyroxmangite. The tephroite appears to show alteration to pyroxmangite. Some of the garnet, concentrated in irregular but continuous stringers, has a semi-opaque appearance under low magnification, but with high magnification and intense illumination, myriads of tiny pyrophanite blebs are clearly seen. Pyrophanite in this specimen has a dark blood-red color. Huebnerite also is present, but this was not observed in a thin section.

(6) *X-mine*—The sample is labeled as having come from a skarn zone, and the location suggests that it was obtained from the contact zone between the Chichibu "Complex" sediments and a Mesozoic granodioritic intrusive. The section shows anhedral alabandite in rhodonite. Carbonate, closely associated with the alabandite, often separates it from the rhodonite, and monazite was tentatively identified as inclusions in the silicate. Rhodonite also includes many pyrophanite grains that exhibit a range of color from crimson-red to greenish-yellow. Again, no correlation can be made between color and grain size. One euhedral grain is distinctive for its zoning; a yellowish-orange periphery grades into a red irregularly-shaped inner zone. Apatite, pyrite and galena are present in minor amounts.

Mineralogy

(1) *Form*—Crystals .003 mm. or less in length appear as elongated blebs and show no definite crystal form. The larger crystals have a tabular habit and many of the separated grains show well-developed crystals faces (Fig. 2). Well-developed cleavage planes were occasionally observed.

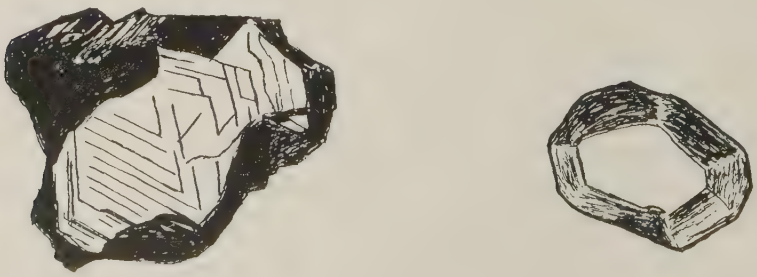

Fig. 2. *Left*—Yellowish-green crystal of pyrophanite oriented with the dominant face (0001) parallel to the plane of the preparation. Such crystals give centered interference figures and exhibit (11$\bar{2}$0) and (02$\bar{2}$1) cleavages. Locality: Ajiro mine. ×570. *Right*—Orange-red crystal of pyrophanite. The euhedral tabular form is typical of many crystals from all six mines described. Interference figure about 5° off center. Locality: Kusugi mine. ×570.

(2) *Physical properties*—In oblique illumination pyrophanite has a wine-red color, but when finely ground (powder for x-ray spindle), a dull brownish-green tint is evident.

In transmitted light, color variation from grain to grain is striking, and greenish-yellow and blood-red crystals are often found in the same slide. Zoning within a given crystal is unusual. Colors are not related to crystal size.

Because of their strong preferred orientation perfectly-centered negative interference figures are easily obtained for grains of any color. The ordinary ray has strong positive relief in a sulphur-selenium mount with an index of 2.25.

The largest grains are about .2 mm. long, but the majority are much smaller. This factor and lack of sufficient quantity of the mineral prevented direct specific gravity measurements. It can be stated that pyrophanite here described has a specific gravity greater than that of Clerici at maximum density at room temperature; that is, greater than 4.20.

The red and yellow grains have similar magnetic susceptibility. With the Frantz Isodynamic Separator set at slope 15° and tilt 12°, the smallest grains are drawn off at .2 ampere. Most of the grains are attracted at .25 ampere and at .3 ampere very few remain in the non-mangetic fraction.

Pyrophanite showed no evidence of attack after treatment with 1:1 HCl at 100° C. for one hour.

(3) *Separatory processes*—Crushed material separations served both to isolate as much pyrophanite as possible and to detect the presence of minerals not apparent in thin section.

To insure preparation of monomineralic particles, specimens were broken to pass through 200-mesh bolting silk. Screened material was then freed from dust by repeated washing in a two-liter beaker and decanting until the supernatant water was clear after 90 seconds of particle settling. Turgitol was used to reduce surface tension to a minimum.

In most instances a partial concentration of pyrophanite was effected with the Frantz Isodynamic Separator. Pyrophanite is slightly more paramagnetic than huebnerite, hausmannite or allanite; slightly less magnetic than tephroite or carbonate.

The ability of pyrophanite to withstand acid attack provided a means by which undesired carbonate, neotocite, sulfides and orthosilicates were effectively removed.

Greatest control was achieved with Clerici solution. Of the acid-insoluble minerals with the same range of magnetic susceptibility as that of pyrophanite, only the heavier garnet could not be separated from pyrophanite by centrifuging in Clerici at maximum practicable density (about 4.20).

Hand-picking of pyrophanites was of little use. Most grains are less

than .07 mm. long, and color differences are only apparent in transmitted light with a magnification of over 100 times.

(4) *Spectrographic data*—Qualitative spectrographic analyses were made of two pyrophanite samples.

About three milligrams of mixed red and yellow pyrophanite were isolated from the Kinko mine sample described. The spectrogram shows intense lines for manganese and titanium. Other lines present are those for iron (estimated at less than one per cent), cerium (strong trace), and lanthanum and chromium (traces).

The third sample described from the Kusugi mine yielded about 10 milligrams of material for analysis. About 10 per cent of this preparation

Table 1. X-ray Diffraction Data for Pyrophanite

Posnjak and Barth			Kinko Mine	
I–I_1	d(Å)	(hkl)	d(Å)*	I–I_1
30	3.75	110	3.74	10
100	2.78	211	2.76	100
90	2.57	$1\bar{1}0$	2.55	70
50	2.25	210	2.25	40
—	2.18	200		
70	1.89	220	1.88	60
80	1.745	321	1.74	70
10	1.655	$\{332\ 2\bar{1}1\}$	1.66	5
70	1.518	310	1.52	50
60	1.480	$\bar{2}11$	1.48	50
—	1.388	$\{300\ 22\bar{1}\}$	1.36	5
40	1.357	$\{432\ 433\}$	1.35	10
20	1.280	$2\bar{2}0$	1.28	5
10	1.200	442	1.20	5
10+	1.129	420	1.130	10
20	1.086	$\{522\ 532\}$	1.089	20
10−	1.058	$\{400\ 430\}$	1.063	5
10	1.010	$\{3\bar{2}1\ 521\ 531\}$	1.016	10
10	.970	$\{41\bar{1}\ \bar{3}21\ 511\}$	.982	10

* Fe filtered with Mn. $\lambda = 1.9373$ Å. Camera radius 57.3 mm.

was garnet; the remainder was pyrophanite, some red, some yellow. Lines for manganese and titanium are again intense. Other elements in evidence are silicon, aluminum, magnesium, iron (estimated at less than two per cent), cerium (trace) and vanadium (weak trace).

(5) *X-ray diffraction data*—A complete and accurate set of diffraction data were obtained only for the Kinko mine pyrophanite. As noted, this pyrophanite ranges in color from blood-red to greenish-yellow. Results are compared with the data of Posnjak and Barth (1934) in Table 1. Intensities listed for the Kinko pyrophanite are visual estimates only.

For the three largest *d* spacings the Kinko pyrophanite has values consistently lower than those listed by Posnjak and Barth. Moreover, the very weak (200) line recorded was not apparent on the Kinko film. However, except for those discrepancies, the two sets of values are in close agreement.

The lines on the Kinko film are sharp, with no suggestion of doublets. Thus the cell sizes for red and yellow varieties do not appear to be significantly different.

Conclusion

The widespread presence of pyrophanite in these "ores" should be viewed in the light of the low over-all iron content of the associated minerals; analytical and spectrographic data indicate that most of these specimens contain less than one per cent iron. Nevertheless, pyrophanite is probably a much more common mineral than previously supposed. In thin section it may easily be mistaken for rutile or priderite (Norrish, 1951); indeed, it was not until a casual check was made of the optic sign of freed crystals that pyrophanite was suspected in these samples.

Though Derby was unable to check his determinations with *x*-ray diffraction work, the similarity of occurrence of his reported pyrophanites with some of those described here would seem to offer circumstantial evidence in support of his results.

The compositional change reflected in the color range of these pyrophanites cannot of course be known until analyses of the red and the greenish-yellow concentrates are available. Pending such analyses, it is suggested that the greenish-yellow color of some of the pyrophanite might be due to the presence of small amounts of cerium.

References

Derby, A. O. (1901), On the manganese ore deposits of the Queluz (Lafayette) District, Minas Geraes, Brazil: *Am. Jour. Sci.*, Ser. 4, **12**, 18–32; esp. p. 21.

——— (1908), On the original type of the manganese ore deposits of the Queluz District, Minas Geraes, Brazil: *Am. Jour. Sci.*, Ser. 4, **25**, 213–216; esp. p. 215.

Hamberg, A. (1890), Über die Manganophylle von der Grube Harstigen bei Pajsberg in Vermland: *Geol. För. Förh.*, Stockholm, **12,** 567–637, esp. pp. 598–604, 632.

Norrish, K. (1951), Priderite, a new mineral from the leucite-lamproites of the west Kimberly area, Western Australia: *Mineral. Mag.*, **29,** 496–501.

Posnjak, E., and Barth, T. F. W. (1934), Notes on some structures of the ilmenite type: *Z. Krist.*, **88,** 271–280.

Smith, W. Campbell, and Claringbull, G. F. (1947), Pyrophanite from the Benallt mine, Rhiw, Carnarvonshire: *Mineral. Mag.*, **28,** No. 187, 108–110.

Manuscript received Dec. 2, 1953

STUDIES IN THE MICA GROUP: POLYMORPHISM AMONG ILLITES AND HYDROUS MICAS

A. A. Levinson, *College of Engineering, The Ohio State University, Columbus 10, Ohio.*

Abstract

Powder and single crystal x-ray studies on specimens called illite or hydrous mica have demonstrated that polymorphism exists among these minerals. The 3-layer trigonal (*3T*), 2-layer monoclinic (*2M*), 1-layer monoclinic (*1M*) and 1-layer monoclinic disordered (*1Md*) structures have been identified. The commonly held concept that all illites have poorly crystallized *2M* structures is disproved. No definite correlation between the type of polymorphic crystallization and either chemical composition or geological occurrence has been observed.

Introduction

In their original description, Grim, Bray and Bradley (1937) concluded that the structure of illite from Gilead, Illinois, is closely related to that of common 2-layer monoclinic (*2M*) muscovite. Two years later Hendricks and Jefferson (1939) described the wide variety of polymorphic forms of mica. Grim, Bradley and Brown (1951, p. 145) state that the demonstration of polymorphism in biotites introduced several structural possibilities of which they had previously been unaware and note that the characterization of illite as a derivative of *2M* muscovite crystallization is based on less rigorous grounds than would be normally desired. In later papers by Grim and his colleagues, and especially in Grim (1953, p. 67), it has been pointed out that "illite" does not refer to a specific structural type of mica. Nevertheless, many persons apparently retain the early concepts as a consequence of the fact that Hendricks and Jefferson (1939) found the *2M* structure to be unique for muscovite. The degree of the dissemination of this concept may be gauged by the fact that many investigators compare material they believe to be illite or hydrous mica (these terms are here used synonomously) with the musocvite spacings reported by Nagelschmidt (1937) and others which have a *2M* structure, or assign indices on the basis of a *2M* structure, unmindful of other structural possibilities. However, the 3-layer muscovite polymorph discovered by Axelrod and Grimaldi (1949) and the lithian muscovite variation reported by Levinson (1953), demonstrate that the muscovite structure is not unique. Thus the structural interrelationship between muscovite and hydrous micas requires reëxamination.

To the writer's knowledge, the brief mention by Yoder and Eugster (1954) of a *1Md* (1-layer monoclinic disordered structure) illite has been the only published attempt to re-evaluate the x-ray data on illite or hydrous mica taking into account the fact that these minerals may

crystallize as some polymorph other than the common *2M* muscovite. The purpose of this paper is to point out that at least three polymorphs exist among micas called illites or hydrous micas (all dioctahedral) and therefore all minerals of this type may not be considered a defect or poorly crystallized *2M* muscovite structure as many investigators have erroneously concluded from the work of Grim et al. (1937).

This work has been aided by generous gifts of illites and hydrous micas from Dr. Robert C. Mackenzie, Macaulay Institute for Soil Research, Aberdeen, Scotland, and a specimen of the hydrous mica from the Yorkshire fireclay received from Dr. A. G. Sadler of the University of Leeds, England, which has been described by Carr, Grimshaw and Roberts (1953). Professor Duncan McConnell, of this department, critically read the mansucript. Dr. H. S. Yoder kindly supplied information on the differentiation of polymorphs in addition to that available in the literature.

Identification of Polymorphs

Grim, Bradley and Brown (1951) in their discussion of mica polymorphism note (p. 145) that in the range from about 4.4 kX to 2.6 kX the most characteristic diffraction lines of the various mica polymorphs may be observed. This corresponds with 2θ for copper radiation of about 20° to 34°. They also present data (p. 166) for distinguishing the polymorphic forms of mica. This information is used as a basis for identification of the structures, although additional aid was obtained from comparison of known *1M*, *2M* and *3T* powder patterns, these structures having been first determined by single-crystal Weissenberg studies. Dr. H. S. Yoder (personal communication) pointed out that a measure of disorder in the *1M* structure may be gauged from the absence or low intensity of the $(11\bar{2})$ and (112) reflections which correspond with (approx.) $d=3.62$ Å and 3.07 Å, respectively.

The 3-layer Trigonal (3*T*) Polymorph

As originally defined by Grim et al. (1937), illite is a general term for the clay-mineral constituents of argillaceous sediments belonging to the mica group. This definition has been modified in such a way that illite has been used as a general name for mica-clay minerals from other environments. Mackenzie, Walker and Hart (1949), for example, have described illite occurring in the decomposed granite at Ballater, Aberdeenshire. This mineral might possibly have been called "sericite" or "phengite" (owing to its high silica) if older terms had been employed. The fact that it is relatively low in potassium and correspondingly high in water justifies the name hydrous mica under any condition.

Specimens of this mica were obtained from Dr. Mackenzie for *x*-ray

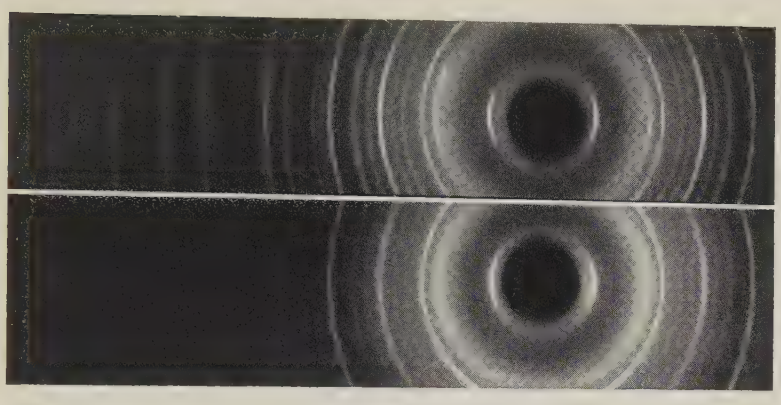

FIG. 1. Powder x-ray photographs of 3-layer trigonal (*3T*) mica polymorphs. Top: Muscovite from Sultan Basin, Washington. Bottom: Illite from Ballater, Aberdeenshire. Filtered copper radiation.

study. Powder photographs of the Ballater mica were compared with photographs of *3T* muscovite* from Sultan Basin, Washington, described by Axelrod and Grimaldi (1949). The patterns are identical (Fig. 1) and it is thus concluded that the illite from Ballater has crystallized with the *3T* structure. (This same polymorph has previously been described as 3-layer rhombohedral or hexagonal by various authors). The d-spacings for the *3T* Ballater illite are given in Table 1 along with new powder data on the *3T* muscovite from Sultan Basin. The data given by Axelrod and Grimaldi (1949) were obtained using unfiltered radiation with the result that several diffraction lines result in part or wholly from β radiation.

The 2-layer Monoclinic (*2M*) Polymorph

Several examples of hydrous micas or illites crystallizing with this structure have been identified. The most interesting one is the hydrous mica from the Yorkshire fireclay described by Carr, Grimshaw and Roberts (1953) because it was possible to obtain single-crystal Weissenberg photographs from several flakes. Figure 2 is believed to be the first single crystal photograph obtained from a hydrous mica. The structure is unmistakably *2M*.

Optical studies of specimens of this mica yield different results from

* The muscovite from Sultan Basin, Washington, described by Axelrod and Grimaldi (1949), has been restudied by the Weissenberg method. The conclusion that this mica is monoclinic on the basis of differences in diffuse scattering has not been confirmed by this writer. The mica is therefore considered to be *3T*, although the 2V of as much as 15° is admittedly anomalous. Smith and Yoder (1954) reached the same conclusion regarding the structure by utilizing the precession method.

TABLE 1. X-RAY POWDER DATA FOR 3-LAYER TRIGONAL POLYMORPHS

A. 3T Muscovite		*B. 3T Illite*	
d(Å)	*I*	*d*(Å)	*I*
9.98	S	9.9	S
4.98	M	4.9	M
4.47	S	4.45	VS
4.29	VW	4.28	W
4.11	VW	4.10	W
3.87	M	3.87	M
3.60	M	3.64	MW
3.34	VS	3.35	VS
3.10	M	3.09	MW d
2.87	M	2.85	M d
2.57	VS	2.56	VS
2.47	M d	2.45	MW
2.38	M	2.39	M
2.24	W	2.235	MW
2.20	W	—	
2.13	M	2.14	M
2.05	VW	—	
2.00	MS	1.988	M
1.96	W	1.940	W
1.72	VW	—	
1.65	M	1.647	M d
1.61	VW	—	
1.52	VW	—	
1.50	M	1.497	S
1.35	M	1.342	MW d
1.30	MW	1.294	M
—		1.266	W
1.25	W	1.243	MW

A. 3T muscovite, Sultan Basin, Wash., described by Axelrod and Grimaldi (1949). Spacings remeasured using filtered copper radiation and 114.59 mm. diameter camera. CuKα=1.5418 Å.

B. 3T illite, Ballater, described by Mackenzie, et al. (1949). Spacings from original paper. FeK$_\alpha$ radiation.

those reported by Carr, et al. (1953). Particularly, the optic angle was reported as small (between 5° and 10°) whereas the optic angles observed by the writer were considerably larger than 10°. In some cases the retardation on flakes in horizontal positions is high and distinct interference figures indicate a 2V of approximately 30° (est.). One index on these flakes was found to be as high as 1.590 whereas 1.578 is reported in the original paper. Thus it seems likely that two phases exist in the hydrous mica from the Yorkshire fireclay although the powder *x*-ray data given by Carr, et al. (1953) suggest the *2M* polymorph.

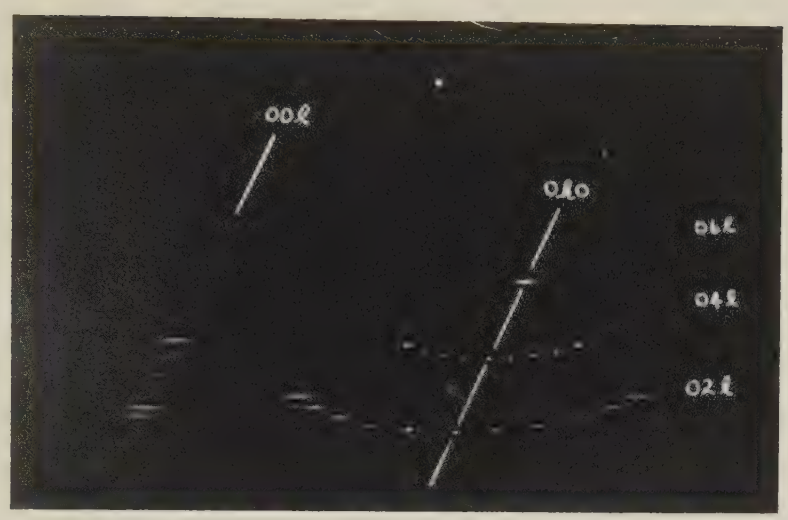

FIG. 2. Zero-level *a*-axis Weissenberg photograph obtained from hydrous mica described by Carr, et al. (1953) showing 2-layer monoclinic (*2M*) polymorph. Unfiltered copper radiation. (020), (021), (022) and (04*l*) reflections were retouched for better reproduction.

Another example of a *2M* structure is furnished by a specimen of illite from Fithian, Illinois, which has been described in the American Petroleum Institute reports as *A.P.I.* specimen number 35. The specimen is a coarse fraction and thus the powder patterns show some quartz lines. Nevertheless the *2M* polymorph can be definitely established. Another specimen from this locality with a *1Md* structure will be described below. Powder diffraction data for the *2M* muscovite polymorph have been reported by several investigators. Those of Nagelschmidt (1937) or Grim, et al. (1937) may be used to identify this structure.

TABLE 2. ANALYSIS OF ILLITE FROM ST. AUSTELL, CORNWALL

SiO_2	53.3
Al_2O_3	26.0
Fe_2O_3	2.5
TiO_2	0.01
MgO	4.4
CaO	0.2
K_2O	8.3
Na_2O	0.3
loss on ign.	5.7
	100.71

Analyzed at the laboratories of English Clays Lovering Pochin and Co. Ltd., St. Austell, Cornwall, England. Mr. I. H. Warren kindly gave permission to publish this analysis.

TABLE 3. X-RAY POWDER DATA FOR 1-LAYER MONOCLINIC POLYMORPHS

1. 1M Lepidolite		*2. 1M Illite*		*3. 1M "Hydromuscovite"*		*4. 1Md Illite*		*5. 1Md Illite*	
d(Å)	*I*	*d*(Å)	*I*	*d*(Å)	*I*	*d*(Å)	*I*	*d*(Å)	*I*
9.98	MS	10.1	S	10.1	S	10.1	S	10.0	VS
4.98	MS	4.98	M	4.98	W	4.98	W	5.0	M
4.53	M	4.50	S	4.48	S	4.48	S	4.46	VS
4.34	VW	4.35	VW	—		—		—	
4.12	VW	4.10	VW	4.09	VW	—		—	
3.86	VW	3.85	VW	3.87	VW	—		—	
3.62	S	3.62	MS	3.65	M	—		—	
3.33	VS	3.32	S	3.34	S	3.33	S	3.32	VS
3.07	S	3.08	MS	3.07	M	3.07	VW	2.97	VW
2.86	M	2.89	MW	2.88	VVW	2.85	VW	2.80	VW
2.68	W	2.67	W	2.67	MW	—		—	
2.58	S	2.57	VS	2.56	S	2.57	VS	2.55	VS
2.48	W	2.47	W	2.46	W	2.46	W d	2.44	W
2.39	MW	2.38	M	2.38	MW	2.38	W d	2.37	WM
2.26	W	2.25	MW	2.25	W	2.25	W d	2.23 2.17	W
—		—		—		—			
2.14	MW	2.14	M	2.13	MW	2.14	W d	2.14	M
1.99	MS	1.99	S	2.00	M d	1.99	W d	1.98	M
1.96	VVW	—		—		—		—	
1.72	VW	1.71	VW	—		—		—	
1.65	M d	1.65	M d	1.64	W d	1.65	W d	1.64	M
1.58	VW	1.58	VVW	—		—		—	
1.51	S	1.50	S	1.50	MS	1.50	S	1.49	VS
1.43	VW	—		—		—		—	
1.38	VW	1.38	VVW	—		—		—	
1.35	VW	—		—		—		—	
1.34	W	1.34	W d	1.34	W	1.34	W d	1.34	W
1.30	M	1.30	M	1.29	W	1.30	MW	1.29	M
1.25	VW	1.25	W	1.25	VW	1.25	W	1.24	W

Data for samples 1 through 4 obtained using filtered copper radiation and 114.59 mm. diameter camera. CuKα=1.5418 Å.

1. *1M* Lepidolite, Brown Derby pegmatite, Colorado.
2. *1M* Illite, St. Austell Clay, Cornwall.
3. *1M* "Hydromuscovite" from decomposed granite, Aberdeenshire.
4. *1Md* Illite, Fithian, Illinois.
5. *1Md* Illite, South Wales, described by Nagelschmidt and Hicks (1943). Spacings from original paper: CoK$_\alpha$ radiation.

THE 1-LAYER MONOCLINIC (*1M*) POLYMORPH

A previously undescribed illite from the St. Austell China Clay deposits, Cornwall, was supplied by Dr. R. C. Mackenzie. Data furnished by Dr. Mackenzie indicate that this material is dioctahedral, that it

gives a *D.T.A.* curve very similar to the Ballater illite discussed above (which has been shown to have a *3T* structure) and that the deposit from which it comes is not of sedimentary origin. An analysis of this illite is presented in Table 2; noteworthy is the high K_2O content.

X-ray study of this Cornwall illite shows that the material is pure and has an essentially well ordered *1M* structure. When compared with *1M* lepidolite the patterns are practically identical except that the illite gives slightly more diffuse lines, as would be expected (Fig. 3). Spacings for this *1M* illite are given in Table 3 and are compared with a *1M* lepidolite as well as other *1M* illites or hydrous micas described below.

Another specimen received from Dr. Mackenzie is the hydromuscovite mentioned by MacEwan (1951, the "*HM*" in Table 4, p. 133). Inasmuch as identification apparently depends on how these terms are defined, illite would also be a suitable name for this material. Dr. Mackenzie notes that it gives a *D.T.A.* peak of the illite type and that it originated from a boulder of decomposed granite in glacial drift in Aberdeenshire. The *x*-ray patterns show a small amount of quartz contamination but this does not interfere with the identification of the polymorph. The structure is *1M* and the pattern compares closely with that of the Cornwall illite described above. The most noticeable difference is the low intensity of the reflection with $d = 2.88$ Å on the former as compared with the medium intensity of this reflection in the latter (Fig. 3).

A specimen of illite from Fithian, Illinois, was purchased from Ward's Natural Science Establishment. Powder *x*-ray photographs were extremely poor and show only a few discernible reflections in addition to several orders of the basal pinacoidal reflections (Fig. 3). In the range of approximately $d = 4.48$ Å to $d = 2.57$ Å, for example, there is little more than a faint haze with the exception of the strong basal reflection at $d = 3.33$ Å. (112) and ($11\bar{2}$) reflections ($d = 3.07$ and 3.62 Å) are either extremely weak or absent. The absence or low intensities of these reflections is the yardstick used by Dr. Yoder (personal communication) for designation of the *1Md* (disordered *1M*) structure, resulting from random stacking of the mica layers. This specimen of illite from Fithian is thus interpreted as a *1Md* structure and is analogous to disordered kaolinite recently described by Robertson, Brindley and Mackenzie (1954). The *1Md* structure has been noted in illite from Illinois by Yoder and Eugster (1954). Another polymorph, the *2M*, from the same general locality has been described above.

A specimen of the illite (fine fraction) described by Nagelschmidt and Hicks (1943) from South Wales has also been obtained for study. *X*-ray studies gave essentially identical results with those reported in the original paper. However, a few weak reflections observed only on aggregate

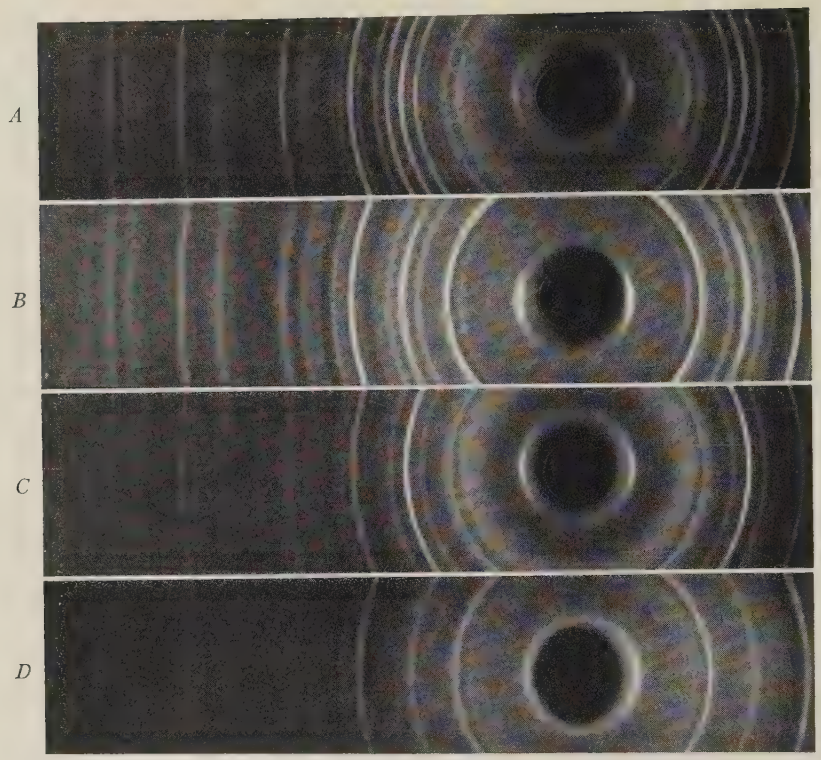

FIG. 3. Powder x-ray photographs of 1-layer monoclinic (*1M*) mica polymorphs. Filtered copper radiation. *A*. *1M* lepidolite, Colorado. *B*. *1M* illite, St. Austell Clay, Cornwall. *C*. *1M* "hydromuscovite," Aberdeenshire. (Small amount of quartz contamination.) *D*. *1Md* (disordered) illite, Fithian, Illinois.

diagrams by Nagelschmidt and Hicks (1943) were observed on the powder diagrams in the present investigations; they consist of the kaolinite reflections at 7.1 and 3.55 Å. The x-ray powder photographs appear very similar to those obtained from the *1Md* illite from Fithian, Illinois. (112) and ($11\bar{2}$) reflections are extremely weak or absent; the structure is therefore considered another example of a *1Md* illite.

DISCUSSION

It has been shown that minerals which have been called illite, hydromuscovite and hydrous mica have crystallized as the 3-layer trigonal (*3T*), 2-layer monoclinic (*2M*), 1-layer monoclinic (*1M*) and 1-layer monoclinic disordered (*1Md*) mica polymorphs. The demonstration of polymorphism in these "clay-micas" makes untenable the commonly held concept that all dioctahedral micas of this type are poorly crystallized *2M* muscovite. Caution must be exercised in indexing powder diffraction patterns because, for example, the 10.0 Å line corresponds with

(001) in *1M* and *1Md* polymorphs, (002) in the *2M* polymorph and (003) in the *3T* polymorph. The reader is referred to Grim, Bradley and Brown (1951, p. 166) for the correct indices of some reflections common to all polymorphs.

The cause of these polymorphic variations is not known. They do not appear to be related to any evident geological, environmental or chemical variations. It is interesting to note that both the *2M* and *1Md* polymorphs have been observed in illites from Fithian, Illinois. The *3T* and *1M* polymorphs have been observed only in non-sedimentary environments, specifically in decomposed granites. The *2M* and *1Md* polymorphs studied were found in micas only from sedimentary environments.

Mackenzie, et al. (1949) have noted that the Ballater illite gives a *D.T.A.* curve different from that of any previously described illite or hydrous mica. It would be logical to suggest, therefore, that some variations among such curves may be caused by differences inherent in the various polymorphic modifications.

References

Axelrod, J. M., and Grimaldi, F. S. (1949), Muscovite with small optic axial angle: *Am. Mineral.*, **34,** 559–572.

Carr, K., Grimshaw, R. W., and Roberts, A. L. (1953), A hydrous mica from Yorkshire fireclay: *Mineral. Mag.*, **30,** 139–144.

Grim, R. E. (1953), Clay Mineralogy: McGraw-Hill, New York.

Grim, R. E., Bray, R. H., and Bradley, W. F. (1937), The mica in argillaceous sediments: *Am. Mineral.*, **22,** 813–829.

Grim, R. E., Bradley, W. F., and Brown, G. (1951), The mica clay minerals; *X*-ray identification and crystal structures of clay minerals: Chapter V, pp. 138–172, *Mineralogical Society of Great Britain.*

Hendricks, S. B., and Jefferson, M. E. (1939), Polymorphism of the micas: *Am. Mineral.*, **24,** 729–771.

Levinson, A. A. (1953), Studies in the mica group; Relationship between polymorphism and composition in the muscovite-lepidolite series: *Am. Mineral.*, **38,** 88–107.

MacEwan, D. M. C. (1951), The montmorillonite minerals (montmorillonoids): *X*-ray identification and crystal structures of clay minerals: Chapter IV, pp. 86–137, *Mineralogical Society of Great Britain.*

Mackenzie, R. C., Walker, G. F., and Hart, R. (1949), Illite occurring in decomposed granite at Ballater, Aberdeenshire: *Mineral. Mag.*, **28,** 704–713.

Nagelschmidt, G. (1937), *X*-ray investigations on clays. Part III. The differentiation of micas by *x*-ray powder photographs: *Zeit. Krist.*, **97,** 514–521.

Nagelschmidt, G., and Hicks, D. (1943), The mica of certain coal-measure shales in South Wales: *Mineral. Mag.*, **26,** 297–303.

Robertson, R. H. S., Brindley, G. W., and Mackenzie, R. C. (1954), Mineralogy of kaolin clays from Pugu, Tanganyika: *Am. Mineral.*, **39,** 118–138.

Smith, J. V., and Yoder, H. S. (1954), Theoretical and *x*-ray study of the mica polymorphs (abstract): *Am. Mineral.*, **39,** 343–344.

Yoder, H. S., and Eugster, H. P. (1954), Syntheses and stability of the muscovites (abstract): *Am. Mineral.*, **39,** 350–351.

Manuscript received Dec. 16, 1953

PHOSPHATE MINERALS OF THE BORBOREMA PEGMATITES: I—PATRIMONIO

JOSEPH MURDOCH, *University of California at Los Angeles, California.*

ABSTRACT

The beryl-tantalite pegmatites of northeastern Brazil carry a considerable number of phosphates, both primary and secondary, which are to be considered in a projected series of papers covering individual localities, individual minerals, or groups of localities. The mineral arrojadite, reported as occurring in most of these pegmatites, is known with certainty only from the original locality, and minerals locally so called constitute a wide range of species. The first report is on the "alto" Patrimonio, where amblygonite and lithiophilite are the primary phosphate minerals. Hydrothermal and other alteration has formed brazilianite (a second Brazilian occurrence for this mineral), crandallite, wardite and apatite, from the amblygonite. Eosphorite, hureaulite, metastrengite, stewartite, ferrisicklerite, heterosite, rockbridgeite(?), and a number of unidentified minerals, have been derived, mainly by oxidizing solutions, from the lithiophilite. Lepidolite with minor microlite, beryl and tantalite, are primary accessory minerals. Brazilianite and wardite occur sometimes in measurable, although small crystals. Details of observations on various unknowns are included, with the hope that some may be identified by the writer or other observers at some future date.

INTRODUCTION

This paper is the first of a projected series of reports on the phosphate minerals of the beryl-tantalite pegmatites of northeastern Brazil. These pegmatites have been described in some detail by several authors: W. D. Johnston, Jr., P. M. A. Rolff, S. C. de Almeida, L. J. De Moraes, D. Guimaraes, H. C. A. De Souza, F. H. Pough and others. Johnston (1945), gives an extensive bibliography on these occurrences. These writers have paid particular attention to the minerals of economic value, (Pough, 1945, has described simpsonite), and the following brief outline of the geologic picture has been taken from their writings. For a more detailed description of general paragenesis and distribution, the reader is referred to the original papers.

The region in general is one of Precambrian gneisses and mica schists, intruded by granites and cut by pegmatites and quartz veins. Pre-cretaceous (?) erosion reduced the area to a peneplane—the Borborema "planalto," later overlain by Cretaceous and younger sandstones. The present erosion cycle has stripped off most of these cover-rocks, and in the Paraíba-Rio Grande do Norte area has cut into the peneplane surface, forming relatively steep-walled valleys, exposing batholithic granite masses as monadnocks, and leaving many pegmatites standing as walls or eminences above the surrounding terrane, because of their greater resistance to erosion. From these projecting masses has come the local name "alto" given to the pegmatite outcrops in general, even when they

do not rise above the surrounding surface. In the northern area, notably in the State of Ceará, the peneplane surface is less dissected, and the pegmatites show no relief, merely appearing as patches or strips of white quartz on the essentially flat surface.

The pegmatites may be classified as "homogeneous" or "heterogeneous," depending on their mineralogy and texture. The former are simple granite pegmatites, of relatively uniform texture and mineral distribution, with quartz, muscovite, and microcline which has been more or less albitized. They are in general rather regular dikes, and are extremely numerous in the area. The latter (heterogeneous) are usually lenticular in horizontal section, and show a high degree of mineralogic differentiation, which produces a more or less well-developed zonal pattern. They are also numerous, but far less so than the homogeneous type. Field evidence does not indicate a different source for the two types, but the accessory minerals in the heterogeneous dikes are more abundant, often in large crystals, and afford an economic source of beryllium, tantalum and sometimes tin.

The beryl-tantalite pegmatites may be grouped roughly into three

Fig. 1

areas: the Picuí-Parelhas, Quixeramobin-Cachoeira and Cascavel-Cristais regions, the first two of which are shown on the accompanying key map (Fig. 1).

According to Johnston, (1945) p. 1040 these pegmatites have been formed by an orderly sequence of crystallization, with little or no evidence of replacement, except for some late stage albitization. This sequence is normally divided into four zones, beginning at the margins with abundant, usually coarse-grained muscovite. Next comes a mixture of normal quartz-feldspar-muscovite with a texture like that of ordinary granite pegmatites. Inside this is a zone characterized by enormous feldspar crystals, up to several meters in dimensions and tons in weight. Most of the beryl, tantalite and spodumene occur here, as do also the primary phosphates, which appear as patches and nodules in the quartz and feldspar. The final, innermost zone is essentially massive quartz, usually milky, but sometimes a curious bluish gray, or a beautiful rose-pink. Many large crystals of beryl appear here also, although large portions of the core may be absolutely barren. Occasional vugs in this quartz are lined with quartz crystals, which may be accompanied by apatite.

Beryl and tantalite have apparently been essentially unaffected by later solutions or by weathering processes, but spodumene may show extensive kaolinization, and in some cases is completely altered. The associated phosphates, however, have been affected by extensive alteration, both hydrothermal and superficial, with the resulting development of a considerable number of later minerals, many of which occur intimately intergrown with each other, in fine-grained aggregates. Many of the pegmatites are lithium-bearing, with lepidolite or spodumene, or both, appearing in considerable amount. Here the primary phosphates are lithiophilite, amblygonite, or graftonite, any one of which may be the source of a series of alteration products. In the absence of lithium, phosphates such as triplite do not appear to have produced such a variety of secondary minerals.

The author was privileged, when on sabbatical leave from the University of California at Los Angeles in 1948, to visit approximately twenty of these pegmatites, and to collect specimens, mainly of the phosphate minerals, for laboratory study. I wish here to express my thanks to the following: the University of California, for a research grant which made the trip possible; the Divisão de Fomento da Producão Mineral, and its Director Dr. A. I. Erichsen, for facilitating arrangements for transportation and guidance in the field; Dr. Onofre Chavez, engineer of the D.N.P.M. at Campina Grande, who was assigned to me as guide and mentor, since without him I should not have been able to accomplish my task; Dr. W. D. Johnston, Jr. for invaluable aid in infor-

mation and introductions; and finally, Señor Silveira Danton, of Silveira Brasil & Cia, who presented me with a magnificent large crystal of tantalite for the University Museum.

Patrimonio

The "alto" Patrimonio is a few hundred yards south of the little town of Pedra Lavrada, in the State of Paraíba (see index map, Fig. 2). It forms a gentle eminence on the landscape, rather than a wall-like outcrop, since it is lenticular rather than tabular in form. It is one of the smaller heterogeneous pegmatites which have been mined, and is not described in detail in the literature. It was originally (1914–1918) opened for mica, which was a rather poor quality of ruby muscovite, and reported production was only a few kilograms. A production of 45 tons of beryl and 2.9 tons of tantalite was reported for 1940-1942, and in 1943 the records show about 200 kilograms of bismutite and native bismuth, with small amounts of mangano-tantalite, tantalite and betafite (?). Lazulite and "arrojadite," some uranium ochres, aquamarine beryl, and smoky and bluish quartz, were also noted from this dike.

The general pattern of mineral distribution apparently follows roughly Johnston's zoning, with a quartz-rich central core. Little detail of this pattern was observable at the time of the writer's visit, especially since the pegmatite had not been worked actively for some years, and the outcrops were obscured by vegetation and by rubble of the dumps. The

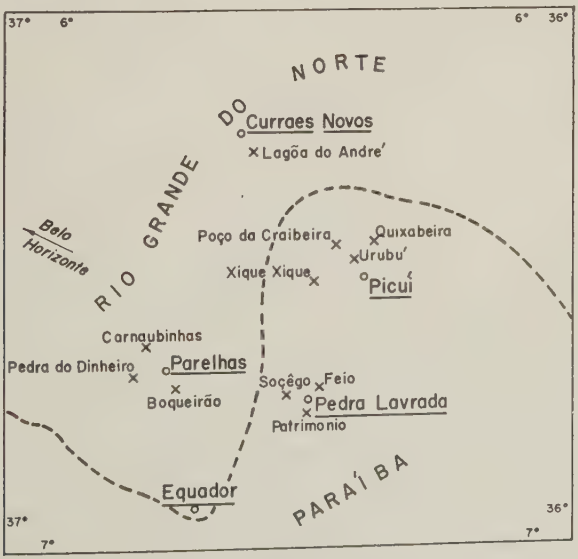

Fig. 2

principal primary minerals are quartz and microcline, with lesser muscovite and albite (cleavelandite). The minor minerals include beryl, tantalite, lepidolite, amblygonite and lithiophilite. These last two are the source of a considerable number of alteration productions which will be discussed in some detail. The ordinary early minerals were not collected, but their appearance was normal, and they do not need further consideration here.

The beryl and tantalite had been quite thorougly mined out before my visit, so their characteristic occurrence could not be checked by observation. Specimens of lepidolite, amblygonite, lithiophilite and others, were collected only from fragments on the dumps, so that their exact relationship to the zonal distribution of the dike could not be directly determined. However, judging by their relationship to quartz and feldspar in the dump fragments, there seems to be no reason to assume other than the usual space-relationships. Accordingly, it may be assumed that here the principal phosphates were deposited only moderately late in the sequence of dike crystallization, and occurred along with beryl and tantalite in irregular masses in the quartz and feldspar of Johnston's third zone. In the following sections the various minerals of the deposit will be considered individually. Arrojadite was not observed in the Patrimonio deposit, but should be discussed here because of its supposed widespread occurrence. One of the early phosphates has been named arrojadite, and was described from the "alto" Serra Branca, by Guimmaraes (1942). It has been reported by casual observers from many of the pegmatites of this region, and Rolff (1946A) p. 31 says that it is frequently altered to a varied assortment of minerals ranging in color through yellow, blue, olive green, etc., to black, the most common product being vivianite, followed by purpurite. The present writer has found, however, that true arrojadite is rare or absent from any but the original locality, that vivianite is almost never formed, and that purpurite is relatively uncommon. Nevertheless, the varicolored series noted by Rolff is frequently present in the lithia-bearing pegmatites, and forms an interesting group. The alteration sequence ranges from huréaulite, through sicklerite (or ferri-sicklerite) to purpurite (or heterosite), with several other varieties, to purple or blue meta-strengite (phosphosiderite), and black manganese oxides. Most of the alterations appear to be due to descending oxidizing solutions. Descriptions of the individual minerals, with discussion of their relationships, are given in the following sections.

Lepidolite and Microlite

Pale lilac lepidolite occurs in massive aggregates of small (2–3 mm.) platy grains intergrown with clear quartz, some cleavelandite and an

occasional grain or poorly developed crystal of colorless to faintly yellowish microlite. This microlite was identified by its isotropic character, high index of refraction, and spectroscopic determination of major calcium and tantalum with small sodium, and very small niobium, aluminum, etc. The *x*-ray powder pattern checks closely with that of type material from Topsham, Maine, in the Harvard collection, as shown in the accompanying Table 1.

Table 1. X-ray Data for Powder Photographs of Microlite
Cu radiation Ni filter, spacings in Ångstrom units, $\lambda = 1.5418$

Patrimonio		*Topsham*		*Patrimonio*		*Topsham*	
d/n	*I*	*d/n*	*I*	*d/n*	*I*	*d/n*	*I*
6.64	½			1.204	½	1.20	½
6.01	8	5.78	2	1.195	3	1.194	5
?3.48	½			1.16	3	1.163	4
3.33	½			1.145	1	1.141	1
3.14	5	3.10	2	1.093	½	1.092	½
3.01	10	2.97	10	1.065	1	1.063	3
2.61	5	2.58	3	1.051	½	1.047	1
		?2.43	½	1.012	½	1.008	½
2.39	2	2.37	1	1.004	2	1.0025	3
2.00	3	2.00	2	.9749	½	.9717	1
1.84	7	1.835	10	.9440	½	.9407	1
1.76	3	1.755	2	.9250	½	.9216	2
1.59	½	1.61	1	.9140	½	.9113	3
1.57	7	1.567	10	.8879	½	.8850	½
1.50	2	1.50	2	.8822	3	.8810	4
1.46	2	1.456	2	.8695	½	.8694	3
1.356	2	1.352	3				
1.295	½	1.302	2				
1.265	½	1.270	½				

Amblygonite

Massive cleavable amblygonite was found in irregular fragments on the dump. In the specimens collected it is milky white in color and carries clear-cut veins and irregularly bounded patches of later minerals which appear to be hydrothermal in origin. Some of these minerals are in good or poor crystals, some in fibrous aggregates, and some in powdery form as very fine-grained patches. In this group appear apatite, brazilianite, wardite, crandallite, carbonatian apatite and some species so far unidentified. Some specimens show fracture-coating of dehrnite (?) along with carbonatian apatite. A few well-formed crystals of manganotantalite, with a little massive orangeite (?) were found on one amblygonite specimen. Clusters and nests of muscovite occur here and there in

the massive amblygonite. Analysis of the amblygonite (Table 2) shows it to be fairly high in fluorine, and low in hydroxyl. A second generation of amblygonite, very fine grained and associated with eosphorite, was noted in veinlets cutting across lithiophilite.

TABLE 2

	Amblygonite (1)	*Lithiophilite* (2)
Al_2O_3	31.50	—
Fe_2O_3	1.78	0.60
FeO	—	19.53
MnO	—	24.30
MgO	—	0.18
Na_2O	0.44	0.18
K_2O	—	0.07
Li_2O	10.47	8.99
P_2O_5	46.56	44.74
F	11.24	—
H_2O^+	0.02	—
H_2O^-	0.11	—
	102.12	98.59
$-F=O$	4.75	
	97.47	

(1) E. L. MARTIN, *analyst.*
(2) L. C. PECK, *analyst.*

BRAZILIANITE

Narrow (5-10 mm.) veins in massive amblygonite show numerous small glassy grains, and occasional poor to fairly good crystals of a colorless mineral which goniometric measurements and *x*-ray powder photographs prove to be brazilianite. This is the fourth known occurrence for this mineral, and the second for Brazil. The other localities are: the original find in the Conselheira Pena district, Minas Geraes; the Palermo pegmatite near North Groton, N. H.; and the Smith mine near Newport, N. H. The Patrimonio crystals are relatively simple, somewhat elongated on [001], and measured crystals show the following forms: {110} usually well-developed and always present; {101} usually present and prominent; {010} always present though invariably narrow; {320}, {130}, {670?}, {111}, {121}, {301?}, {311}, {321}, {112}, sometimes present but never prominent. Some of the crystals are to be found in a fine granular matrix of crandallite, along with lavender apatite crystals. As observed in thin section, fine-grained brazilianite was deposited along the walls of a fissure in the amblygonite, and followed by deposition of larger grains and

terminated crystals embedded in, or projecting from the walls into the fine-grained crandallite, which filled the remaining space. In one instance, brazilianite is somewhat coarser textured, appearing as sub-parallel or radiating prismatic groups, none of which show crystal faces. Here it is associated with glassy wardite, a yellowish green isotropic mineral which may be orangeite and an unidentified pink phosphate.

Wardite

Glassy, granular wardite, sometimes in imperfect crystals, occurs associated with brazilianite in several of the veins and patches of later minerals in the amblygonite. One or two crystals were measurable, and showed {001}, {012}, and {011}. It is somewhat difficult to distinguish from brazilianite by inspection, but is usually in larger grains, and often shows its perfect basal cleavage. *X*-ray powder photographs confirm its identity, and cleavage flakes show anomalously biaxial segments as reported in crystals from Montebras. Dana (1951) p. 940.

Crandallite

This mineral occurs only as fine powdery aggregates filling in the space between lavender apatite, brazilianite and wardite, in veins in amblygonite. It was identified by micro-chemical tests, confirmed by *x*-ray powder pattern. Associated with it are at least two other minerals in fine prismatic or fibrous form. This matrix is so fine grained and intergrown that the optical properties are confused, but they may be members of the apatite group, since carbonatian apatite has been found in some of the specimens.

Apatite

Apatite occurs in various fashions in the deposit. In massive amblygonite, there are large patches of imperfect crystals of dark green manganapatite, essentially contemporaneous with its host. In the veins or replacement patches in the ambygonite, carbonatian apatite appears as pale lavender or bluish prisms up to 2–3 mm. across, heavily striated vertically, and usually with a colorless center. A basal section shows biaxial segments in the lavender portion, with a sensibly uniaxial core. These crystals are somewhat later than most of the brazilianite, and occur principally in regions which were originally cavities, but which have since been filled in with powdery crandallite. An area of massive greenish material adjoining the crandallite filling is shown in thin section to be a feathery aggregate of carbonatian apatite prisms intergrown with numerous prismatic grains of an unidentified mineral.

Hydroxyl-manganapatite also occurs as fine-textured veins cutting

massive altered lithiophilite, ferri-sicklerite, etc. Here the mineral is very fine grained, waxy in luster and pale orange on the borders of the veins, white and sugary in the midportion.

Carbonatian apatite occurs as a drusy to botryoidal crust coating lithiophilite and its alteration products, and also as a fine-grained, almost waxy coating, also on lithiophilite, and partly altered to a very soft unknown mineral.

A late stage of apatite appears as minute, water-clear grains and crystals in narrow veins cutting across spongy aggregates of late alteration products or lining the surfaces of cavities in such minerals as metastrengite, pyrolusite (?), etc. Here it seems to be almost the last mineral to be deposited.

Lithiophilite

Lithiophilite occurs in fair-sized masses of irregular shape, essentially contemporaneous with the primary quartz and feldspar of the pegmatite. When perfectly fresh it is practically colorless, but it is often brownish due to partial oxidation, or greenish yellow from abundant inclusions of later minerals. Chemical analysis of selected pure mineral shows a moderate excess of MnO over FeO, so that it is lithiophilite rather than triphilite. The analysis is given in Table 2.

Huréaulite

Huréaulite occurs in crystalline crusts, occasionally with measurable crystals showing {100}, {110}, {201}, {111}, and {311}. These crusts are cavity or fracture fillings in lithiophilite. In color the mineral varies from salmon pink to colorless. Chemical tests show only a very small amount of FeO, which apparently varies with the depth of color of individual samples. Huréaulite is one of the fairly early oxidation products of lithiophilite, and is apparently confined to this mineral, not being observed in ferri-sicklerite. Huréaulite is essentially contemporaneous with a yellowish-green mineral (mineral *A*, which colors much of the lithiophilite), underlying it in part and covering it in part.

Ferri-sicklerite and Heterosite

Ferri-sicklerite where present forms an alteration zone around fresh cores of lithiophilite, and as is usually the case, is in crystallographic continuity with it, so that cleavage surfaces on one mineral are continued uninterruptedly on the other. Locally, further oxidation has formed purple patches of heterosite, still with the same orientation crystallographically. The last stage of oxidation is the formation of porous or powdery black manganese oxides of indeterminate character, which sometimes carry small amounts of phosphorus. Little or no iron is left in these

oxides, but the element does occasionally appear in the form of cellular or powdery limonite. Frequently other secondary phosphates are formed directly or indirectly by the oxidation and hydration of the lithiophilite, usually later than huréaulite or mineral *A*, and earlier than the oxide coatings.

Meta-strengite

This is one of the late-formed minerals, and occurs as fine botryoidal crusts, or porous, sometimes crumbly, masses of minute crystals. Less commonly it appears as fine-grained compact patches in ferri-sicklerite, and in one or two cases as pseudomorphs after imperfect, nearly square prisms of an earlier unknown mineral, possibly lithiophilite. In color meta-strengite is quite variable, ranging from a rather bright light blue, which is commonest, to blue-violet, purple, or even pink. In some cases it appears to have faded to almost colorless. Chemical tests show a small amount of manganese, but not enough material is available from this locality to make a quantitative determination. The *x*-ray powder pattern matches exactly that of analyzed material from another locality. In general it is earlier than the manganese oxides, but sometimes it seems to be later, forming crusts or cavity linings superimposed on the latter.

Stewartite

Occasional acicular or bladed crystals or irregular grains, of canary yellow stewartite occur in the meta-strengite, and are in general somewhat later than the latter.

Variscite

Pale pink to colorless variscite was observed as a finely drusy coating on one of the fracture surfaces of a highly oxidized specimen. In part this mineral coats even the manganese oxides. Identification was made on the basis of optical and chemical properties, and confirmed by *x*-ray powder pattern.

Eosphorite

One specimen of massive lithiophilite shows a vein of massive flesh-colored or colorless coarsely crystalline material with one good cleavage, associated with fine sugary white amblygonite. Occasional crystal faces show striations on the somewhat elongated grains. This mineral has a hardness of about 4—5, and is optically biaxial negative, with 2 V near 10°; moderate dispersion $v > r$; index of refraction close to 1.64 for β. The mineral is insoluble in HCl, but on moderate heating turns dark brown and becomes soluble. Chemical tests show P, Fe small, Mn moderate, Al large, no Ca. The *x*-ray powder pattern matches very closely that of

the childrenite-eosphorite group. The index of refraction and low iron content indicate eosphorite, which seems probable in spite of lack of solubility, and the very small value for 2 V.

Unidentified Minerals

A considerable number of minerals in the secondary groups occur in such small quantity or in such intimate intergrowth with others, and in such small particles, that optical determinations are difficult, and only qualitative chemical tests are possible. In none of these cases has identification been possible, but all available information will be given in their descriptions, in the hope that some other worker may encounter better material, and be able to complete an identification It has been possible to get x-ray powder patterns for most of these, but none has been found to match anything in the *A.S.T.M.* or Harvard files. In many cases, too, optical determinations have been only approximate. The unknowns will be designated by letters.

Mineral A = Tavorite*

This mineral occurs as a minor alteration product of lithiophilite, along cleavages, fractures, and in solution cavities. It is quite soft, yellowish green in color, and usually in microscopic spherules. Rarely it forms separate crystals, or crystal aggregates, but in no case in individuals large enough to make any determination of the symmetry. Optically, it is biaxial positive, with 2 V about 70°–80°. Pleochroism is moderate, pale yellow to colorless. Dispersion strong, with $r > v$. The index of refraction is variable, from 1.77 to 1.81, and extinction is oblique to elongation of the grains. Chemically, it is easily soluble in acid, giving micro-tests for Fe and P; Ca and Mn are absent; no water given off in the closed tube, but the mineral quickly turns bright red-brown at moderate heat. The x-ray powder pattern shows the following spacing and intensities for the strongest lines: 4.96 Å—3; 4.68—5; 3.93—3; 3.41—3; 3.29—10; 3.03—7. The complete pattern rather closely matches that of amblygonite.

Mineral B

This mineral appears as dark brown, nearly square prismatic crystals, crudely developed, and showing two perfect cleavages at approximately 90°, parallel to the prism direction. Hardness 3–4; streak pale yellow-brown; optically biaxial positive, with 2 V very small; beta is close to 1.75; pleochroism slight, pale to darker brown; extinction parallel to

* This mineral is apparently identical with the mineral tavorite, identified and described by Lindberg and Pecora (1954) after the submission of this manuscript to the editor.

prism edges. It is readily soluble in acid, and gives tests for Fe, Mn and P. Gives off water readily in a closed tube. Its age relationship to lithiophilite could not be determined, as the two do not occur in contact. Where found, it was in some cases replaced by compact meta-strengite, which forms imperfect pseudomorphs. *X*-ray powder photographs show spacings which do not match any recorded pattern. Spacings and intensities of the stronger lines are as follows: 8.6 Å—3; 6.6—3; 4.76—3; 4.36—4; 4.11—3; 3.52—4; 3.38—3; 2.83—10; 2.43—3; 2.37—3; 1.52—3.

Mineral C

In the crumbly crystalline coating of late alteration products, one of the minerals is canary yellow in color, occurring as minute square flat crystals, tetragonal in aspect, showing a flat pyramid and base. Optically it appears to be uniaxial negative, with omega about 1.78. Some sections which are square in cross section, and also some which are diamond shaped, show abnormal blue interference colors with crossed nicols. The mineral is soluble in acid, giving tests for ferric iron and phosphorus, but not for calcium or manganese. It may be hydrous, but not enough pure material could be isolated to check this. Spacings and intensities of the stronger *x*-ray powder spacings are as follows: 4.48 Å—10; 3.20—3; 3.10—3.

Mineral D

Another finely-crystalline mineral occurring in similar powdery crusts, is dark red-brown, in extremely small platy or tabular crystals, with index well above 1.83. It appears to be biaxial negative, with 2 V very small. Extinction is symmetrical, and pleochroism is strong, pale yellow to dark red-brown. The obtuse bisectrix is not far from normal to the plates. It is soluble in acid, and gives tests for ferric iron, Mn, P, and probably H_2O, though this is not sure, because of possible admixture of impurities. The *x*-ray powder pattern is practically identical with those of two other minerals from this locality (Minerals *E* and *F*), although their optical and physical properties are different. Prominent lines with spacing and intensity for all three are as follows: 8.65 Å—10; 5.60—5; 2.74—6.

Mineral E

This mineral is compact, fine grained, olive green in color with yellow streak. Index near 1.75. Soluble in acid, and gave tests for ferric iron, ferrous iron, a little Mn, some Ca, and little or no water. A variant of this has a somewhat higher index, and no Ca. The mineral in general in the hand specimen resembles alluaudite from Varuträsk, Sweden, but the *x*-ray powder patterns do not match.

Mineral F

Mineral F is yellow-brown in color, apparently pseudomorphous after some earlier mineral, as it shows large cleavage surfaces, but is actually fine grained. Optically it is biaxial negative, with index much above 1.76, and with no pleochroism. It is soluble in acid, and gave tests for ferric iron, Ca and Mn. Physically it somewhat resembles xanthoxenite, but the x-ray powder patterns do not match.

Mineral G

This mineral occurs as radiating clusters of blades intergrown with a mass of other secondary minerals. It is deep red-brown in color, with one perfect cleavage. Optically it is biaxial negative, with 2 V about 5°, and β well over 1.76. The obtuse bisectrix is nearly normal to the platy surface. Pleochroism is strong, from nearly colorless to dark brown. The mineral is readily soluble in acid and gave tests showing much Mn, little Fe, and some water in the closed tube. An identical mineral is found in two other pegmatites of the region, Boqueirão and Taboa. Spacings and intensities of the stronger lines of the x-ray powder pattern are as follows: 8.6 Å—10; 2.90—4; 2.75—4.

Mineral H

A deep green colored mineral occurring in patches in lithiophilite, and as compact fine-grained masses, is close to rockbridgeite, and may be this species.

Various other minerals of unknown character also occur here in minor amounts, mostly in the porous, friable crusts, and include some manganese oxides; patches of reddish material suggesting salmonsite (index near 1.68, biaxial negative? 2 V small); minute black crystals, green by transmitted light, which have index about 1.76, biaxial (?) negative (?) with large 2 V, and giving tests for Fe, Mn, and P; also a powdery yellow-brown fibrous mineral, possibly an oxidized vivianite.

References

Johnston, W. D., Jr. (1945), Beryl-tantalite pegmatites of northeastern Brazil: *Geol. Soc. Am. Bull.*, **56**, 1015–1070.

Pough, F. H. (1945), Simpsonite and the northern Brazilian pegmatite region: *Geol. Soc. Am. Bull.*, **56**, 505–514.

Rolff, P. A. M. de A, (1946*A*), Minerais dos Pegmatitos da Borborema: *Departmento Nacional da Producão Mineral, Bol.* **78**, 24–76.

Rolff, P. A. M. de A, (1946*B*), Reservas Minerais do município de Picuí: *Departmento Nacional da Producão Mineral, Bol.* **80**, 1–54.

de Almeida, S. C., Johnston, W. D., Jr., Leonardos, O. H., Scorza, E. P. (1944), The beryl-tantalite pegmatites of Paraíba and Rio Grande do Norte, northeastern Brazil: *Ec. Geol.*, **39**, 206–223.

Guimaraes, Djalma (1942), Arrojadita, um Novo mineral do grupo da wagnerita, Mineralogia No. 5, p. 3–16: *Bol. da Facultade de Filosofia, Ciencias e Letras de Universitade de São Paulo.*

Palache, C., Berman, Harry, and Frondel, Clifford. The System of Mineralogy, 7th Ed. (1951), vol. 2, 1124 pp.

Lindberg, M. L., and Pecora, W. T. (1954), Tavorite and barbosalite: two new phosphate minerals from Minas Geraes, Brazil: *Science*, **119**, 739.

Manuscript received Dec. 22, 1953.

ORDOÑEZITE, ZINC ANTIMONATE, A NEW MINERAL FROM GUANAJUATO, MEXICO[1]

GEORGE SWITZER AND W. F. FOSHAG, *U. S. National Museum, Washington, D. C.*

ABSTRACT

Tin ores from the Santín mine, Guanajuato, Mexico, contain a new mineral having the chemical composition $Zn\ Sb_2O_6$. Chemical analysis gave ZnO 20.07, Sb_2O_5 80.49 SiO_2 and Al_2O_3 n.f.; sum 100.56 per cent. It occurs in small pale to dark brown tetragonal crystals showing the forms {001}, {011} and {110}, and usually twinned on {013}. Unit cell dimensions are $a=4.67$, $c=9.24$ Å, space group $P4/mnm$. The structure is the trirutile type, and the mineral is isostructural with tapiolite ($FeTa_2O_6$), bystromite ($MgSb_2O_6$), and many other artificial antimonates and tantalates. Its physical and optical properties are as follows: cleavage none, fracture conchoidal, hardness $6\frac{1}{2}$, specific gravity 6.635 (calculated 6.657), luster adamantine, uniaxial (+), $n>1.95$. Ordoñezite occurs in small veinlets in rhyolitic rocks associated with cassiterite, cristobalite, tridymite, hematite, sanidine, topaz, and fluorite.

INTRODUCTION

In 1941 a collection of cassiterite was acquired by the U. S. National Museum from the Santín mine, Cerro de las Fajas, Santa Caterina, Guanajuato, Mexico. Several specimens were analyzed spectrographically to determine the cause of a wide color range. Two had zinc and antimony as major constituents. Further investigation revealed that this material was a new mineral having the composition $ZnSb_2O_6$. It has been named ordoñezite (or-dohn′-yez-ite), in honor of the late Ezequiel Ordoñez, formerly head of the Instituto de Geologia de Mexico, and one of Mexico's greatest geologists.

The writers wish to thank the Lucius Pitkin Company, New York City, for making the first spectrographic analyses, K. J. Murata of the U. S. Geological Survey for additional spectrographic analyses, and J. J. Fahey, also of the Survey for a specific gravity determination.

CHEMISTRY

A spectrographic analysis of ordoñezite is given in Table 1.

The results of a chemical analysis of the same sample are given in Table 2.

Ordoñezite is insoluble in acids and was put into solution by sintering with sodium peroxide in a platinum crucible at 480° C. The antimony was precipitated as the sulfide in sulfuric acid solution, the sulfide redissolved, and titrated with 0.1 N potassium permanganate. Zinc was precipitated as the sulfide in 0.01 N sulfuric acid and ignited at 900° C. to

[1] Publication authorized by the Secretary, Smithsonian Institution, Washington, D. C.

TABLE 1. SPECTROGRAPHIC ANALYSIS OF ORDOÑEZITE FROM THE SANTÍN MINE, GUANAJUATO, MEXICO (USNM R9127; K. J. MURATA, ANALYST)

Per Cent	Element
>1	Zn, Sb
0.X	Al, Si
0.0X	Mg, Sn, Fe, Na, Cu
0.00X	Ca, Mn, Ti, Li, In

Not found: As, Pb, Cd, Co, Ni, U, Cr, Bi, Ge, Mo, W, Tl, Ag, Ga, Ba, Sr, Be, B, Zr, P, Nb, Y, La.

TABLE 2. CHEMICAL ANALYSIS OF ORDOÑEZITE FROM THE SANTÍN MINE, GUANAJUATO, MEXICO

	1	2		3
ZnO	20.07	0.247	1	20.10
Sb_2O_5	80.49	0.249	1.01	79.90
SiO_2	n.f.			
Al_2O_3	n.f.			
	100.56			100.00

1. Ordoñezite. USNM R9127. G. Switzer, analyst.
2. Molecular ratios.
3. Theoretical composition of $ZnSb_2O_6$.

convert it to the oxide. Silicon and aluminum were sought for but not found.

X-RAY DATA

Ordoñezite gives an *x*-ray powder pattern identical with that of artificial $ZnSb_2O_6$, and is isostructural with bystromite ($MgSb_2O_6$) and tapiolite ($FeTa_2O_6$). The *d* spacings of these compounds are compared in Table 3.

The crystal structure of $ZnSb_2O_6$ has been determined by Byström, Hök and Mason (1942). It has a trirutile-type structure, with space group $P4/mnm$, and unit cell dimensions $a=4.66$ *k*X, $c=9.24$ *k*X.

Rotation and zero layer photographs of an ordoñezite crystal gave $a=4.67$ Å, $c=9.24$ Å (both values ± 0.01 Å). From this the axial ratio is $c=1.979$.

The unit cell contains $Zn_2Sb_4O_{12}$. The calculated density is 6.657 (measured 6.635).

TABLE 3. COMPARISON OF X-RAY *d* SPACINGS OF ORDOÑEZITE, ARTIFICIAL $ZnSb_2O_6$, BYSTROMITE AND TAPIOLITE

Ordoñezite[1]		$ZnSb_2O_6$[2]		Bystromite[3]		Tapiolite[4]		*hkl*[5]
I	*d*	*I*	*d*	*I*	*d*	*I*	*d*	
10	4.58			40	4.63	10	4.60	100
20	4.11			70	4.19	10	4.21	101
90	3.26	v. st.	3.30	100	3.32	90	3.34	110
10	2.65	w.	2.69	30	2.69	10	2.71	112
80	2.55	st.	2.58	90	2.57	80	2.58	103
40	2.31	m.	2.33	50	2.34	50	2.37	200
20	2.23	w.	2.24	20	2.25	20	2.26	113
20	2.07	w.	2.08					210, 202
20	2.02	w.	2.03	30	2.04	10	2.06	211
10	1.90	m.	1.89					114
100	1.72	v. st.	1.72	90	1.73	100	1.74	213
		v. w.	1.71					105
50	1.64	st.	1.64	40	1.65	70	1.68	220
		v. w.	1.63					204
		v. w.	1.55					222
30	1.54	st.	1.54	20	1.54	30	1.53	006
50	1.47	st.	1.52	40	1.48	60	1.50	310
40	1.39	st.	1.39					116
60	1.38	st.	1.38			50	1.39	303, 205
30	1.28	m.	1.28	10	1.28	30	1.29	206
10	1.24	—	1.24					314
60	1.19	st.	1.19	30	1.19	50	1.21	323

[1] Ordoñezite, Santín mine, Guanajuato, Mexico; USNM R9127; camera radius 114.59 mm; $\lambda Cu = 1.5418$ Å.

[2] Artificial $ZnSb_2O_6$. Data from Byström, Hök and Mason (1942), *d* converted from *k*X to Å.

[3] Bystromite, Sonora, Mexico. Data from Mason and Vitaliano (1952), *d* in Å.

[4] Tapiolite, Chanteloube, France. USNM 86267, camera radius 114.59 mm., $\lambda Cu = 1.5418$ Å.

[5] Values of *hkl* from Byström, Hök and Mason (1942).

MORPHOLOGY

Ordoñezite occurs as drusy or stalactitic masses of repeatedly twinned tetragonal crystals having a maximum size of 2 mm. Two twin crystals of excellent quality were measured. One with (100) as pole gave for two faces of {011}, $H = 26° 51'$ and $26° 46'$ respectively, corresponding to rho values of $63° 09'$ and $63° 14'$. From these, $c = 1.9797$, in excellent agreement with $c = 1.979$ obtained from *x*-ray measurements. The second crystal was mounted to rotate about the intersection of (100) and the twin plane. Measurements made with the crystal in this position were

plotted on a stereographic net and rotated about [100] to place [001] vertical. This identified the twin plane as (013), the same as that reported for tapiolite. Only {110} and {011} were observed on the twin crystals.

A few very small single crystals of ordoñezite were found, one of which was used to determine unit cell dimensions by the Weissenberg method. Only faces of {110} and {011} gave measurable signals. {001} is present but etched.

The appearance of typical ordoñezite crystals is shown in Fig. 1.

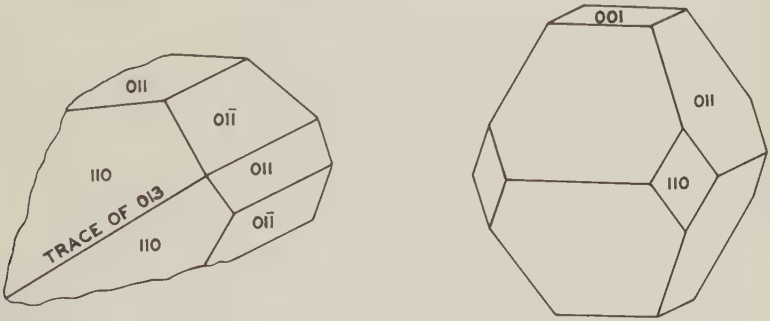

FIG. 1. Twin and single crystals of ordoñezite from the Santín mine, Guanajuato, Mexico.

PHYSICAL AND OPTICAL PROPERTIES

Ordoñezite has the following physical properties: cleavage none, fracture conchoidal, hardness $6\frac{1}{2}$, specific gravity 6.635 (4° C.), luster adamantine, color very light to very dark brown, variable from colorless to pearl gray, olive buff to dark olive, light yellowish olive, bone brown (Ridgeway), transparent.

The optical properties of ordoñezite are: uniaxial (+); indices of refraction much higher than the highest liquid available (1.95), and probably considerably higher than 2.0.

OCCURRENCE

Rhyolitic rocks with veinlets or fractures carrying cassiterite and associated minerals are found in many parts of Mexico. In almost every rhyolitic area in the country, from Sonora and Chihuahua on the north to Chiapas on the south, some cassiterite can be found. A small tin mining industry is based upon these cassiterite occurrences, operated by *gambusinos* or pocket-hunters. One of the characteristic features of these occurrences is the association of the high temperature forms of silica, cristobalite and tridymite, with the cassiterite. Quartz, chalcedony, or

opal may also be present, but their association with the cassiterite is less intimate. Hematite is a very common associate of the tin mineral; magnetite is rarer. Also present in the ores are sanidine, topaz, fluorite, and rarely zeolites.

Genth (1887) reported the analyses of some of these Mexican cassiterite ores in which were found appreciable to large amounts of lead, zinc, bismuth, antimony, and arsenic. Ingalls (1895) quotes two analyses of pig tin from Mexican ores which show appreciable quantities of lead and bismuth, and large quantities of antimony. These impurities in the tin ores and the smelted metal suggest the presence of unrecognized accessory minerals. Arsenic and lead may be ascribed to mimetite (Diablo mine, Durango; Cabires mine, Michoacan, Zimapan, Hidalgo); antimony and zinc minerals have not been reported previously.

The Santín mine is one of these small tin occurrences in rhyolitic rocks. It can be reached most easily from San Luis de la Paz to Victoria to Santa Catarina (42 miles) by car, and Santa Catarina to Rancho Ruscia ($4\frac{3}{4}$ miles) by trail. Rancho Ruscia lies at the western foot of Cerro de las Fajas, a high hill of bedded lava flows, whose banded appearance gives the hill its name. The Santín mine lies on the lower south slope of the Cerro de las Fajas, only a short distance from the ranchhouse. The mine has been described briefly by Foshag and Fries (1942).

The rock of the Santín mine is broken by a system of small fractures that appear to be confined, principally, to a narrow east-west zone. These fractures carry a little clay and the ore mineral cassiterite. According to Sr. Martin Sutti, owner of the mine, pockets of ore occur along these fractures but the individual pockets seldom yielded more than 75–100 kilograms of cassiterite. Much of the ore from the Santín mine consisted of beautiful branching groups of seal brown cassiterite crystals. According to Sutti, the cassiterite in the upper portions of this small mine was botryoidal, becoming more crystallized with depth.

Ordoñezite occurs sparingly with the cassiterite. An analysis of a 15 ton lot shipped from the mine showed 2.16 per cent of Sb_2O_3, indicating an ordoñezite content of about three per cent. Associated minerals, in addition to the cassiterite, are hematite, quartz, cristobalite, hyalite, and montmorillonite. Cassiterite and hematite were the earliest minerals to form, followed by ordoñezite. The ordoñezite may rest directly upon the rock, or upon an earlier crust of red cassiterite, or cassiterite and hematite. Small prismatic crystals of quartz perch directly upon cassiterite or ordoñezite, and are distinctly later. Cristobalite, as small white drusy balls, was found on a few groups of cassiterite crystals, but not in direct association with ordoñezite. Hyalite is rare upon quartz. The sequence of mineral deposition in these fractures was (1) cassiterite and hematite,

(2) ordoñezite, (3) cristobalite, (4) quartz, (5) hyalite and (6) montmorillonite.

These cassiterite occurrences in rhyolitic rocks are believed to be deposited from aqueous vapor solutions resulting from the congelation of lava flows, as a late stage in their crystallization. Morey and Hesselgesser (1951) have demonstrated the appreciable solubility of silica in superheated steam, and Foshag (1926) has shown how such vapors can yield cristobalite and tridymite. Hematite shows an appreciable solubility in such vapors, but the solubility of cassiterite is quite low.

References

Byström, Anders, Hok, Brita, and Mason, Brian, (1942), The crystal structure of zinc meta antimonate and similar compounds: *Ark. Kemi, Mineral., Geol., Bd.* **153,** no. 4, 1–8.

Foshag, William F. (1926), The minerals of Obsidian Cliff and their origin: *Proc. U. S. Nat. Mus.*, **68,** 1–18.

Foshag, William F., and Fries, Carl, Jr. (1942), Tin deposits of the Republic of Mexico: *Bull. U.S. Geol. Surv.*, **935-C,** 155–158. Los yacimientos de estaño de la Republica Mexicana: *Comite Directivo para la investigacion de los recursos minerales de Mexico, Bol.* **8,** 49–51 (1946).

Genth, F. A. (1887), On the occurrence of tin ores in Mexico: *Contr. to Mineralogy, No.* **XXIX**; *read before the Am. Philosophical Soc.*, March 18, 1887.

Ingalls, Walter Benton (1895), The tin deposits of Durango, Mexico: *Trans. Am. Inst. Min. Engrs.*, **25,** 146–163.

Mason, Brian, and Vitaliano, Charles J. (1952), Bystromite, magnesian antimonate, a new mineral: *Am. Mineral.*, **37,** 53–57.

Morey, George W., and Hesselgesser, James H. (1951), The solubility of some minerals in superheated steam at high pressures: *Econ. Geol.*, **46,** 821–835.

Manuscript received Jan. 11, 1954

ION SUBSTITUTION IN THE DIOPSIDE-FERROPIGEONITE SERIES OF CLINOPYROXENES

Hisashi Kuno, *Geological Institute, Tokyo University, Tokyo, Japan.*

Abstract

Evidence is presented to show that there is a complete variation in composition from augite to pigeonite passing through subcalcic augite. Under ordinary conditions of crystallization of magmas, subcalcic augite does not form; an immiscibility gap exists between augite and pigeonite. However, subcalcic augite forms only when part of Si^{4+} in Si—O chain of pyroxene is replaced by Fe^{3+}, rendering it possible for Ca^{2+}, Mg^{2+}, and Fe^{2+} to enter the pyroxene structure in all proportions. The Si^{4+}—Fe^{3+} substitution is probably favored by rapid cooling at comparatively high temperature. The course of crystallization of clinopyroxenes in the Izu-Hakone province, Japan, is from salite close to diopside, passing through augite, to ferropigeonite. Throughout the greater part of this course, Ca^{2+} of the salite is successively replaced by Fe^{2+}, while the proportion of Mg^{2+} remains nearly constant.

Introduction

This paper presents the results of the study of clinopyroxenes from volcanic rocks. The principal purpose was to solve the question whether augite and pigeonite (according to the nomenclature proposed by Poldervaart and Hess, 1951) crystallizing from magmas are continuous or is there an immiscibility gap between the two.

There is some diversity of views regarding the limit of miscibility in natural pyroxenes. Asklund (1925), Hess (1941), Edwards (1942), and Poldervaart and Hess (1951) postulate an immiscibility gap between the augite series (including ferroaugite) and the pigeonite series (including ferropigeonite, or pigeonite with Mg^{2+}: Fe^{2+} less than 1:1), although most of them consider that this gap disappears when the pyroxenes become rich in Fe^{2+} as the crystallization proceeds. This conclusion is largely based on the facts that neither clinopyroxenes having compositions intermediate between the augite and pigeonite series, namely subcalcic augite and ferroaugite, have been found in nature nor the continuous zoning between the two series has been observed. In rare cases, 2 V values change continuously from one series to the other, but Hess (Poldervaart and Hess, 1951) attributes this to an anomalous value of 2 V caused by the substitution of Al^{3+} for Si^{4+} in more than the normal amount. Edwards (a contribution to Benson's paper, 1944) regards subcalcic augite as formed metastably during rapid cooling of magmas and states that under such condition Ca^{2+} of clinopyroxenes can be replaced by Fe^{2+} without causing any undue distortion of the crystal structure.

However, the occurrence of subcalcic augite and the continuous zoning were noticed by some petrologists who concluded that a complete miscibility obtains even in less ferriferous pyroxenes (Barth, 1931*a*; Mac-

donald, 1944; Benson, 1944; Kuno, 1950). Kuno (1950) recognized the existence of the immiscibility gap between the two series with Mg^{2+}: Fe^{2+} ratio ranging from 100:0 to about 57:43.

It has been demonstrated by synthetic experiments (Bowen, 1914; Bowen, Schairer, and Posnjak, 1933) that at high temperatures clinopyroxenes form a complete solid solution except for a narrow range of composition near $FeSiO_3$. Thus, clinoenstatite-diopside solid solution is obtained at temperatures above 1300° C. and hedenbergite-ferrosilite solid solution above 950° C. While Atlas (1952) who studied subsolidus relation of the system clinoenstatite-diopside found the existence of an immiscibility gap and determined the maximum temperature of the solvus at about 1380° C.

The immiscibility gap found by Atlas extends probably towards the field of ferriferous pyroxenes, and the solvus is represented by a domed surface the crest of which would incline toward the Fe-rich side until its temperature attains a value below 950° C. at the hedenbergite-ferrosilite end of the field, as illustrated by Barth (1951).

Since the observed temperatures of basaltic lavas in active volcanoes are usually between 1200° C. and 1000° C., it is likely that the crystallization of magnesian clinopyroxenes of the basaltic magmas takes place below the temperature of the crest of the solvus surface and therefore two separate clinopyroxenes are formed.

On the other hand, the crystallization temperature of more ferriferous clinopyroxenes in strongly fractionated magmas would be above that of the crest of the solvus surface. This is indicated by the occurrence of

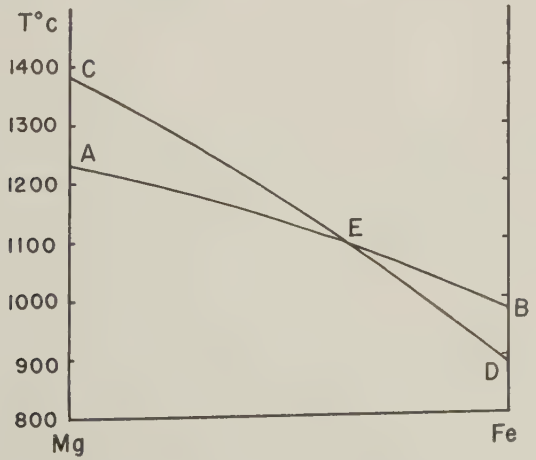

Fig. 1. Change of the crystallization temperature of magmas (*AB*) and the temperature of the crest of the solvus surface for clinopyroxenes (*CD*).

the members of the hedenbergite—ferrosilite solid solution in the Skaergaard intrusion which were first formed as members of the wollastonite solid solution and later inverted to the low temperature form (Wager and Deer, 1939, Muir, 1951).

This relation is shown diagrammatically in Fig. 1. The curve AB of the figure represents the temperatures of crystallization of the common mafic magmas at various stages of fractionation. The curve CD shows the temperature of the crest of the solvus surface.

The focus of discussion among the petrologists above cited is concerned with the location of the point E which is the intersection of the two curves.

To settle this question it is necessary to determine the range of the $Mg^{2+}:Fe^{2+}$ ratio of the pyroxenes which link the augite series with the pigeonite series, and also to examine the crystal structural relation of the two series.

Acknowledgments

This study was carried out in the Department of Geology, Princeton University, in close cooperation with Professor H. H. Hess. The writer's cordial thanks are due to the staff of the Department for many courtesies received, especially to Professor Hess for criticism of the results and for reading the manuscript. During this study, the writer was supported by the grant from The Geological Society of America (project No. 578-51) which is greatly appreciated.

Before and after his visit to Princeton, the writer engaged in the same study in the Geological Institute, Tokyo University, with the financial support by the grant from the Japanese Government Expenditure for Scientific Research.

The writer is also indebted to Dr. Kōzō Nagashima, Messrs. Takashi Katsura and Yukio Konisi for chemical analyses of pyroxenes from Hakone, Wadaki, Hatu-sima, and Ō-sima, to Assistant Professor Ryōhei Morimoto for the permission of the publication of the analyses of pyroxenes from Ō-sima made by Mr. Jōyo Ossaka, and to Dr. Akio Miyashiro for helpful discussions on the crystal chemical aspect of the problem.

X-ray Study

The chemical compositions of the pyroxenes used for the present study are listed in Tables 1–5 and are plotted in Fig. 2.

The figure shows that the diopside from St. Lawrence Co., N. Y. (Hess, 1949), and the pyroxenes Nos. 5, 6, 9, and 15 have compositions lying approximately on a straight line, and the pyroxene No. 1 close to it. This line represents the variation of the pyroxene composition largely con-

TABLE 1. COMPOSITIONS OF SALITES

	Phenocrysts		
	1	2	3
SiO_2	49.79	49.86	50.87
Al_2O_3	4.92	5.48	3.22
Fe_2O_3	0.79	2.42	0.49
FeO	5.88	4.23	7.51
MgO	14.84	15.02	14.14
CaO	22.70	22.34	23.87
Na_2O	0.20	0.00	0.32
K_2O		0.00	0.10
H_2O^+	n.d.	0.20	n.d.
H_2O^-	0.00	0.11	0.05
TiO_2	0.43	0.41	0.48
P_2O_5	tr.	0.00	n.d.
MnO	0.00	0.15	0.07
Total	99.55	100.22	101.12
Atomic no. on basis of 6 oxygen atoms			
Si^{4+}	1.851	1.837	1.883
Al^{3+}	0.149 } 2.000	0.163 } 2.000	0.117 } 2.000
Al^{3+}	0.065	0.076	0.011
Ti^{4+}	0.011	0.011	0.013
Fe^{3+}	0.022	0.066	0.013
Fe^{2+}	0.183	0.130	0.231
Mn^{2+}	0.000 } 2.024	0.004 } 2.000	0.002 } 2.026
Mg^{2+}	0.827	0.831	0.784
Ca^{2+}	0.903	0.882	0.946
Na^{1+}	0.013	0.000	0.022
K^{1+}		0.000	0.004

1. Salite in olivine eucrite (HK33010901e), an ejected block in tuff of Taga Volcano. Southwest of Wadaki near Aziro, north Izu. *Analyst*, Y. KONISI.
2. Salite in olivine-salite basalt tuff of Taga Volcano. Locality same as above. *Analyst*, S. Tanaka (Kuno and Sawatari, 1934).
3. Salite in hypersthene-salite dacite pumice (HK36082106) of Hakone Volcano. Just west of Odawara. *Analyst*, K. NAGASHIMA.

trolled by successive replacement of Ca^{2+} of the diopside by Fe^{2+} while the proportion of Mg^{2+} remains nearly constant.

These pyroxenes were selected for investigation with the North American Philips x-ray spectrometer. The method employed was nearly the same as that already described by Hess (1952) except that in this study the powder of pyroxene was mounted on glass slide together with

Table 2. Compositions of Augites

	Phenocrysts		Groundmass	
	4	5	6	7
SiO_2	51.20	51.44	50.8	50.72
Al_2O_3	2.71	2.09	2.5	0.98
Fe_2O_3	2.76	1.01	0.7	0.35
FeO	4.94	6.73	13.6	21.10
MgO	15.43	16.45	17.4	12.23
CaO	22.62	19.94	14.3	13.35
Na_2O	0.24	0.32	n.d.	0.33
K_2O	0.12	0.17	n.d.	0.13
H_2O^+	n.d.	n.d.	n.d.	n.d.
H_2O^-	0.06	0.36	n.d.	0.09
TiO_2	0.27	0.75	0.2	0.15
P_2O_5	n.d.	n.d.	n.d.	n.d.
MnO	0.05	0.21	0.4	0.37
SrO	n.d.	n.d.	n.d.	0.09
Total	100.40	99.47	99.9	99.89
Atomic no. on basis of 6 oxygen atoms				
Si^{4+}	1.885	1.911	1.906	1.960
Al^{3+}	0.115 } 2.000	0.089 } 2.000	0.094 } 2.000	0.040 } 2.000
Al^{3+}	0.000	0.005	0.019	0.006
Ti^{4+}	0.009	0.022	0.007	0.005
Fe^{3+}	0.080	0.027	0.018	0.014
Fe^{2+}	0.150	0.208	0.425	0.680
Mn^{2+}	0.002	0.007	0.014	0.012
Mg^{2+}	0.853 } 2.007	0.917 } 2.011	0.979 } 2.036	0.710 } 2.011
Ca^{2+}	0.891	0.794	0.574	0.554
Na^{1+}	0.018	0.022	0.000	0.023
K^{1+}	0.004	0.009	0.000	0.005
Sr^{2+}	0.000	0.000	0.000	0.002

4. Augite in olivine-augite basalt (HK47081901) of the Taga Volcano. Just east of Tyōzyagahara, west of Usami, north Izu. *Analyst*, K. Nagashima.
5. Augite in hypersthene-olivine-augite andesite (HK35090603) of Hakone Volcano. Yagurazawa-tōge, just north of Sengokubara, northern caldera wall of Hakone. *Analyst*, K. Nagashima.
6. Augite in olivine basalt (HK47040503) of Taga Volcano. Awarada-tōge, west of Usami, north Izu. *Analyst* Y. Konisi. The analysis corrected for 0.5% ilmenite impurity.
7. Augite in olivine basalt (HK47030801) of the Hatu-sima Basalt Group. Southeastern coast of Hatu-sima, north Izu. *Analyst*, K. Nagashima.

TABLE 3. COMPOSITIONS OF SUBCALCIC AUGITES AND FERROAUGITE

	Groundmass		
	8	9	10
SiO_2	49.68	49.72	49.98
Al_2O_3	0.78	0.59	0.04
Fe_2O_3	3.29	3.74	1.64
FeO	18.15	18.12	23.22
MgO	16.19	16.44	12.73
CaO	9.90	9.56	11.11
Na_2O	0.65	0.42	0.29
K_2O	0.15	0.07	0.16
H_2O^+	0.10	0.17	n.d.
H_2O^-	0.00	0.00	0.12
TiO_2	0.56	0.73	0.27
P_2O_5	n.d.	n.d.	n.d.
MnO	0.59	0.78	0.27
SrO	n.d.	n.d.	0.16
Total	100.04	100.34	99.99
Atomic no. on basis of 6 oxygen			
Si^{4+}	1.896	1.903	1.958
Al^{3+}	0.037	0.028	0.000
Ti^{4+}	0.018 } 2.000	0.021 } 2.000	0.009 } 2.000
Fe^{3+}	0.049	0.048	0.033
Fe^{3+}	0.047	0.058	0.014
Fe^{2+}	0.579	0.576	0.759
Mn^{2+}	0.018	0.025	0.009
Mg^{2+}	0.927	0.943	0.747
Ca^{2+}	0.405 } 2.035	0.392 } 2.027	0.465 } 2.029
Na^{1+}	0.050	0.028	0.024
K^{1+}	0.009	0.005	0.009
Sr^{2+}	0.000	0.000	0.002

8. Subcalcic augite in hypersthene-augite basalt (HK50100803) extruded in September, 1950, from the Mihara-yama crater. Western rim of the crater, Ō-sima Island, Izu. *Analyst*, J. OSSAKA. The analysis corrected for 0.5% ilmenite impurity.
9. Subcalcic augite in hypersthene basalt (HK38031201), extruded in 1778 from the Mihara-yama crater. Western caldera floor, Ō-sima Island, Izu. *Analyst*, J. OSSAKA.
10. Subcalcic ferroaugite in coarse-grained segregation vein (HK36092301d) in hypersthene-olivine basalt lava of the Okata Basalt Group. Sea cliff at Okata, Ō-sima Island, Izu. *Analyst*, K. NAGASHIMA. The analysis corrected for 0.5% ilmenite impurity.

Table 4. Compositions of Pigeonites

	Groundmass		
	11	12	13
SiO_2	52.84	50.56	50.28
Al_2O_3	0.44	1.41	2.03
Fe_2O_3	1.06	0.12	2.33
FeO	16.89	23.17	21.70
MgO	23.51	16.10	14.77
CaO	4.06	7.05	8.02
Na_2O	0.19	0.26	n.d.
K_2O	0.00	0.23	n.d.
H_2O^+	n.d.	n.d.	0.00
H_2O^-	0.22	0.07	
TiO_2	0.22	0.58	0.59
P_2O_5	n.d.	n.d.	0.00
MnO	0.56	0.54	0.38
SrO	0.00	n.d.	n.d.
Total	99.99	100.09	100.10
	Atomic no. on basis of 6 oxygen		
Si^{4+}	1.956	1.939	1.927
Al^{3+}	0.018 } 2.000	0.061 } 2.000	0.073 } 2.000
Al^{3+}	0.000	0.003	0.019
Ti^{4+}	0.007	0.018	0.018
Fe^{3+}	0.019	0.005	0.064
Fe^{3+}	0.012	0.000	0.000
Fe^{2+}	0.522	0.741	0.692
Mn^{2+}	0.018	0.016	0.014
Mg^{2+}	1.305 } 2.030	0.927 } 2.027	0.849 } 1.985
Ca^{2+}	0.160	0.290	0.329
Na^{1+}	0.013	0.018	0.000
K^{1+}	0.000	0.009	0.000
Sr^{2+}	0.000	0.000	0.000

11. Pigeonite (microphenocrysts) in hypersthene-olivine andesite (HK47122401) of Hakone Volcano. Tengu-zawa, southeast of Hatazyuku, in the southeastern caldera wall of Hakone. *Analyst*, K. Nagashima (Kuno and Nagashima, 1952).
12. Pigeonite in andesite free from pyroxene phenocrysts (HK47122301a) of Hakone Volcano. Upper course of the Sukumo-gawa valley near the confluence of Kiwada-zawa, southeastern caldera wall of Hakone. *Analyst*, K. Nagashima.
13. Pigeonite (with admixture of augite) in aphyric andesite (HK33081909a) of Hakone Volcano. Saru-sawa, south of Yumoto, eastern caldera wall of Hakone. *Analyst*, I. Iwasaki (Kuno, 1940).

TABLE 5. COMPOSITION OF PIGEONITE AND FERROPIGEONITES

	Phenocrysts			
	14	15	16	17
SiO_2	50.40	49.30	49.72	48.90
Al_2O_3	1.99	0.68	0.90	3.86
Fe_2O_3	0.13	3.83	1.72	4.65
FeO	21.30	23.17	27.77	25.35
MgO	18.28	15.38	12.69	6.87
CaO	6.43	3.14	3.80	7.96
Na_2O	1.33	n.d.	0.23	0.58
K_2O	0.02	n.d.	0.12	0.20
H_2O^+	n.d.	n.d.	1.27	0.57
H_2O^-	n.d.	n.d.	0.08	0.35
TiO_2	0.55	0.60	0.85	0.12
P_2O_5	n.d.	n.d.	n.d.	n.d.
MnO	n.d.	2.44	0.98	0.51
Total	100.43	98.54	100.13	99.92
Atomic no. on basis of 6 oxygen				
Si^{4+}	1.907	1.930	1.965	1.940
Al^{3+}	0.091 } 2.000	0.033	0.035 } 2.000	0.060 } 2.000
Al^{3+}	0.000	0.000 } 2.000	0.008	0.121
Ti^{4+}	0.002	0.019	0.026	0.005
Ti^{4+}	0.014	0.000	0.000	0.000
Fe^{3+}	0.005	0.018	0.000	0.000
Fe^{3+}	0.000	0.095	0.052	0.138
Fe^{2+}	0.672	0.760	0.915 } 1.970	0.838 } 1.924
Mn^{2+}	0.000 } 2.089	0.080	0.033	0.017
Mg^{2+}	1.037	0.909 } 1.976	0.751	0.409
Ca^{2+}	0.261	0.132	0.161	0.338
Na^{1+}	0.100	0.000	0.019	0.048
K^{1+}	0.000	0.000	0.005	0.010

14. Pigeonite (with admixture of augite) in augite-pigeonite-hypersthene andesite (HK33022001) of Hakone Volcano. North of Hakone-tōge, southern caldera wall of Hakone. *Analyst*, T. SAMESHIMA (Kuno, 1952).
15. Ferropigeonite in remelted quartz diorite (HK37090503), an ejected block in pumice of Hakone Volcano. Northeast of Yumoto, eastern flank of Hakone. *Analyst*, T. KATSURA.
16. Ferropigeonite in ferropigeonite andesite. Loch Scridain, Mull, Scotland. *Analyst*, E. G. RADLEY (Hallimond, 1914).
17. Ferropigeonite (with admixture of ferroaugite) in ferropigeonite andesite (HK40110106). North of Ōkubo-yama, Minami-Aizu, Hukusima Prefecture. *Analyst*, T. INOUE (Kuno and Inoue, 1949).

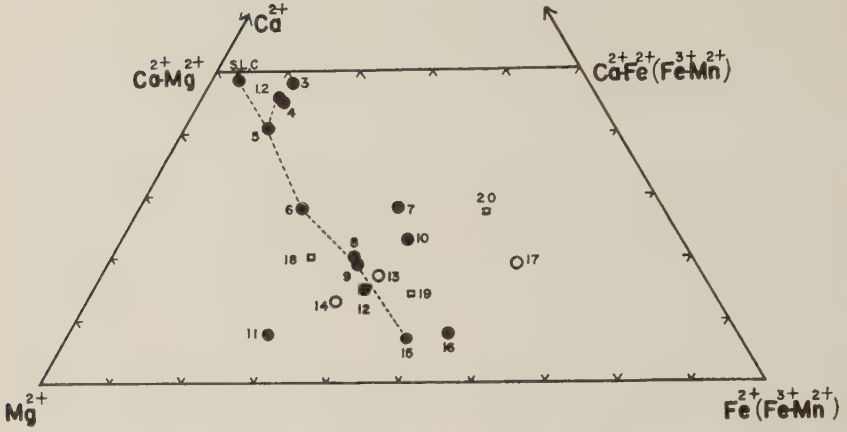

FIG. 2. Compositions of clinopyroxenes in atomic per cent. The numbers refer to those in Tables 1–5 and 10. S.L.C.—diopside from St. Lawrence Co. Solid circle—single pyroxene phase. Open circle —mixture of two clinopyroxene phases. Square—pyroxene whose composition was determined by partial analysis and by optical constants.

silicon powder used as an internal standard for calibration.

The unit cell dimensions a', b, and c', were determined from the 2θ angles for the reflections {750}, {660}, {260}, {060}, {350}, {600}, {440}, {150}, {510}, {041}, {330}, {002}, {310}, {220}, {021}, {020}, and {200}, and the angle β from 2θ for $\{53\bar{1}\}$, {531}, {331}, $\{31\bar{1}\}$, $\{22\bar{1}\}$, {131}, {311}, and {221} and the already known values of a', b, and c'. All measurements were made with Cu K_α radiation filtered by nickel. The values of a and c were then calculated from a', c', and β. The cleavage angle $110 \wedge 1\bar{1}0$ were calculated from a' and b.

A part of the results of this study has been already published (Kuno and Hess, 1953). It has been demonstrated that all the common clinopyroxenes belong to the same space group as diopside C_{2h}^6, $C\ 2/c$, and that the unit cell dimensions change continuously with the ratio $Ca^{2+}:Mg^{2+}:Fe^{2+}$ $(+Fe^{3+}+Mn^{2+})$ of the pyroxenes.

The x-ray powder diffraction patterns for these pyroxenes are shown in Fig. 3, and the unit cell dimensions a, b, and c, and the angles β and $110 \wedge 1\bar{1}0$ are listed in Table 6 and plotted in Fig. 4.

The angles β and $110 \wedge 1\bar{1}0$ show straight-line variation from the diopside to the ferropigeonite. The value of a also changes continuously throughout the series. No discontinuity is to be seen between the augite and the ferropigeonite.

A curve is drawn to show the variation of the b values of the clinopyroxenes with Al^{3+} content less than 0.05 (the diopside and the py-

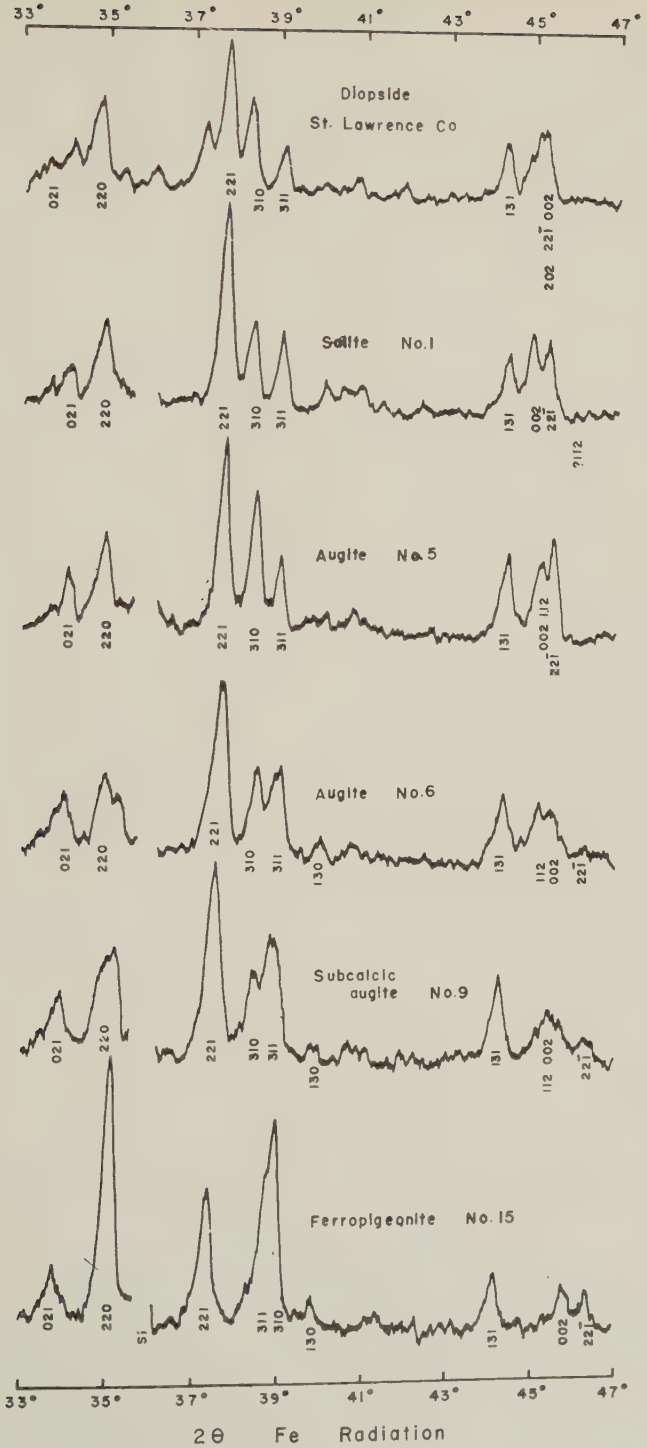

FIG. 3. *X*-ray powder diffraction patterns for the pyroxenes of the diopside-ferropigeonite series.

Table 6. Unit Cell Dimensions and the Crystallographic Angles of the Diopside—Ferropigeonite Series

	Diopside St. Lawrence Co. $Ca_{49}Mg_{47}Fe_4$	No. 1 Salite, Wadaki $Ca_{46}Mg_{43}Fe_{11}$	No. 5 Augite, Yagurazawa-tōge $Ca_{41}Mg_{47}Fe_{12}$
a	9.750 Å	9.742 Å	9.744 Å
b	8.930	8.901	8.909
c	5.249	5.268	5.260
β	74°10′	73°55′	73°28′
$110 \wedge 1\bar{1}0$	87°12′	87°07′	87°18′
	No. 6 Augite, Awarada-tōge $Ca_{28}Mg_{49}Fe_{23}$	No. 9 Subcalcic augite Ō-sima $Ca_{19}Mg_{46}Fe_{35}$	No. 15 Ferropigeonite Yumoto $Ca_7Mg_{45}Fe_{48}$
a	9.722 Å	9.716 Å	9.712 Å
b	8.925	8.944	8.959
c	5.242	5.242	5.251
β	72°57′	72°20′	71°27′
$110 \wedge 1\bar{1}0$	87°40′	88°02′	88°26′

roxenes Nos. 9 and 15, Table 7). The b values of Nos. 1, 5, and 6 which contain higher Al^{3+} (Table 7) lie below this standard curve. Two curves are drawn tentatively, one representing the b values for pyroxenes with Al^{3+} about 0.2 and another for those with Al^{3+} about 0.1. The effect of Al^{3+} is also seen in the c value; the values for the pyroxenes Nos. 1 and 5 lie above the standard curve constructed for the c value of the pyroxenes with lower Al^{3+} content.

Table 7. Atomic Numbers of Al^{3+} in Pyroxenes on the Basis of 6 Oxygens

	St. Lawrence Co.	No. 1	No. 5	No. 6	No. 9	No. 15
Al^{3+}	0.018	0.214	0.094	0.113	0.028	0.033

The Al^{3+} content does not appear to affect the a value.

The contraction of b length of the unit cell and the expansion of c are also found in orthorhombic pyroxenes, although in the latter the expansion of c takes place only to a limited extent (Hess, 1952).

It might be suggested that the expansion of c is caused by the substitution of the Al^{3+} ions for the smaller Si^{4+} ions, while the contraction of b

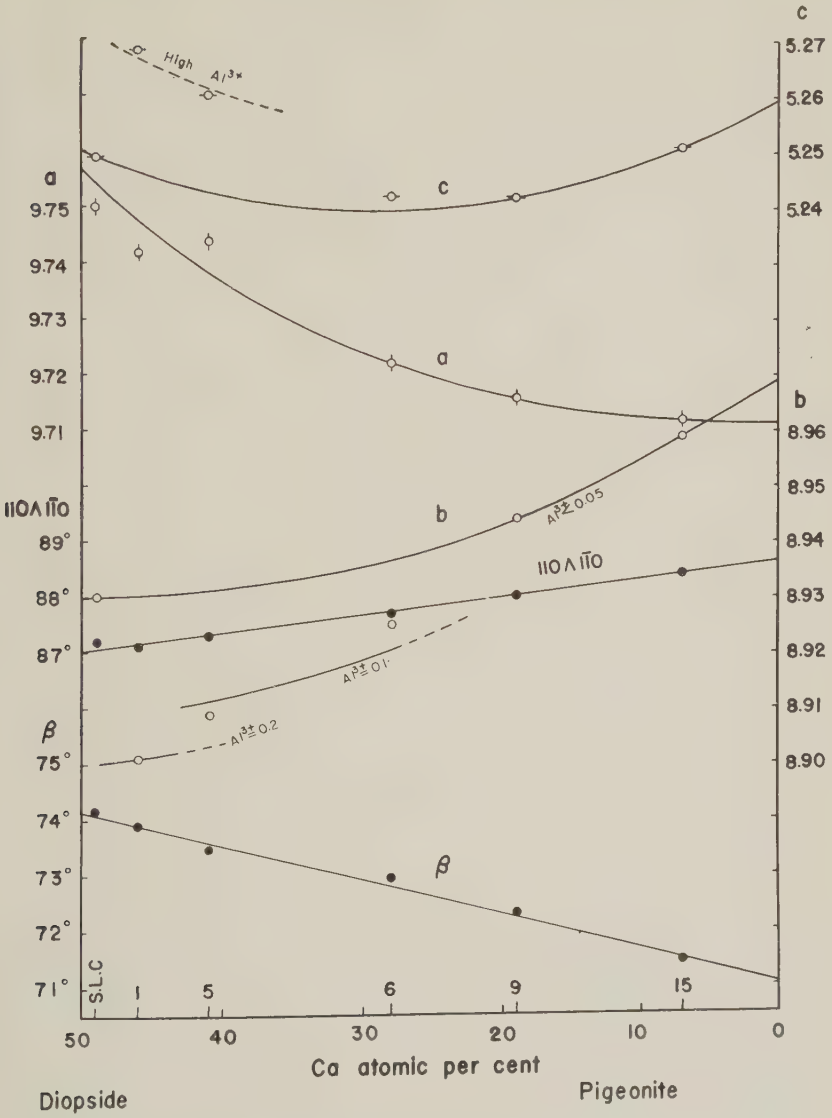

FIG. 4. Variation of the unit cell dimensions and crystallographic angles for the diopside-ferropigeonite series.

by the substitution of the Al^{3+} ion for the larger Mg^{2+} ion. Hess (1952), on the other hand, considered that, in orthopyroxenes, the substitution of Al^{3+} for Si^{4+} at first increases the c value but larger amounts of Al^{3+} causes the SiO_3 chain to zigzag in the 010 plane and hence no more increase of c. The zigzag in the 010 plane and the substitution of Al^{3+} for

Mg^{2+} result in the contraction of b without changing a. In any case, the more marked increase of c in the clinopyroxenes than in the orthopyroxenes is probably due to the higher proportion of Al^{3+} in the Si^{4+} position in the former.

The crystal structure of the clinoenstatite-pigeonite-ferrosilite series appears to be unique among clinopyroxenes belonging to C_{2h}^6. As shown in Table 8, the angle $110 \wedge 1\bar{1}0$ of this series is about 1° larger than those of any other clinopyroxenes, and the angle β from 4° to 1° lower than those of the latter except spodumene.

Table 8. Crystallographic Angles of Clinopyroxenes

	Diopside (Kuno and Hess, 1953)	Hedenbergite (Kuno and Hess, 1953)	Acmite (Dana, 1900)	Spodumene (Dana, 1900)	Jadeite (Yoder, 1950)
$110 \wedge 1\bar{1}0$	87°12′	86°46′	87°04′	87°00′	87°02′
β	74°10′	75°40′	73°11′	69°40′	72°44.5′
	Clinoenstatite (Kuno and Hess, 1953)	Pigeonite No. 11 (Kuno and Hess, 1953)	Ferropigeonite No. 15	Ferropigeonite from slag (Bowen, 1933)	Ferrosilite from lithophysae (Bowen, 1935)
$110 \wedge 1\bar{1}0$	88°04′	88°17′	88°26′	88°40′	89°10′
β	71°38.5′	71°27′	71°27′	71°31′	n.d.

The angle β for ferrosilite is probably about 71° 35′ as inferred by extrapolation, and this value and the value of $110 \wedge 1\bar{1}0$ for the same pyroxene are very different from those of hedenbergite with which it forms a solid solution. This departure of the angles from those of the Ca-rich pyroxenes might explain the extreme rarity of ferrosilite.

The subcalcic augite No. 9 shows a strong zoning from pigeonite to augite, and one might doubt that the mineral consists of a mixture of two separate phases, pigeonite and augite, and that the apparently continuous zoning is due to anomalous value of 2V. In Fig. 5 the powder diffraction pattern of the pyroxene No. 9 is compared with that of a mixture of the augite No. 7 and the pigeonite No. 11 in the ratio 1:1.

The mixture shows double peaks in the pattern while No. 9 shows single broad peaks at the corresponding positions. It is safe to conclude that the subcalcic augite represents a single phase.

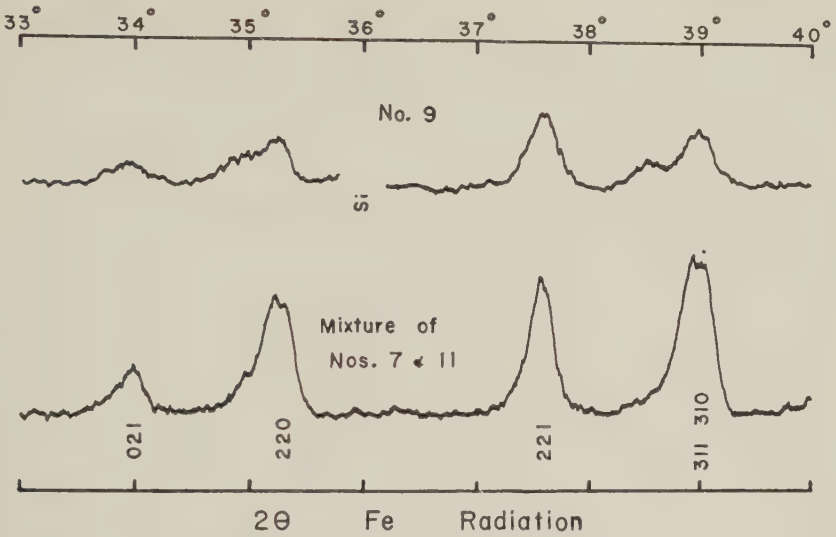

FIG. 5. *X*-ray powder diffraction patterns in the single pyroxene No. 9 and of the mixture of the two pyroxenes Nos. 7 and 11.

TABLE 9. OPTICAL CONSTANTS OF THE PYROXENES

	Diopside* St. Lawrence Co.	No. 1	No. 5	No. 6
α (mean)	1.6718	1.690	1.690	1.691
β (mean)	1.6785	1.696	1.696	1.697
γ (mean)	1.7013	1.715	1.716	1.718
Range of β	none	0.009	0.008	0.006
(+) 2V (in 010)	56°5	59°	51°	44°
Range	3°5	3°	5°	10°
Dispersion	$r>v$	$r>v$	$r>v$	no disp.
	No. 8	No. 9	No. 10	No. 15
α (mean)	1.709	1.711	1.719	1.713
β (mean)	1.711	1.713	1.722	1.713
γ (mean)	1.738	1.739	1.745	n.d.
Range of β	0.042	0.043	0.068	0.003
(+) 2V (in 010)	28°	25°	29°	11°
Range	30°	41°	47°	20°
Dispersion	$r<v$	$r<v$	no disp.	$r<v$

* Hess, 1949.

Optical Study

The mean values of refractive indices and 2V of the pyroxenes of the diopside-ferropigeonite series are given in Table 9.

The 2V value changes continuously through this series. The refractive indices of the pyroxenes Nos. 1 and 5 are much higher than those of the diopside, probably due to the high Al^{3+} content, and the range of refractive indices of the subcalcic augite No. 9 is very great.

In Table 9 are also given the optical constants of the subcalcic augites Nos. 8 and 10. The 2V values of these pyroxenes and of No. 9 vary continuously from about 10° (core) to about 40° (margin), the optic plane being always parallel to 010. The values between 20° and 35° are quite common, although these values were considered previously as extremely rare in clinopyroxenes.

Similar continuous zoning has been observed in some other crystals as shown in Table 10. Their mean compositions are plotted in Fig. 2.

Table 10. Zoning in Clinopyroxenes

	No. 18	No. 19	No. 20
β	1.685–1.731	1.704–1.710	1.710–1.733
(+) 2V	0° (core) →39° (margin) (in 010)	46° (core) →0° (margin) (in 010)	0° (core) →51° (margin) (in 010)
Composition	$Ca_{20}Mg_{53}Fe_{27}$* (mean)	$Ca_{37}Mg_{34}Fe_{29}$ (core) $Ca_{10}Mg_{42}Fe_{48}$ (margin)	$Ca_{10}Mg_{42}Fe_{48}$ (core) $Ca_{37}Mg_{13}Fe_{50}$ (margin)

* Partial analysis by Nagashima.

The subcalcic augite No. 18 occurs in the groundmass of basalt from Okata, Ō-sima Island, Izu, and shows quite similar zoning as those in Nos. 8, 9, and 10.

Porphyritic clinopyroxenes (No. 19) in andesite from Weiselberg, Germany, consist of augite and ferropigeonite (Kuno, 1947). Where the two types of pyroxenes occur in the same crystal, they are either zoned continuously as shown in Fig. 6 or bounded distinctly from one another.

Clinopyroxene crystals (No. 20) about 1 mm. in length occur in pegmatitic schlieren in a dolerite sheet at Semi, Yamagata Prefecture, Japan. Some of the crystals are zoned continuously but others show discontinuous zoning.

Crystal Chemistry

The general formula for pyroxenes may be written as follows (Berman, 1937; Hess, 1949):

$(W)_{1-p}\ (X,\ Y)_{1+p}Z_2O_6$
$W = Ca^{2+}, Sr^{2+}, Na^{1+}, K^{1+}$
$X = Mg^{2+}, Fe^{2+}, Mn^{2+}, Ni^{2+}$
$Y = Al^{3+}, Fe^{3+}, Cr^{3+}, Ti^{4+}$
$Z = Si^{4+}, Al^{3+}, Ti^{4+}, Fe^{3+}$

The atomic proportions of the pyroxenes listed in Tables 1–5 are calculated on the assumption that the number of atoms in the Z group always amounts to 2.000. If addition of Al^{3+} to Si^{4+} does not satisfy the number of atoms required for the Z group, then Ti^{4+} and Fe^{3+} are also added until the total number of these atoms becomes 2.000. Al^{3+}, Ti^{4+}

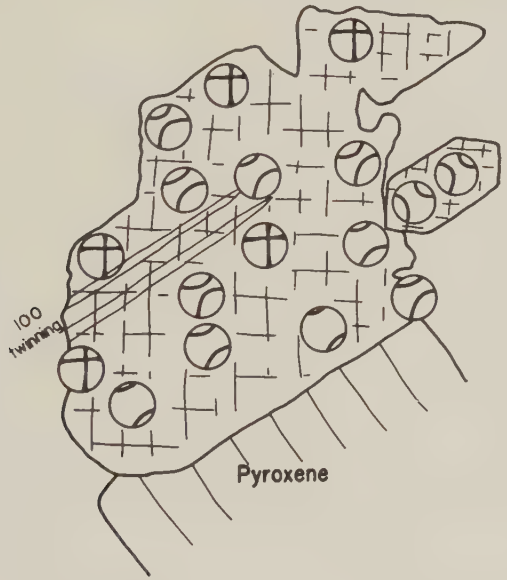

FIG. 6. Variation of the optic angle 2V in a pyroxene phenocryst (0.25 mm. long) in andesite from Weiselberg.

and Fe^{3+} left after this allotment then constitute the Y group. The total number of atoms of the W, X, and Y groups for the pyroxenes listed in the tables except Nos. 14 and 17 approximately equals 2.000, indicating that these pyroxenes have the theoretical compositions. In the case of the pyroxenes Nos. 14 and 17, the cause of the departure from the theoretical formula is not known. It is certainly not due to impurities.

In the subcalcic augites Nos. 8, 9, and 10, considerable proportion of Fe^{3+} (0.05 to 0.03) and all of Ti^{4+} enter the Z group, otherwise the compositions do not fit the theoretical formula. In all other pyroxenes except Nos. 11 and 15, Fe^{3+} does not enter this group. In Nos. 11 and 15, the amount of Fe^{3+} in the Z group is only 0.02.

That a part of Si^{4+} in the pyroxene structure can be replaced by Ti^{4+} has been discussed by Barth (1931*b*), Dixon and Kennedy (1933), and Muir (1951), but the replacement by Fe^{3+} has not been anticipated.

The entrance of Fe^{3+} in the tetrahedral position of silicate is demonstrated by the existence of Fe^{3+}-bearing potash-feldspars both as natural and synthetic minerals (Faust, 1936; Rosenqvist, 1951). A small amount of Fe^{3+} enters this position in plagioclase of Skaergaard intrusion (Wager and Mitchell, 1951) and also in anorthite from Wadaki, north Izu (Kuno, 1950).

Ahrens (1952) gave the following ionic radii of the cations for 6-fold co-ordination:

Si^{4+} 0.42, Al^{3+} 0.51, Fe^{3+} 0.64, Ti^{4+} 0.68.

The similarity of the ionic radius indicates that Fe^{3+} and Ti^{4+} are equally capable of replacing Si^{4+}, although other factors such as the ionization potential and electronic charge of the two ions may also affect the capability of substitution.

The partial substitution of Fe^{3+} for Si^{4+} appears to be characteristic of subcalcic augite and ferroaugite, or pyroxenes with compositions lying within the postulated immiscibility gap. Since the analyses listed in the tables were made by many different analysts, the relation cannot be considered to be fortuitous.

As shown in Fig. 2, the analyzed pyroxenes other than Nos. 8, 9, 10, and 18 consist either of a single phase with Ca^{2+} content more than 25 per cent or less than 15 per cent or of a mixture of the two phases.

About 10 excellent analyses of porphyritic augites from Japanese volcanic rocks could be cited. They all have Fe^{3+} in the *Y* group. Hess (1949) listed 44 first-class analyses of clinopyroxenes, and only one of them (No. 40) has Fe^{3+} in the *Z* group. This pyroxene is aegirinaugite and may be set aside from the present discussion.

Of the 23 clinopyroxenes from the Skaergaard intrusion listed by Muir (1951), only three (Nos. 11, 13, and 14) contain Fe^{3+} in the *Z* group, but the amount of Fe^{3+} in this group is less than 0.02. In another pyroxene (No. 12), the amount of Fe^{3+} in the *Z* group attains 0.038, but the revised analysis of this pyroxene by Muir revealed that all Fe^{3+} enters the *Y* group.

At temperatures of dry melts, Ca^{2+} of diopside can be replaced by Mg^{2+} and Fe^{2+}, probably in all proportions except for those corresponding to ferrosilite. However, at temperatures prevailing in ordinary magmas, this replacement can take place until the ratio $Ca^{2+}:Mg^{2+}+Fe^{2+}=25:75$ is attained. This limit is represented approximately by the pyroxenes Nos. 6 and 7. Further replacement causes undue distortion of the structure, and the pyroxenes just beyond this limit (subcalcic augite and ferroaugite) are no longer stable, breaking up into two phases, namely,

that with Ca^{2+} more than 25 per cent and that with Ca^{2+} less than 15 per cent. The structure of the latter pyroxene is probably suitable for accommodating the smaller ions Mg^{2+} and Fe^{2+} in place of the larger ion Ca^{2+}, and therefore can form at ordinary magmatic temperature as a stable phase.

However this distortion of the structure is released by the entrance of the large Fe^{3+} ion in the tetrahedral position, and therefore subcalcic augite and ferroaugite can form.

Conditions Necessary for the Formation of Subcalcic Augite

The temperature of crystallization of the subcalcic augite No. 8 has been measured. The lava from which the mineral was separated was extruded from the Mihara-yama crater, Ō-sima Volcano, in the middle of September, 1950. At the lava fountain, the temperature was 1100° C. (Minakami, 1951 *a*), and at the rim of the crater about 500 meters away from the fountain, it was from 1070° C. to 1030° C. as measured by the writer using an optical pyrometer. At 1030° C. the lava was still fluid. Where the temperature fell below 1000° C., the lava nearly stopped moving. Examination of the specimens of the lava showed that the final movement was due to the fluidity of the glass present interstitially between pyroxene and plagioclase. The rock specimen for the pyroxene separation was collected on October 8th at the crater rim when it was still hot. It contains also a little interstitial glass. Scoriaceous fragments ejected from the lava fountain are made up largely of glassy groundmass with some scattered phenocrysts.

Thus it may be concluded that the groundmass pyroxene (No. 8) started to crystallize at some temperature a little below 1100° C. and ceased to grow at about 1000° C.

The subcalcic augite No. 9 was separated from the 1778 lava of the same crater. Judging from the similarity of the chemical composition and surface feature of this lava to those of 1951 lava, the temperatures of these lavas at the time of extrusion were nearly the same. The temperature of the 1951 lava at the lava fountain was estimated as about 1200° C. (Minakami, 1951 *b*).

The subcalcic ferroaugite No. 10 and the subcalcic augite No. 18 occur in basaltic segregation veins in the same olivine-pyroxene basalt flow.

Pyroxenes having similar compositions (2V from 30° to 20°) occur in the groundmass of basalts but are rare in that of andesites. They are extremely rare, if not entirely absent, in gabbros and dolerites, as has been pointed out by many authors.

Since the common gabbros and dolerites were formed probably at temperatures nearly the same as those observed in the Ō-sima lavas, the conclusion may be drawn that rapid cooling at comparatively high

temperatures favors the formation of subcalcic augite and ferroaugite and also pyroxenes with continuous zoning.

It may be assumed that at high temperatures the magma consists of Si^{4+}—O^{2-}, Al^{3+}—O^{2-}, Ti^{4+}—O^{2-}, and Fe^{3+}—O^{2-} tetrahedra and freely moving cations. During rapid cooling, Si^{4+}—O^{2-} tetrahedra would be linked with Fe^{3+}—O^{2-} tetrahedra to form the $(Si^{4+}, Fe^{3+})O_3^{2-}$ chain of pyroxene. This framework would be able to accommodate Ca^{2+}, Mg^{2+}, and Fe^{2+} without limitation in their proportion. On the other hand, during slow cooling, $(Si^{4+}, Fe^{3+})O_3^{2-}$ chain might be once formed but equilibrium adjustment would take place and Fe^{3+} in the chain would be successively replaced by Si^{4+} and Al^{3+}, resulting in the ordinary $(Si^{4+}, Al^{3+})O_3^{2-}$ chain. This framework would be able to take up Ca^{2+}, Mg^{2+}, and Fe^{2+} to a certain limited extent. Even during slow cooling, some crystals in a rock or some part of a crystal would have the $(Si^{4+}, Fe^{3+})O_3^{2-}$ framework which has escaped from equilibrium adjustment. This would account for the rare occurrence of continuously zoned pyroxenes as phenocrysts and as crystals in some dolerite pegmatites.

The crystal chemical aspect pictured above may be expressed in another way.

Thus, where a small proportion of Fe^{3+} enters the tetrahedral position in pyroxenes, the temperature of the solvus for such pyroxenes becomes lower than that for the normal pyroxenes. The temperatures of magmas now lie above this solvus temperature, and therefore subcalcic augite and ferroaugite can form as stable phases.

Referring to Fig. 1, the curve *CD* is displaced downward for the series of pyroxenes with some Fe^{3+} in the tetrahedral position, so that the point *E* moves toward the point *A* of the figure. The point lies at least on the Mg-rich side of the point No. 18 of Fig. 2 ($Mg^{2+}:Fe^{2+}=65:35$) for pyroxenes with about 0.040 Fe^{3+}.

On the other hand, the normal magnesian pyroxenes of the common mafic magmas crystallize below the solvus temperature, and the point *E* lies at about $Mg^{2+}:Fe^{2+}=35:65$ as determined by Wager and Deer (1939).

The position of the point *E* also moves easily according to the temperatures of the magmas. In andesitic magmas, the point *E* moves further toward the Fe-rich side, as shown by the pyroxene No. 17 which consists of two distinct clinopyroxenes with the average ratio $Mg^{2+}:Fe^{2+}=29:71$.

Poldervaart and Hess (1951) and Kuno and Nagashima (1952) used the term "two-pyroxene boundary" for the line in the ternary diagram Ca^{2+}—Mg^{2+}—Fe^{2+} which has the same significance as the point *E* of the binary diagram Fig. 1. However the term was first introduced by Tsuboi (1932) for the boundary line in the ternary diagram which sepa-

rates the field of augite from that of hypersthene. The term should be used according to the original definition by Tsuboi.

Crystallization of Pyroxenes from Japanese Magmas

The course of crystallization of clinopyroxenes in a strongly fractionated basaltic magma has been completely traced by Muir (1951). The trend of differentiation of the basaltic and andesitic magmas of Izu-Hakone province, Japan, is slightly different from that of the Skaergaard magma (Kuno, 1953). The crystallization of clinopyroxenes in the pigeonitic rock series of this province (Kuno, 1950) can be discussed on the basis of the analyses plotted in Fig. 2, although the figure also includes two pyroxenes from other localities which represent the later stage of the pyroxene crystallization in this province.

The pyroxenes Nos. 1, 2, and 4 are early-formed phenocrysts in basaltic magmas. They were separated before orthopyroxene starts to crystallize, and have compositions close to diopside; only a small proportion of Ca^{2+} of diopside is replaced by Fe^{2+}. These pyroxenes have high contents of Al^{3+} mostly in tetrahedral position.

The pyroxene No. 3 which forms phenocrysts in dacite pumice has an exceptionally high content of Ca^{2+}.

The pyroxene No. 5 forms phenocrysts in mafic hypersthene-augite andesite and represents a slightly more advanced stage of crystallization.

As the crystallization proceeds, the amount of Ca^{2+} replaced by Fe^{2+} increases continuously until the limit of miscibility, approximately represented by Nos. 6 and 7, is attained. Nos. 6 and 7 are later-formed crystals in basaltic magmas (groundmass).

Upon further crystallization, the ratio $Ca^{2+}:Mg^{2+}+Fe^{2+}$ in the pyroxene becomes lower than 25:75, and Ca^{2+} can no longer be replaced either by Fe^{2+} or Mg^{2+} except when rapid cooling at high temperatures obtains. At this stage, the composition of the magma becomes andesitic and its temperature is usually not high enough to permit this replacement even if rapid cooling obtains, so that the pyroxenes split into two phases, one with Ca^{2+} higher than 25 per cent and another lower than 15 per cent. Such a stage is represented by the pyroxenes Nos. 13, 14, and 17, including intratelluric crystals and groundmass grains.

In certain cases, rapid cooling of high-temperature magma results in the formation of the pyroxenes with Ca^{2+} content between 25 and 15 per cent. Such pyroxenes are found in the groundmass of pyroxene basalts (Nos. 8, 9, 10, and 18).

In more advanced stages of the crystallization of the andesitic magmas, Ca^{2+} of the pyroxenes is largely replaced by Fe^{2+}, resulting in pigeonites and ferropigeonites with $Ca^{2+}:Mg^{2+}+Fe^{2+}$ less than 15 per cent. The

compositions of such pyroxenes are shown by the analyses Nos. 12, 15 and 16. Optical examination of groundmass pyroxenes of salic andesites showed that they have compositions close to those of Nos. 15 and 16.

The latest stage of the pyroxene crystallization is represented by ferropigeonite occurring in cavitites of dacite (Kuno, 1950). It has a composition $Ca_8Mg_{28}Fe_{64}$.

Thus throughout the main part of the course of crystallization of pyroxenes, Ca^{2+} of the magnesian salite is successively replaced by Fe^{2+} and the content of Mg^{2+} of the pyroxenes remains nearly constant.

In the Skaergaard intrusion, the earliest pyroxene has the same composition as the salite of Japan. In the earlier stage of the pyroxene crystallization, Ca^{2+} is replaced by Fe^{2+} to a certain extent, and thereafter the main trend is controlled by the Mg^{2+}—Fe^{2+} substitution. The earlier trend is comparable to the main trend of the Japanese pyroxenes.

The pyroxene No. 11 is a member of a series which follows a different course of crystallization. In this series, orthopyroxene separates first and is followed by successively more calcic clinopyroxenes (Kuno and Nagashima, 1952). Thus Mg^{2+} of the pyroxene No. 11 is gradually replaced by Ca^{2+} and Fe^{2+} until the pyroxene has composition of subcalcic augite or Ca-poor augite. This course of crystallization eventually joins the other course already pictured.

According to Tsuboi (1932), the pyroxenic components of magmas lying in the upper part of Fig. 2 separate Ca-rich clinopyroxene first, while those in the lower part of the same figure separate orthopyroxene first. The boundary between the two fields is the "two-pyroxene boundary."

The compositions of groundmass pyroxenes in equilibrium with phenocrysts of Ca-rich clinopyroxene alone should lie above this boundary line, while those in equilibrium with phenocrysts of orthopyroxene alone below this line. The former is represented by the pyroxenes Nos. 6 and 7, and the latter by Nos. 9 and 18. Therefore, in Fig. 2, the two-pyroxene boundary should be located below the points Nos. 6 and 7 and above the points Nos. 9 and 18. These are groundmass pyroxenes of basalts.

Again, the compositions of groundmass pyroxenes in equilibrium with phenocrysts of both Ca-rich clinopyroxene and orthopyroxene should lie on the two-pyroxene boundary. Such pyroxenes are Nos. 8, 12, and 13. Nos. 12 and 13 occur in rocks without pyroxene phenocrysts, but that they are in equilibrium with Ca-rich clinopyroxene and orthopyroxene phenocrysts is certain from the mineral assemblage of the associated lavas. They are pyroxenes of medium andesites and their compositions lie well below the boundary line already located. Most of the groundmass

pyroxenes of salic andesites in equilibrium with phenocrysts of both Ca-rich clinopyroxene and orthopyroxene have compositions closer to the Mg^{2+}—Fe^{2+} base of Fig. 2.

Thus the location of the two-pyroxene boundary moves toward the base of the figure as the proportion of the salic components of the magmas increases. If a tetrahedron is constructed with the *Wo-En-Fs* triangle as its base and with the salic components as its apex, the two-pyroxene boundary surface would rise from the base and gradually ap-

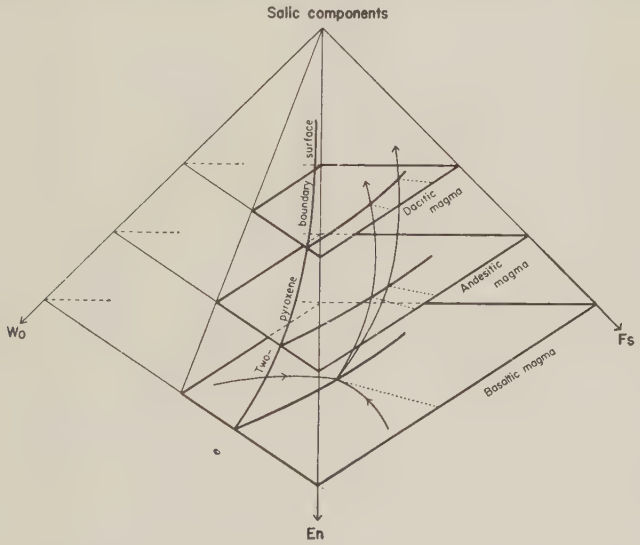

Fig. 7. Two-pyroxene boundary surface in a tetrahedron with *Wo-En-Fs* as its base and salic components as its apex. Three sections cut parallel to the base with different proportions of salic components are shown. The arrow heads indicate courses of crystallization of Japanese magmas.

proach the salic components-*En-Fs* face of the tetrahedron as shown in Fig. 7. The magmas would change their compositions along the curved courses of the figure, the difference of the courses depending on the original compositions and the degree of fractionation. In the triangular diagram Fig. 2, only the projections of various points lying on this surface are shown.

References

Ahrens, L. H. (1952), The use of ionization potentials. Part 1. Ionic radii of the elements: *Geoch. Cosm. Acta*, **2**, 155–169.

Asklund, B. (1925), Petrological studies in the neighbourhood of Stavsjö at Kolmården. Granites and associated basic rocks of the Stavsjö area: *Sver. Geol. Undersök., ser. C, Årsbok*, **17**, 1–121.

Atlas, L. (1952), The polymorphism of $MgSiO_3$ and solid-state equilibria in the system $MgSiO_3$—$CaMgSi_2O_6$: *J. Geol.*, **60,** 125–147.

Barth, T. F. W. (1931*a*), Crystallization of pyroxenes from basalts: *Am. Mineral.*, **16,** 195–208.

Barth, T. F. W. (1931*b*), Pyroxen von Hiva Oa, Marquesas-Inseln und die Formel titanhaltiger Augit: *Neues Jahrb. Min., Abt. A*, **64,** 217–224.

Barth, T. F. W. (1951), Sub-solidus diagram of pyroxenes from common mafic magmas: *Norsk Geol. Tids.*, **29,** 218–221.

Benson, W. N. (1944), The basic igneous rocks of Eastern Otago and their tectonic environment: *Tr. Roy. Soc. New Zealand*, **74,** 71–123.

Berman, H. (1937), Constitution and classification of natural silicates: *Am. Mineral.*, **22,** 333–415.

Bowen, N. L. (1914), The ternary system: diopside—forsterite—silica: *Am. J. Sci.*, **38,** 207–264.

Bowen, N. L. (1933), Crystals of iron-rich pyroxene from a slag: *J. Wash. Acad. Sci.*, **23,** 83–87.

Bowen, N. L. (1935), "Ferrosilite" as a natural mineral: *Am. J. Sci.*, **30,** 481–494.

Bowen, N. L., and Schairer, J. F. (1935), The system, MgO—FeO—SiO_2: *Am. J. Sci.*, **29,** 151–217.

Bowen, N. L., Schairer, J. F., and Posnjak, E. (1933), The system, CaO—FeO—SiO_2: *Am. J. Sci.*, **26,** 193–284.

Dana, J. D. (1900), System of mineralogy, 6th ed.: 352.

Dixon, B. E., and Kennedy, W. Q. (1933), Optically uniaxial titanaugite from Aberdeenshire: *Zeit. Krist., A*, **86,** 112–120.

Edwards, A. B. (1942), Differentiation of the dolerites of Tasmania: *J. Geol.*, **50,** 451–480; 579–610.

Faust, G. T. (1936), The fusion relations of iron-orthoclase, with a discussion of the evidence for the existence of an iron-orthoclase molecule in feldspars: *Am. Mineral.*, **21,** 735–763.

Hallimond, A. F. (1914), Optically uniaxial augite from Mull: *Mineral. Mag.*, **17,** 97–99.

Hess, H. H. (1941), Pyroxenes of common mafic magmas: *Am. Mineral.*, **26,** 515–555; 573–579.

Hess, H. H. (1949), Chemical composition and optical properties of common clinopyroxenes: *Am. Mineral.*, **34,** 621–666.

Hess, H. H. (1952), Orthopyroxenes of the Bushveld type, ion substitutions and changes in unit cell dimensions: *Am. J. Sci., Bowen vol.*, 173–187.

Kuno, H. (1940), Pigeonite in the groundmass of some andesite from Hakone Volcano: *J. Geol. Soc. Japan*, **47,** 347–351.

Kuno, H. (1947), Occurrence of porphyritic pigeonite in "weiselbergite" from Weiselberg, Germany: *Proc. Japan Acad.*, **23,** 111–113.

Kuno, H. (1950), Petrology of Hakone Volcano and adjacent areas, Japan: *Bull. Geol. Soc. Am.*, **61,** 957–1020.

Kuno, H. (1952), Explanatory text of the geological map of Atami (in Japanese): *Geol. Surv. Japan*, sheet 123, 1–141.

Kuno, H. (1953), Formation of calderas and magmatic evolution: *Tr. Am. Geoph. Union*, **34,** 267–280.

Kuno, H., and Hess, H. H. (1953), Unit cell dimensions of clinoenstatite and pigeonite in relation to other common clinopyroxenes: *Am. J. Sci.*, **251,** 741–752.

Kuno, H., and Inoue, T. (1949), On porphyritic pigeonite in andesite from Ōkubo-yama, Minami-Aizu, Hukusima Prefecture: *Proc. Japan Acad.*, **25,** 128–132.

KUNO, H., AND NAGASHIMA, K. (1952), Chemical compositions of hypersthene and pigeonite in equilibrium in magma: *Am. Mineral.*, **37,** 1000–1006.

KUNO, H., AND SAWATARI, M. (1934), On the augites from Wadaki, Izu, and from Yoneyama, Etigo, Japan: *Jap. J. Geol. Geogr.*, **11,** 327–343.

MACDONALD, G. A. (1944), Pyroxenes in Hawaiian lavas: *Am. J. Sci.*, **242,** 626–629.

MINAKAMI, T. (1951*a*), Report on the volcanic activities in Japan during 1948–1950: *Intern. Ass. Vulc., Brussel, August* **1951,** 1–18.

MINAKAMI, T. (1951*b*), On the temperature and viscosity of the fresh lava extruded in the 1951 Oo-sima eruption: *Bull. Earthq. Res. Inst.*, **29,** 487–498.

MUIR, I. D. (1951), The clinopyroxenes of the Skaergaard intrusion, eastern Greenland: *Mineral. Mag.*, **29,** 690–714.

POLDERVAART, A., AND HESS, H. H. (1951), Pyroxenes in the crystallization of basaltic magma: *J. Geol.*, **59,** 472–489.

ROSENQVIST, I. TH. (1951), Investigations in the crystal chemistry of silicates. III. The relation haematite—microcline: *Norsk Geol. Tids.*, **29,** 65–76.

TSUBOI, S. (1932), On the course of crystallization of pyroxenes from rock-magmas: *Jap. J. Geol. Geogr.*, **10,** 67–82.

WAGER, L. R., AND DEER, W. A. (1939), Geological investigations in East Greenland. Pt. III. The petrology of the Skaergaard intrusion, Kangerdlugsuaq, East Greenland: *Medd. om Gronland,* **105,** no. 4, 1–352.

WAGER, L. R., AND MITCHELL, R. L. (1951), The distribution of trace elements during strong fractionation of basic magma—a further study of the Skaergaard intrusion, East Greenland: *Geoch. Cosm. Acta,* **1,** 131–208.

YODER, H. S. (1950), The jadeite problem, part I: *Am. J. Sci.*, **248,** 225–248.

Manuscript received Jan. 12, 1954

SYNTHETIC ZINC SULFIDE POLYTYPE CRYSTALS*

Lester W. Strock and Vincent A. Brophy, *Sylvania Electric Products Inc., Bayside, Long Island, New York.*

Abstract

Polytype crystals of ZnS or SiC consist of structures based on unit cells whose [*c*] axis spacing is some multiple of the number of layers on one atom sort contained in the simple hexagonal (2-layer) or rhombohedral (3-layer) polymorph prototypes. Known examples of polytypism in ZnS and SiC are summarized, and their genesis as a result of introducing periodic breaks in the stacking sequence of hexagonal layers is emphasized, as distinct from occasional or random (non-periodic) breaks which produce diffuse scattering of *x*-rays. Vapor phase grown ZnS crystals have complex growth habits and are shown to consist of mixed structures in the majority of cases regardless of external morphology, so that coalescence of different structures in our synthetic crystals is on a much finer scale than observed for the natural ZnS polytypes or for SiC. In addition to intimate mixtures of 2- and 3-layer structures—wurtzite and zincblende (or rhombohedral, Buck and Strock) —the vapor phase grown crystals also show the Frondel and Palache 4- and 6-layer polytype structures as minor phases in the same crystal. In one small crystal (0.01×0.1 mm), 2-, 3-, 4-, 5-, 6-, 7-, 8-, 9-, and 11-layered structures have been observed. Many crystals show very intense diffuse *x*-ray reflections for planes in zones for which $(h+2k)$ is not divisible by 3, which is not observed in the natural polytypes, but in natural wurtzite crystals from Thrace by Jagodzinski and Laves. The development of a *TB* system of notation is introduced as a means of relating periodic sequence breaks to polytype structures. This is based on the orientation of ZnS_4 tetrahedra in adjacent layers of the structure—and is generally applicable to similar structures. The value N^* defines the layer where a break occurs and for each value of N^* a specific structure is derived. It is being related to impurity content of crystal growing atmospheres and growth habits.

Polytypism in Zinc Sulfide

The three new crystal modifications of zinc sulfide, recently reported by C. Frondel and C. Palache (1) are the structural equivalents of three well known silicon carbide structures. In the nomenclature of L. Ramsdell (2) they are *4H* and *6H* (i.e. four and six layer hexagonal lattice unit cells) and *15R* (i.e. a five layer rhombohedral lattice unit cell, but referable for comparison with the others to a 15-layer hexagonal cell). Crystals in which these structures have been identified were discovered in clay-ironstone concretions near Etna, Allegheny County, Pennsylvania, by D. M. Seaman and H. Hamilton (3).

Frondel and Palache have described their new ZnS structures as *polymorphs*, and Ramsdell continually refers to the SiC modifications interchangeably as *types* or *polymorphs*. In the present paper we adhere to the suggestion of N. W. Thibault (4) and follow Baumhauer (5) in referring to the various modifications of ZnS and SiC as polytypes or as

* Paper presented at Toronto meeting of The Mineralogical Society of America, Nov. 11, 1953.

examples of "polytypism." Frondel and Palache have stated that ordinary wurtzite is the prototype of the "polymorphs" described by them. Their statement is true for the *4H* and *6H* structure but is not true for *15R*, since the latter is based on a rhombohedral lattice. The prototype of *15R* would be, at the time of their paper, a hypothetical rhombohedral modification of ZnS. Since a simple *3R* polymorph of ZnS has now been discovered and reported by D. Buck and L. W. Strock (6), we have a more complete understanding of their structural relationship and can use a more restricted nomenclature in describing them. Specifically, we restrict the term *polymorph* to structures characterized by different lattices; for example, in ZnS these are cubic face centered *sphalerite*, hexagonal close packed *wurtzite* and rhombohedral (*new modification found in vapor phase grown crystals*). The term *polytype* is any possible structural modification which alters the [*c*] axis dimension of the smallest unit cells referable to the above lattice types by some multiple of a single layer, in the case of ZnS and SiC, without altering the structure in the plane perpendicular thereto. This is simply a more precise restatement of Baumhauer's definition of "polytypism"* in light of more recent knowledge regarding these structures. Structures based on the smallest unit cells of the polymorphs are thus prototypes of the polytypes. Consideration of any more general aspect and examples of polytypism will be discussed elsewhere. Doubling or trebling the [*c*] axis spacing produces 4-layer and 6-layer polytypes respectively from the *prototype wurtzite* in case of ZnS, and from a *hypothetical*† *2-H prototype* in case of SiC. The prototype of a 15-layer polytype is the new rhombohedral polymorph in the case of ZnS. We have not seen any reference to the corresponding polymorph of SiC.

Our work on ZnS crystals grown from the vapor phase has shown that the phenomenon of polytypism, in case of natural ZnS, is only one limited phase of the much broader problem of its crystal growth and that there is not complete parallelism between the structural phenomena exhibited by ZnS and SiC.

Polytypism in Silicon Carbide

Many more polytypes have been discovered for SiC than for ZnS,

* "Polytypism" is defined by Baumhauer (p. 253) as a special example of polymorphism whereby different crystallographic and molecular structures of a substance, and thus essentially different modifications, are involved; for which, however, the axial ratio remains unchanged so that only a difference in crystal habit seems to exist. It should be noted that Baumhauer's original definition is based on a critical study of the crystal faces observed on 3 types of SiC, and their internal symmetry as determined by *x*-ray Laue photographs and not on structural studies or even cell size measurements.

† No *2-H* or wurtzite type SiC structure has been reported.

e.g. 14 are listed by L. S. Ramsdell and J. A. Kohn (7). The 14 modifications are: cubic; four hexagonal polytypes *4H*, *6H*, *8H*, *10H;* and nine rhombohedral polytypes *15R*, *21R*, *27R*, *33R*, $51R_a$, $51R_b$, *75R*, *84R* and *87R*. L. S. Ramsdell and R. S. Mitchell (8) have since reported a *19H* structure, and announced the existence of 141, 168, 192 layer structures based on a rhombohedral lattice as determined on Buerger precession films. Further, G. S. Zhdanov and Z. V. Minervina (9) have reported a rhombohedral modification with 270-layers, and G. Honjo, S. Miyake and T. Tomito (10) a 594-layer rhombohedral structure. There is, thus, experimental evidence for the existence of at least 20 different SiC structures at present. These include the modifications described by Baumhauer as Types I, II, and III, which are the above listed *15R*, *4H*, and *6H*, respectively.

Polytypism as Example of Periodic Breaks in Hexagonal Stacking Sequence

The various polytypes may be derived from their prototype polymorphs by the introduction of breaks in the normal stacking sequence of the prototypes at periodic intervals along [*c*]. For example, breaking the hexagonal wurtzite sequence *ABABAB* to *ABACABAC* . . . generates the *4H* polytype sequence *ABAC*. Similarly, breaking the sequence *ABC ABC A* . . . (which is cubic) to *ABCACBA* . . . generates the *6H* hexagonal polytype sequence *ABCACB*. These relationships are conveniently and clearly visualized, as done by L. S. Ramsdell (2), by plotting the positions of either atom sort of the structure on the plane $(11\bar{2}0)$, and drawing lines between nearest neighbors in adjacent horizontal layers intersecting this plane. The lines drawn (with exception of cubic or *3R*) are zigzag or Ramsdell diagrams. The five layer rhombohedral ZnS polytype thus consists of breaks at the third and fifth layers, in the otherwise linear sequence of cubic or simple rhombohedral structures. The 16th layer begins a fourth 32-sequence cycle at the same geometrical type of position, so that a 15-layer hexagonal cell may also be used to describe this structure. It is designated as *15R* to state both the number of layers in the equivalent hexagonal cell, and that its lattice is rhombohedral.

We may look upon these sequence breaks as disorders in the fundamentally simple sequence of stacking up hexagonal net layers. In the case of the natural ZnS polytypes such disorders are highly periodic, i.e. an *ordered disordered*. This is also true of SiC structures.

Random Breaks in Stacking Sequence in ZnS

H. Jagodzinski and F. Laves (11) called attention to an apparent dif-

ferent sort of disorder in natural wurtzite from Thrace, which causes elongation of x-ray diffraction single crystal reflections from certain planes. Other spots in their spectra were identified as produced by twins oriented with respect to the main specimen. The cause of the diffuse x-ray reflections was attributed to disorder in the [c] direction of the wurtzite crystals, and designated as "one dimensional disorder." Jagodzinski and Laves recognized their observation on natural wurtzite to be an example of the same phenomenon encountered by O. S. Edwards and H. Lipson (12) on heat treated samples of powdered cobalt, and studied theoretically by A. J. C. Wilson (13). The theoretical treatment of this problem has been extended by H. Jagodzinski (14, 15, 16). Both theoretical treatments concentrate on explaining the diffuseness of x-ray reflections as a result of the probability that a stacking fault (i.e. a break in the characteristic and repeating sequence of the structure) occurs on the average at some given number of layers in the structure. The entire emphasis on these treatments has been on random stacking faults.

Simultaneous Occurrence of Polytypes and Random Stacking in ZnS Grown from Vapor

If an ordered stacking sequence break in wurtzite generates definite polytype structures in one environment (as in the Frondel-Palache polytypes) and random stacking sequence breaks generates "one dimensional disordered" crystals (as in the Jagodzinski-Laves crystals) from another environment, then it is not surprising to discover both phenomena occurring together in crystals grown in a third environment under different conditions. We have actually encountered this condition in studies of synthetic crystals of ZnS grown from the vapor phase by F. Kremheller and D. Bracco of the Physical Chemistry Section, Physics Laboratories, Sylvania Research Center, as well as in crystals grown in vacuum by us.

H. Müller (17) has expanded the Jagodzinski treatment of relating diffuse scattering to stacking faults in crystals by introducing two constants into the x-ray intensity formula which express the probabilities that the crystal will continue to develop either a 2- or a 3-layer structure as it adds new layers during its growth. Müller's work represents an improvement over Jagodzinski in so far as a 4-layer polytype is actually used in his intensity calculations, and the intensity of its x-ray reflections are handled on the same basis as the 2- and 3-layer structures. Müller finds that it is possible to relate α and β probability values for a few crystals such that not only calculated intensities for peak reflections agree well with experimental observations on mixed polytypes, but that the calculated intensity distribution along rows of constant hk connecting

these peaks resemble the experimentally observed ones. However, the majority of Müller's crystals, he admits, cannot be interpreted by his theoretical formula. Müller's paper contains single crystal x-ray photographs which reveal the co-existence of mixed polytypes and random disorder along [c] in ZnS. He states that he finds the Frondel and Palache 15-layer structure, which we have not found to date. We had observed the co-existence of mixed polytypes and random disorder on [c] before the appearance of Müller's paper.

Some Experimental Data on Vapor Phase ZnS Crystals

We report here the following summary of those portions of our data which contribute to a more complete understanding of the ZnS structure problem as reviewed above.

(1) *External Morphology and Growth Habit:* Many crystals tend to form interpenetrating sets of thin plates at an early state—some so oriented as to be planes of one single crystal, while others belong to different crystal individuals twinned in various ways. The subsequent growth then proceeds on, or between these initial planes to incorporate them more or less completely into a crystal mass showing many re-entrant angles and angular flutings in the zone of the hexagonal axis, and complex terraces parallel to the hexagonal basal plane. There is no suggestion of cubic symmetry or habit on any crystal so far examined regardless of internal structure shown by x-rays. The highly developed striation of faces is due to the crystal growing through stacking up thin crystal plates of hemimorphic symmetry each imperfectly registered with its neighbor. Goniometer measurements and morphology studies are naturally very difficult on such crystals. The most complex crystals were those grown in open gas stream tube furnaces in atmospheres of H_2S with hydrogen or argon from sublimed ZnS powders. The only crystals showing simple growth habit were those grown from pumped or unpumped evacuated systems.

The morphology of our synthetic ZnS crystals will be reported in more detail when the relations between morphology and internal structure can be more fully described.

Angle tables of observed forms will be published then. In the meantime, characteristic growth habits are illustrated by the four drawings of actual crystals of Fig. 1, in which complete indices for all faces are given for the orientation of axes selected.

The position of both Miller-Bravais axes (a_1 and a_2) and gnomonic axes p and q are indicated in the top plan drawing of each crystal. The indices refer to a 2-layer hexagonal (wurtzite) cell, so oriented as to make the pyramids of 43° 21′ and 62° 05′ the (10.2) and (10.1) forms respec-

tively, the orientation used in Dana's (18) Seventh Edition, which fixes the common pyramid form observed on many of our crystals as (10.4).

Crystal 1*A* is representative of many crystals examined, in that the morphology is different for different parts of an individual crystal. The differences in external morphology can, at times, be correlated with differences in internal structure. In this example, the lower thicker portion of the crystal consists of a 3-layer structure, while the top consists of a mixture of 2-, 3-, 4- and 6-layer structures. The entire crystal is slightly under 1 mm. in length, is colorless and very transparent. Fine striations, parallel to the edges of the basal plane, encircle the entire crystal with the exception of the vertical faces of the top portion. Note that the prominent vertical forms $(2\bar{1}.0)$ and $(\bar{1}2.0)$ of the lower 3-layer structure portion are absent in the top mixed structure portion, while the prominent (10.0) and (01.0) forms of the top are absent (or nearly so) on the bottom portion. The prominent forms of the top are rotated 30° with respect to the prominent bottom forms. The deeply striated faces lead to complex multiple signals on the optical goniometer due to their diffraction grating behavior; so that it is frequently necessary to use narrow line signals and monochromatic light to determine the true angles on such crystals.

The crystal of Fig. 1*B* illustrates the origin of many of the typical striations present. The crystal, approximately 1 mm. high, is obviously built up of individual thin plates stacked perpendicular to [*c*]. Each plate, as revealed by the detail at each corner, preserving the morphology and symmetry of the whole crystal, namely, terminated on one end by pyramids of the form $(1\bar{1}.4)$ and on the other by $(00.\bar{1})$ while joined on their basal planes. The separate faces present on the corner of the illustration continue around the entire crystal accounting for its finely striated surface which extends to all faces, including the terminal tip of the crystal. Internally the crystal is colorless and transparent. It is a further example of the terraced habit illustrated in Fig. 1*A*, and occurs in the same lot of material. It is composed of only 3-layer structure but there is no trace of cubic habit.

The crystal of Fig. 1*C* illustrates further examples of striation, not necessarily due to the same cause as in Fig. 1*B*, and lack of cubic growth habit in spite of 3-layer internal structure. To what extent this is due to the 3-layer structure actually being the newly discovered rhombohedral phase, has not yet been determined. In Fig. 1*C*, the terminal faces are not striated, and the basal plane is a good reflecting surface, but frequently not 90° from the vertical zone faces. Its ρ angles vary in different individuals from the same preparation from a few minutes to 1° 40′.

SYNTHETIC ZnS CRYSTALS

VAPOR PHASE GROWN

WURTZITE INDICES

A

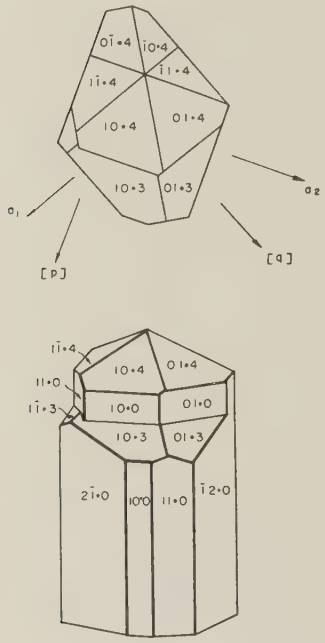

Body: 3-Layer Structure

Tip: Mixture of 2+3+4+6 Layer Structures

All Faces Striated ⊥ to [c], Except Vertical Zone of Tip.

B

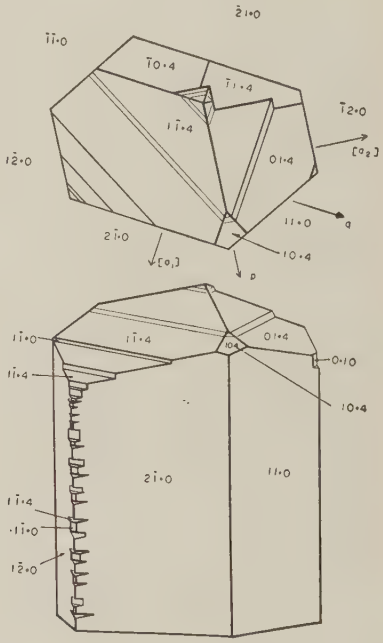

3-Layer Structure

Deep Striations Encircle Crystal ⊥ to [c].

Composed of Many Thin Crystals and Coalesced on (001).

FIG. 1

The unique and characteristic feature of this crystal is the protruding edge which, as is evident by reference to the indexed plan drawing, is the rudiment of a (10.0) tabular habit containing the a_2 and [c] axes of the crystal. The large number of faces in the [c] axis zone make these small crystals almost cylindrical in cross section and the identification of forms difficult, especially in the region of the protruding (10.0) plate. Other crystals have developed many similar protruding plates parallel to other forms, making the vertical zone of such crystals a complicated series of vertical grooves and ridges with dozens of extremely narrow faces. Obviously these fluted crystals cannot be measured accurately. Under the microscope they reveal a remarkable uniformity in the manner in which their horizontal striations cut across all the vertical surface details at

C

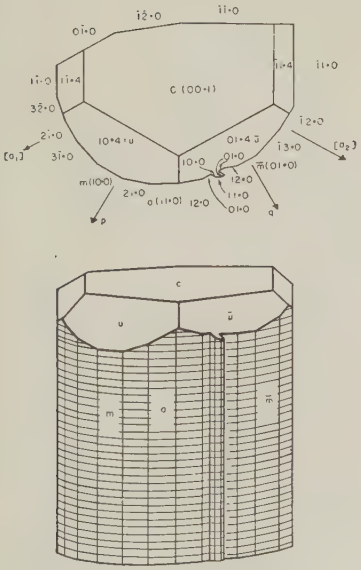

3-Layer Structure Single Crystal with Protruding (100) Face.

D

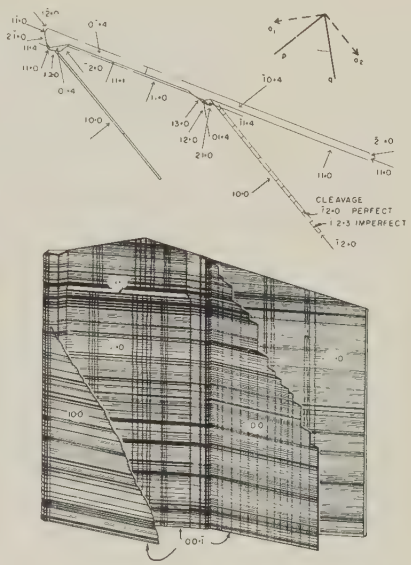

3-Layer Structure Single Crystal Containing 2 Plate Habits and Thin Prismatic Crystal 11[c] Often Developing as Individual Habits.

FIG. 1

the same height in the crystal, as illustrated for the single protruding (10.0) plate in Fig. 1*C*. The tendency to develop with only 5 of the 6 possible terminal faces of the same form is a very constant feature of this and many other lots of crystals.

The crystal of Fig. 1*D* also shows a pure 3-layer internal structure. Shown in comparable orientation and indexed, like the other on a *2-H* cell, the unique feature pointed out for crystal 1*C* is developed to an extreme degree in 1*D*. The crystal has developed two tabular habits to similar extents; one parallel to (10.0), (already shown as a protruding plane in 1*C*) and the other parallel to (11.0). The former is approximately 10 μ and the latter approximately 15 μ thick. This is not a twin, as shown by x-ray measurements on each portion. The two thickened portions shown in the drawing represent regions where the material is tending to produce an independent, but slender, individual of the same habit as the crystal shown in Fig. 1*C*—including elongation on [*c*], horizontal striations, the same terminal forms (*u*), and the protruding (10.0) plate. The principal portion of the crystal (11.0) plate is terminated on top by

two (u) faces and on the bottom by a basal plane. Although this crystal measured approximately 2 mm. in width, the thin (10.0) wing (plate 10 μ thick) was only 18′ off from its theoretical angle of 30° from (11.0). The two (01.4) faces on the two separated thickened portions differed only by 4′ in measured V angle on the goniometer. The vertical ($\bar{1}$2.0) cleavage is perfect, requiring only little pressure to break narrow strips from the entire length of the crystal. The imperfect cleavage indexed as ($\bar{1}$2.3) is estimated from microscopic observations, as no measurements could be made on the cleavage surfaces. The wavy vertical lines indicate a local thickening of the crystal which does not progress to the point of developing definite reflecting faces. This drawing shows the single unit form (11.1) of wurtzite which was observed in a total of many hundreds of faces measured. Finally, the extreme regularity with which the horizontal striations continue at the same height of the crystal, extending to all lateral developments, is illustrated in Fig. 1*D*. These were observed by ordinary binocular microscopic visual observation, and on high magnification reflected light micrographs. Crystals representing each unit of this complex habit were observed in the same crystal preparation. Other equally characteristic and unique examples of morphology, growth habit, and twinning will be presented in a later paper.

(2) *X-ray Examination of Single Crystals:* A few crystals are found with a 3-layer spacing only on [c]. These were all, early in our work, listed as cubic structure, as they were by all previous workers who used powder methods. Many such 3-layer structures are undoubtedly actually rhombohedral in light of our most recent results. A few other crystals show a 2-layer spacing only on [c], and are accordingly hexagonal. More frequently both 2- and 3-layer structures are present in varying proportions in a crystal which, microscopically, appears to be a uniform crystal entity. A striking characteristic of the crystals grown from gas-streams at atmospheric pressure by A. Kremheller of these laboratories, is that minor amounts of 4- and 6-layer structure also occur frequently in the same individuals containing 2- and 3-layered structure as their major structural component. It has already been pointed out that the top portion of the crystal illustrated in Fig. 1*A* has such a mixed structure. One quadrant of a single crystal rotation photograph about the [c] axis of this tip is reproduced in Fig. 2. First layer line reflections corresponding to four different structures are observed. Those from the 3-layer structure are most intense while those from the 6-layer structure are weakest. The disordered portion of the crystal accounts for the diffuse reflections appearing to join the reflections from (10l) (01l) and (20l) (02l) into an approximate continuous ring, while the (11l) reflections are sharp in comparison and are not joined into a continuous ring of diffuse reflections.

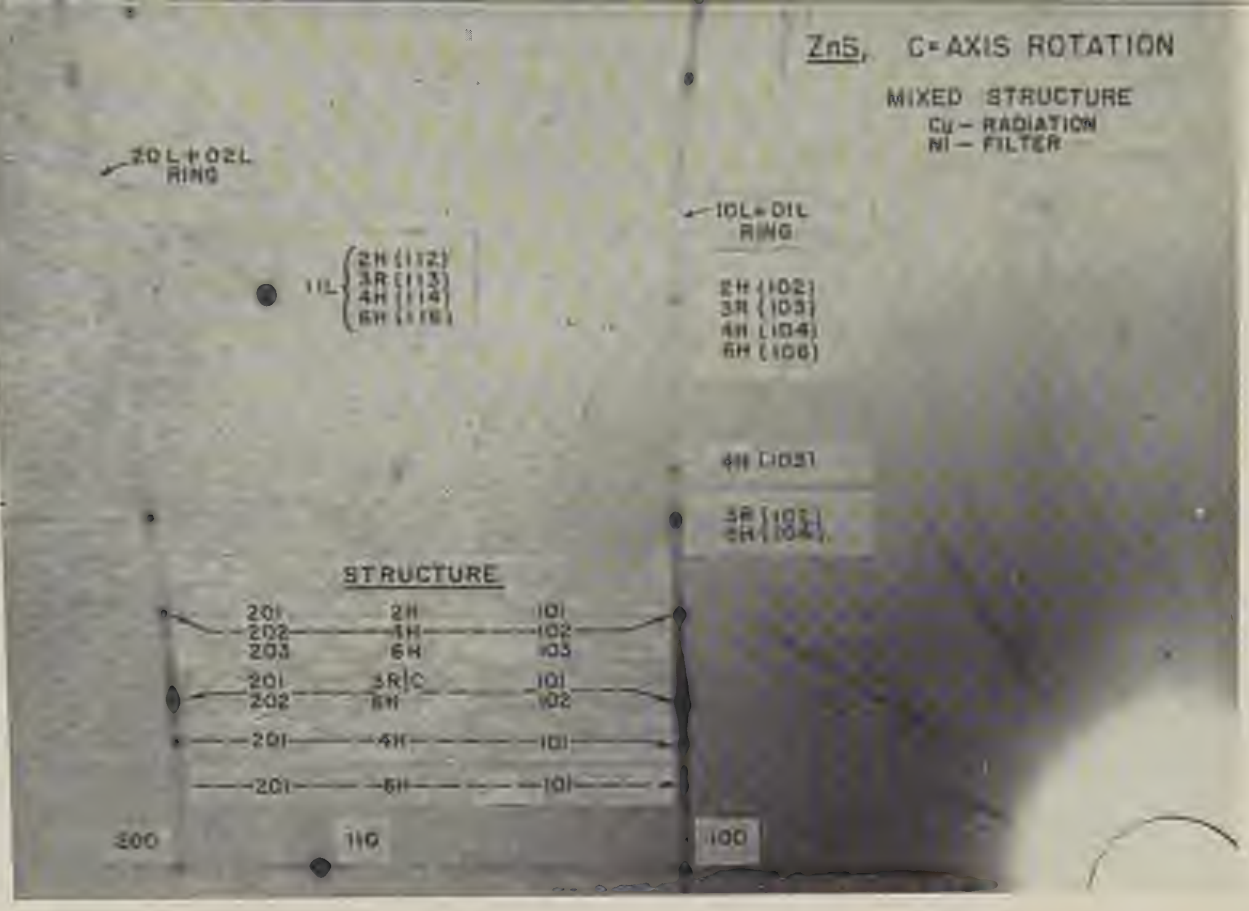
ZnS, C-AXIS ROTATION
MIXED STRUCTURE
Cu – RADIATION
Ni – FILTER
20L+02L RING
10L+01L RING
11L
2H (112)
3R (113)
4H (114)
6H (116)
2H (102)
3R (103)
4H (104)
6H (106)
4H (103)
3R (101)
2H (104)
STRUCTURE
201 2H 101
202 4H 102
203 6H 103
201 3R|C 101
202 6H 102
201 4H 101
201 6H 101
200
110
100

FIG. 2

The diffuse reflections thus lie in zones containing planes for which $h+2k$ is a number not divisible by 3, while sharp reflections lie in zones where $h+2k=n$ (3), where n is an integer or zero.

Crystals grown in evacuated systems by us have so far shown only a small amount of 6-layer structure (no 4-layer) which is distributed more randomly and in smaller parcels thoughout the crystal than in case of crystals grown by Kremheller at atmospheric pressure. One small crystal (approximately 0.01×0.1 mm.) contained nine different structures: i.e. 2-, 3-, 4-, 5-, 6-, 7-, 8-, 9-, and 11-layered ones. The temperature of transition, and stability range of these various structures (including the cubic-hexagonal) is still being studied; as the problem is now confused by the discovery of the previously unrecognized rhombohedral intermediate phase, as well as by the unknown influence of specific impurities.

(3) *Derivation of Polytype Structures by Periodic Sequence Breaks:* Because of the large number of polytypes which have been observed in both ZnS and SiC, considerable thought has been given to the manner in which they are generated. Obviously they can form by a periodically repeated break in the basic stacking sequence, as stated above. There are two such sequences; namely, one with a periodicity of 2-layers, the other with a 3-layer periodicity on [c]. To examine the consequence of such breaks in terms of the three termed ABC notation is difficult. A convenient notation has been developed in a two termed TB notation. This TB notation states the orientation of the ZnS_4 tetrahedra in adjacent (001) planes of all hexagonal close packed structures, and of cubic close packed structures in comparable orientation. In a 2-layer structure the tetrahedra are oriented differently in adjacent layers, which is designated as a TB structure. In structures containing $TBTB$ . . . sequences, the tetrahedra have one face (three corners) in the (001) plane and an apex (the fourth corner) in an adjacent plane. This fourth corner belongs to a group of three corners of a tetrahedron face in the adjacent (001) plane. The tetrahedra faces are rotated 60° in the second plane (T orientation) with respect to the first plane (B orientation). In a 3-layer structure, the tetrahedra faces are all in the same orientation in adjacent (001) planes. The former, with a (TB) structure, is thus designated as possessing a *rotated sequence;* and the latter, with a (TTT . . . or BBB . . .) structure, as possessing a *parallel sequence* throughout the entire crystal in case of a pure homogeneous structure type.

We have examined the consequence of introducing breaks in each type of sequence at a progressively greater number of layers out from the initial growth layer. It is readily shown that for each type of sequence, and for each position of sequence break (N^* = number of layers from zero layer at which a break occurs), the structure will be represented by either

a hexagonal or rhombohedral lattice with a finite number of layers in its unit cell characteristic of N^*.

For example, breaking the *rotated sequence* at $N^*=2, 4, 6, 8, \ldots$ produces structures based on a hexagonal lattice with unit cells of 4-, 8-, 12-, 16-layers. Breaks at $N^*=1, 3, 5, 7, \ldots$ produce structures based on rhombohedral lattices with unit cells of 1-, 3-, 5-, 7-layers (or expressed on a hexagonal lattice with cells of 3-, 9-, 15-, 21-layers).

Corresponding breaks in the *parallel sequence* at $N^*=1, 2, 3, 4, 5, \ldots$ generates structures based on hexagonal cells, containing 2-, 4-, 6-, 8-, 10-layers.

The consequence of breaking these fundamental sequences in crystals growing in both directions along [*c*] have also been examined, but the results are beyond the scope of this paper. A corresponding study is underway for relating polytype structures to disorders created in a crystal already in the solid state.

We want to emphasize here our belief and preliminary observations that the value of N^* is determined primarily by the impurities in the crystal growing atmosphere. It is the first particle to attach at a growing surface which determines the structure over the entire area to which growth extends from this initial growth center, and if this particle happens to be an impurity particle, it may break an already established sequence. The kinetics of the growth process, and its relation to structure is being studied in different ZnS crystal growing atmosphere compositions.

Conclusions

Our studies on polytype genesis have pointed up the close relationship between random disorder and "ordered disorder" in ZnS crystals, and emphasized the need for further studies on the role of mixed polytype structures on external morphology and physical properties of zinc sulfide.

References

1. Frondel, Clifford, and Palache, Charles, Three new polymorphs of zinc sulfide: *Am. Mineral.*, **35**, 29–42 (1950).
2. Ramsdell, Lewis S., Studies on silicon carbide: *Am. Mineral.*, **32**, 64–82 (1947).
3. Seaman, David M., and Hamilton, Howard, Occurrence of polymorphous wurtzite in western Pennsylvania and eastern Ohio: *Am. Mineral.*, **35**, 43–50 (1950).
4. Thibault, Newman W., Morphological and structural crystallography and optical properties of silicon carbide (SiC): *Am. Mineral.*, **29**, 249–278; 327–362 (1944).
5. Baumhauer, H., Über die vershiedenen Modifikationen des Carborundums und die Erscheinung der Polytypie: *Zeit. Krist.*, **55**, 249–259 (1915).
6. Buck, D. C., and Strock, Lester W., Trimorphism in zinc sulfide: *Am. Mineral.*, **39**, 318 (1954).
7. Ramsdell, L. S., and Kohn, J. A., Developments in silicon carbide research: *Acta Cryst.*, **5**, 215–224 (1952).

8. Ramsdell, L. S., and Mitchell, R. S., A new hexagonal polymorph of silicon carbide, 19H: *Am. Mineral.*, **37,** 56–59 (1953).
9. Zhadnov, G. S., and Minervina, Z. V., *J. Exp. Theor. Physics*, **17,** 3 (1947).
10. Honjo, G., Miyake, S., and Tomita, T., Silicon carbide of 594 layers: *Acta Cryst.*, **3,** 396–397 (1950).
11. Jagodzinski, H., and Laves, F., Eindimensional Fehlgeordnete Kristallgitter: *Schweiz. Min. u. Petrogr. Mitteilungen*, **28,** 456–467 (1948).
12. Edwards, O. S., and Lipson, H., Imperfections in the structure of cobalt (I) Experimental work and proposed structure: *Proc. Roy. Soc. Lond.* [A]**180,** 268–277 (1942).
13. Wilson, A. J. C., Imperfections in the structure of cobalt (II). Mathematical treatment of proposed structure: *Proc. Roy. Soc. Lond.* [A]**180,** 277–285 (1942).
14, 15, 16. Jagodzinski, H., Eindimensional Fehlordnung in Kristallen und ihr Einfluse auf die Röntgeninterferenzen: *Acta. Cryst.*, **2,** 201–207; 208–214; 298–304 (1949).
17. Müller, Hermann, Die eindimensionale Umwandlung Zinkblende-Wurtzite und die dabei auftretenden Anomalien: *Neues Jb. Min. Geol. u. Pal.*, **84,** 43–76 (1952).
18. Dana's System of Mineralogy, 7th Ed., New York, N. Y., Vol. 1, p. 227 (1944).

Manuscript received Jan. 11, 1954

THE QUANTITATIVE ESTIMATION OF KAOLINITE BY DIFFERENTIAL THERMAL ANALYSIS

A. R. Carthew, *Division of Building Research, Commonwealth Scientific and Industrial Research Organization, Melbourne, Australia.*

Abstract

The effect of variations in the amount, particle size, and degree of crystallinity of kaolinite on the area and shape of the endothermic peak at about 600° C. in the differential thermal curve of this mineral has been investigated. An empirical relationship has been established between the slope ratio of the peak and the ratio of the area to the width of the peak at half its amplitude and provides a method of quantitatively estimating kaolinite, regardless of its particle size distribution and degree of crystallinity.

Introduction

In the examination of clays by the differential thermal method of analysis, the kaolinite content of a sample has often been estimated from the area of the endothermic peak at about 600° C. on the differential thermal curve. This has been justified by the theoretical work of Speil (1944) and Kerr and Kulp (1948) who have shown that the area of a peak on a differential thermal curve is proportional to the mass of the reacting substance. However, these theories do not take into account the effect of the degree of crystallinity and particle size of a substance upon the heat of reaction. The theoretical work of Shearer (1949) suggests that changes in particle size in the colloid range would have little influence on the heat of reaction, but Speil (1944) has found that the area of the endothermic peak at about 600° C. on the differential thermal curve of kaolinite decreases with decreasing particle size of the kaolinite. Grim (1947) has found that variations in size and perfection of crystallinity of particles of kaolinite appear to be reflected in variations in the intensity of the thermal reactions of the mineral. Also, Cole and Carthew (1953), in determining the kaolinite content of some clays, were not able to obtain agreement between estimates from differential thermal curves and those from chemical analyses without assuming that kaolinites of different degrees of crystallinity and/or particle size distribution have different heats of dehydration.

The effect of the degree of crystallinity and particle size distribution of kaolinite on the endothermic peak of the differential thermal curve has therefore been investigated and a method is proposed for quantitatively estimating kaolinite, regardless of these factors.

Equipment and Procedure

The method of differential thermal analysis has been described in detail by Norton (1939), Grim and Rowland (1942) and others. The dif-

ferential thermal analysis equipment used in this investigation is that described by Carthew and Cole (1953) except that the sample block is now of 24-12 W (chromium-tungsten) heat-resistant steel, which does not scale or deform as did the 18-8 stainless steel previously used.

The procedure for packing the sample into the block was modified to ensure that the sample was uniformly distributed through the sample cavity. The sample was first packed into a hole of similar size to the sample cavity in a separate steel block, and, if necessary, calcined alumina was added to produce the usual tightness of packing obtained with finger tamping. The sample and calcined alumina were then removed from the hole and intimately mixed before being packed into the sample cavity. The rate of heating was 10° C. per minute.

The Effect of Various Factors on the Differential Thermal Curve of Kaolinite

In this paper, kaolinite refers only to the mineral of that name and does not include the minerals "fireclay" and halloysite. The differential thermal curve of kaolinite shows a large endothermic peak at about 620° C. and an intense exothermic one at about 980° C. The endothermic reaction is the loss of (OH) from the kaolinite structure and the exothermic reaction is the crystallization of γ-alumina from the amorphous product of the decomposition of the kaolinite. In addition to these two peaks, the differential thermal curve of very well crystallized kaolinite shows a slight endothermic dip immediately before the exothermic peak. This reaction is the breakdown of the meta-kaolin structure which remains after the dehydration of the kaolinite.

(1) *Amount*

To study the effect of varying amounts of kaolinite on the endothermic peak at about 620° C., differential thermal curves were prepared (Fig. 1) from different weights of a fairly pure kaolinite (checked by x-ray examination) from Gordon, Victoria. This kaolinite is well crystallized, as shown by its differential thermal curve (*A*, Fig. 1).

The areas of the endothermic peaks of the differential thermal curves were measured by planimeter and are set out in Table 1. From Fig. 2 it can be seen that the relation between the area of the peak and the weight of kaolinite is not strictly linear. This departure from linearity is due to the variation of the thermal conductivity of the material in the sample cavity with different weights of kaolinite.

The shape of the endothermic peak was determined by measuring the ratio of the slope of the low temperature to the high temperature sides of the peak (the slope ratio) and the width of the peak at half its amplitude

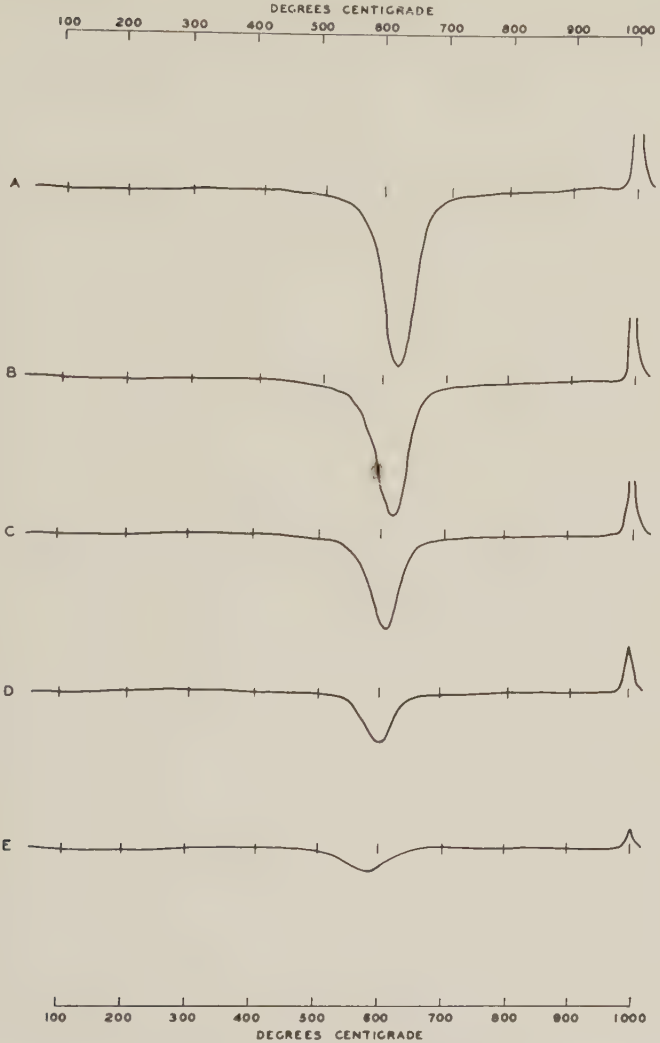

FIG. 1. Differential thermal curves of various weights of kaolinite. *A*, 0.8g; *B*, 0.65g; *C*, 0.5g; *D*, 0.3g; *E*, 0.15g.

(henceforth referred to as the width of the peak). The slope ratio was measured by the method of Bramao *et al.* (1952), the slope of the sides being taken as that of the tangents to the sides from the deepest point of the peak. The slope ratios and widths of the endothermic peaks of the curves shown in Fig. 1 are listed in Table 1, except for curve *E* in which the peak was too shallow for accurate measurement. The slope ratio ap-

Table 1. Characteristics of the Endothermic Peak for Various Weights of Gordon Kaolinite

Weight	Area of Peak	Slope Ratio	Width of Peak	Ratio A/W
0.8g.	11.9 sq. cm.	1.18	1.46 cm.	8.15
0.65	9.35	1.24	1.41	6.63
0.5	6.3	1.24	1.29	4.88
0.3	3.15	1.22	1.20	2.63
0.15	1.5	—	—	

pears to be independent of the amount of kaolinite, whereas the width of the peak decreases with the amount.

(2) *Particle Size*

To examine the effect of variations in particle size on the endothermic peak, the kaolinite from Gordon, Victoria, was separated into various size fractions by sedimentation methods, including the use of a Sharples supercentrifuge. Fractions in which the equivalent diameters of the particles were > 2, 2-1, 1-0.5, 0.5-0.25, and 0.25-0.1 microns were obtained and differential thermal curves were prepared from 0.8 g. of each fraction.

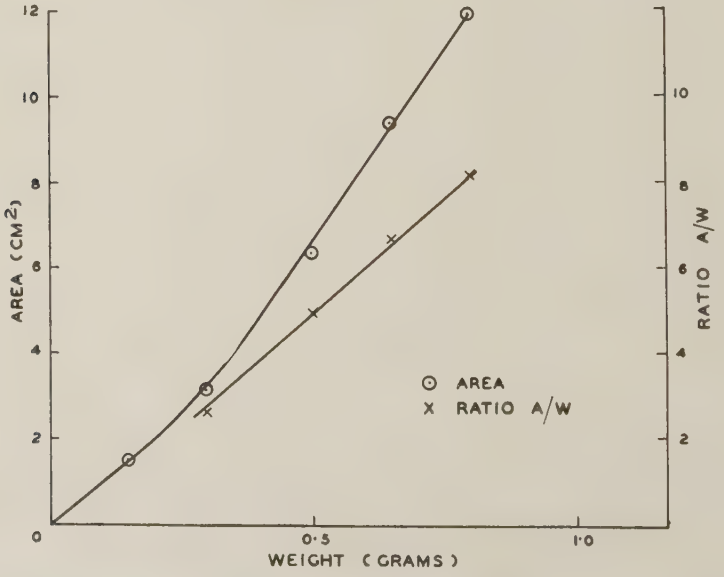

Fig. 2. Relation of the area and the ratio A/W of the endothermic peak to the weight of kaolinite.

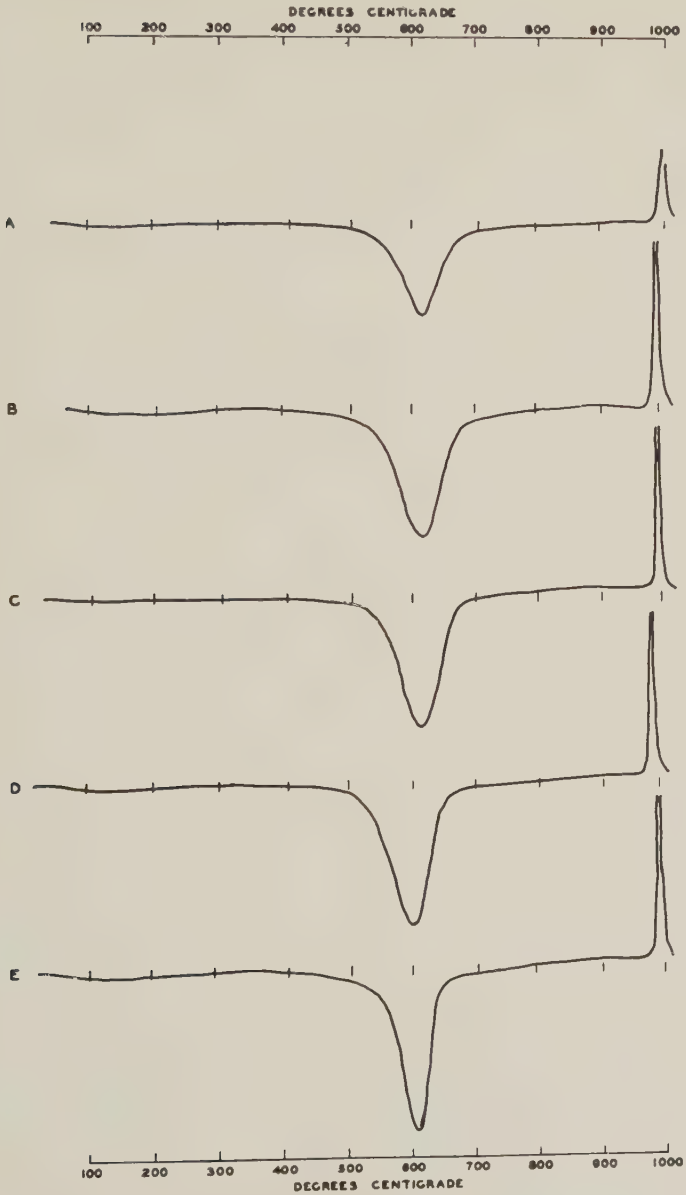

FIG. 3.Differential thermal curves of various particle size fractions of kaolinite. *A*, $>2\mu$; *B*, 2–1μ; *C*, 1–0.5μ; *D*, 0.5–0.25μ *E*, 0.25–0.1μ.

Table 2. Characteristics of the Endothermic Peak for Various Particle Size Fractions of Gordon Kaolinite

Fraction	Area of Peak	Slope Ratio	Width of Peak	Ratio A/W
>2 microns	8.3 sq. cm.	1.25	1.28 cm.	6.48
2–1	11.8	1.25	1.82	6.48
1–0.5	11.9	1.36	1.79	6.65
0.5–0.25	12.4	1.52	1.61	7.70
0.25–0.1	11.5	1.88	1.35	8.52

The kaolinite in every fraction is well crystallized, as can be seen from the differential thermal curves in Fig. 3.

The areas of the endothermic peaks are given in Table 2, and, except for the >2 micron fraction, are very similar. This is contrary to the results of Speil (1944) who has found that the area of the endothermic peak decreases with the particle size of kaolinite. However, Spiel obtained his particle size fractions by a grinding process, which could reduce the degree of crystallinity of the kaolinite. This supposition is supported by the differential thermal curves of his fine particle size fractions. The area of the peak given by the >2 micron fraction cannot be explained by the presence of impurities, as x-ray examination of this fraction has revealed less than 5 per cent quartz as the only impurity.

The slope ratios and widths of the endothermic peaks are listed in Table 2, from which it can be seen that the slope ratio increases as the particle size of the kaolinite decreases whereas the width of the peak, except for the >2 micron fraction, decreases with particle size. This increase in asymmetry of the peak with decreasing particle size has been observed by previous workers. The explanation given by Bramao *et al.* (1952) is that the smaller the particle size of a sample, the greater the number of reaction centres or nuclei formed and the less the amount of kaolinite dehydrated per nucleus. Accordingly, the amount of kaolinite dehydrated by the time the maximum differential temperature is reached (i.e. at the deepest point of the peak) varies inversely with the particle size. Consequently, the return of the differential temperature to zero is faster for the smaller particle size sample, as less kaolinite remains to be dehydrated.

(3) *Degree of Crystallinity*

In this investigation, the term "degree of crystallinity" refers to the perfection of the crystal organization of the kaolinite and not to the size of the crystal.

Table 3. Characteristics of the Endothermic Peak for the 2-1 Micron Fractions of Different Kaolinites

Locality	Area of Peak	Slope Ratio	Width of Peak	Ratio A/W
Gordon, Vic.	11.9 sq. cm.	1.25	1.81 cm.	6.57
S. Aust.	11.0	1.49	1.48	7.43
Langley, S.C., U.S.A.	10.6	1.52	1.34	7.91
Surges Bay, Tas.	10.1	1.56	1.25	8.08
Engadine, N.S.W.	9.7	1.85	1.17	8.29

The effect of variations in the degree of crystallinity of kaolinite on the endothermic peak was studied from samples of five kaolinites from different localities (see Table 3). In order to avoid any effect on the endothermic peaks due to different particle size distributions of these samples, the same particle size fraction of each sample was studied. The 2-1 micron fraction was chosen because the slope ratio varied least in this range of particle size. This fraction was separated from each sample by sedimentation methods and 0.8 g. of it used to prepare a differential thermal curve. The fraction of each sample consisted of fairly pure kaolinite (checked by *x*-ray examination).

The differential thermal curves are shown in Fig. 4 and the areas of the endothermic peaks are given in Table 3. The degree of crystallinity of the kaolinite decreases with the area of the endothermic peak. Previous workers have found that the sharpness of the exothermic peak decreases with the degree of crystallinity of kaolinite, and this effect may be seen in the differential thermal curve of the sample from Engadine (*E*, Fig. 4). This curve also shows an endothermic peak at about 130° C., which is characteristic of poorly crystallized kaolinite and is due to the loss of adsorbed water.

The slope ratios and widths of the endothermic peaks are given in Table 3, the slope ratio increasing as the degree of crystallinity of kaolinite decreases, whilst the width of the peak decreases with the degree of crystallinity. This change in the shape of the peak is very similar to that found with decreasing particle size and may be explained in a similar manner. It is probable that more reaction centres or nuclei are formed in poorly crystallized than in well crystallized kaolinite.

The Quantitative Estimation of Kaolinite

In the quantitative estimation of kaolinite from the endothermic peak of the differential thermal curve, the degree of crystallinity of the kaolinite must be taken into account. This cannot be assessed from the

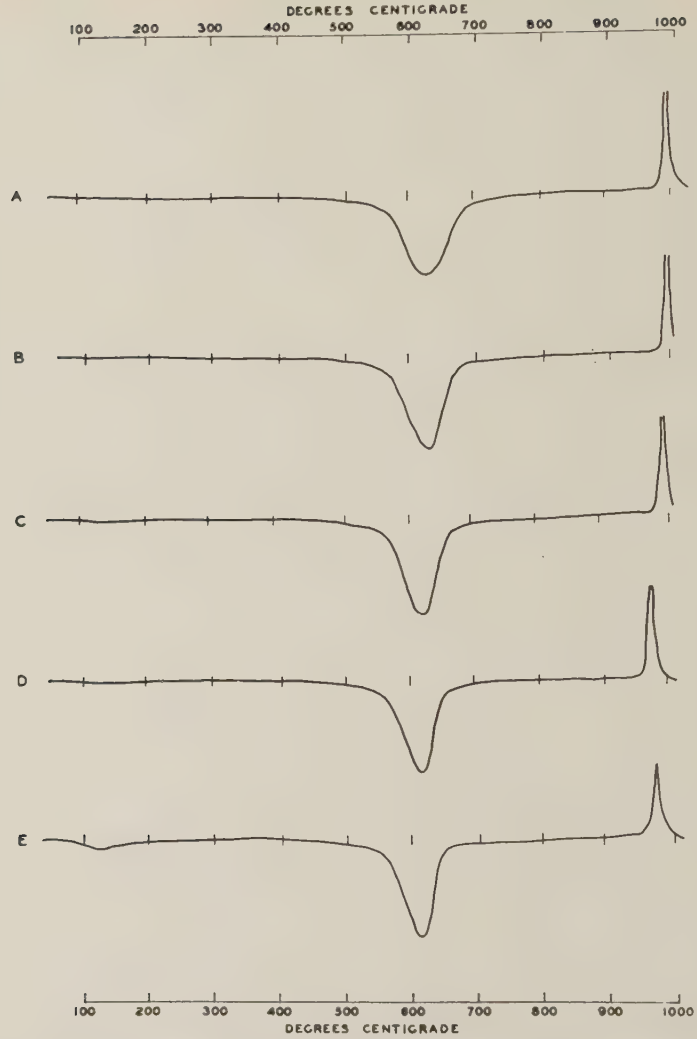

FIG. 4. Differential thermal curves of the 2–1 micron fractions of different kaolinites. *A*, Gordon; *B*, S. Aust.; *C*, Langley; *D*, Surges Bay; *E*, Engadine.

shape of the endothermic peak as the shape is affected also by the particle size distribution of the sample. Furthermore, an empirical relationship between the area of the peak and a characteristic of the shape (such as the slope ratio) is not possible, as the shape of the peak varies with the particle size distribution of kaolinite whilst the area remains constant.

The ratio of the area to the width of the endothermic peak (henceforth referred to as the ratio A/W) has been found to be roughly proportional to the weight of kaolinite (see Fig. 2). From Tables 2 and 3, it is seen that the ratio A/W increases as both the particle size and the degree of crystallinity decrease. Since the slope ratio of the peak also has been shown to increase as the particle size and the degree of crystallinity decrease, the relationship between the slope ratio and the ratio A/W was investigated. The ratio A/W was plotted against the slope ratio for the various particle size fractions and also for the 2-1 micron fractions of the different kaolinites. It was found that one straight line could be drawn through both sets of points (Fig. 5) i.e. the relationship between the ratio A/W and the slope ratio for variations in the particle size of kaolinite is the same as that for variations in the degree of crystallinity. Thus the endothermic peak from 0.8 g. of any kaolinite, regardless of particle size distribution and degree of crystallinity, gives a point on this curve.

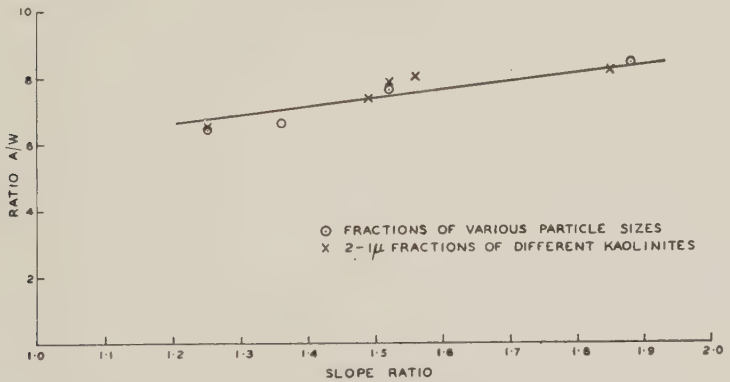

FIG. 5. Relation between the ratio A/W and the slope ratio of the endothermic peak of kaolinite.

Since the ratio A/W has been found to be roughly proportional to the weight of kaolinite, the empirical relationship of Fig. 5 may be used to estimate the kaolinite content of a clay. A differential thermal curve is prepared from 0.8 g. of the clay, the slope ratio of the endothermic peak is measured and the corresponding ratio A/W is read from Fig. 5. The weight of kaolinite in the sample is given by:

$$\frac{\text{Ratio } A/W \text{ (measured from peak)}}{\text{Ratio } A/W \text{ (read from Fig. 5)}} \times 0.8 \text{ grams.} \qquad (1)$$

Estimations by this method of the kaolinite content of clays agree well with those from chemical analyses for both poorly and well crystallized kaolinites. In Table 4 estimations of the kaolinite content of some clays

based on chemical, x-ray and differential thermal evidence (Cole and Carthew 1953) are compared with estimations by the new method and also with estimations based on the area of the endothermic peak without regard to the degree of crystallinity of the kaolinite.

Table 4. Estimations of the Kaolinite Content of Six Clays by Various Methods

Locality of Clay	From Chemical, x-ray and Thermal Evidence*	Using Expression (1)	From Area of Endothermic Peak
St. Helens, Tas. (1)	75%	80%	62%
St. Helens, Tas. (2)	55	59	38
Sth. Mt. Cameron, Tas.	75	76	64
Surges Bay, Tas.	65	61	45
Dover, Tas. (1)	65	64	47
Dover, Tas. (2)	30	32	21

* Cole and Carthew 1953.

Conclusions

The area of the endothermic peak on the differential thermal curve of kaolinite does not give a strictly linear relationship with the weight of the material when calcined alumina is used as a thermally inert material in the sample.

Variations below 2 microns in the particle size of kaolinite appear to have little effect on the heat of dehydration, which decreases with the degree of crystallinity of kaolinite.

The slope ratio of the endothermic peak is independent of the amount of kaolinite, but increases as both the particle size and the degree of crystallinity of kaolinite decrease.

The ratio of the area to the width at half the amplitude of the endothermic peak is practically proportional to the weight of kaolinite and increases as both the particle size and the degree of crystallinity of kaolinite decrease.

The ratio of the area to the width at half the amplitude of the endothermic peak increases with the slope ratio and this empirical relationship provides a method of quantitatively estimating kaolinite of any particle size distribution and degree of crystallinity.

Acknowledgment

The author wishes to thank Dr. W. F. Cole of this Division for suggesting the problem and for helpful advice during the work.

References

Bramao, L., Cady, J. G., Hendricks, S. B., and Swerdlow, M. (1952), Criteria for the characterisation of kaolinite, halloysite, and a related mineral in clays and soils: *Soil Sci.*, **73,** 273–287.

Carthew, A. R., and Cole, W. F. (1953), An apparatus for differential thermal analysis: *Aust. J. Instr. Technol.*, **9,** 23–30.

Cole, W. F., and Carthew, A. R. (1953), The mineralogical composition of some Tasmanian clays: *Pap. and Proc. Roy. Soc. Tas.*, **87,** 1–12.

Grim, R. E. (1947), Differential thermal curves of prepared mixtures of clay minerals: *Am. Mineral.*, **32,** 493–501.

Grim, R. E., and Rowland, R. A. (1942), Differential thermal analysis of clay minerals and other hydrous materials: *Am. Mineral.*, **27,** 756–761; 801–818.

Kerr, P. F., and Kulp, J. L. (1948), Multiple differential thermal analysis: *Am. Mineral.*, **33,** 387–419.

Norton, F. H. (1939), Critical study of the differential thermal method for the identification of the clay minerals: *J. Am. Cer. Soc.*, **22,** 54–63.

Shearer, J. (1949), Recent developments in identification and analysis of crystalline material in powder form: *J. Roy. Soc. W. Aust.*, **35,** 9–25.

Speil, S. (1944), Application of thermal analysis to clays and aluminous minerals: *U. S. Bureau of Mines, Rep. Inv.* **3764.**

Manuscript received Feb. 16, 1954

NOTES AND NEWS

BERYLLIAN IDOCRASE FROM FRANKLIN, NEW JERSEY

Cornelius S. Hurlbut, Jr., *Harvard University, Cambridge, Massachusetts.*

In 1930 beryllium-bearing idocrase from Franklin, New Jersey, was described by Palache and Bauer (1930). Their analysis reporting over 9 per cent BeO and the statement, "It seems highly probable that beryllium is generally present in this mineral but has not been recognized, being determined as alumina" stimulated great interest in idocrase as a possible commercial source of beryllium.

Several analyses of idocrase from different localities have subsequently been made without finding significant amounts of beryllium. Silbermintz and Roschkowa (1933) in testing fourteen idocrases from various localities found only three samples containing beryllium. These ranged from 0.008–0.18 per cent BeO. Meen (1939) reported 1.07 per cent BeO in idocrase crystals from the Great Slave Lake Region, Canada. In connection with a study of helvite and danalite from New Mexico, Glass, Jahns and Stevens (1944) reported 1.09 per cent BeO in idocrase. Spectrographic analysis of this material by Strock gave 1.06 per cent BeO. In 1932 Mr. E. K. Gedney made an extended tour of the western United States in search for beryllian idocrase. He carried with him a portable laboratory with which to make tests for beryllium. His findings were not published, but in several hundred analyses he found a maximum of 1.5 per cent BeO.

Inasmuch as the Franklin material alone showed appreciable amounts of beryllium, it appeared that the analysis might be open to question. Through the kindness of Mr. L. H. Bauer, two specimens of beryllian idocrase from Franklin were loaned for reanalysis. These presumably were of the same material he had analyzed earlier. Analyses of these specimens have been made by Mr. F. A. Gonyer; one in 1941 and the other in 1951. These are given in Table 1 with the earlier analysis by L. H. Bauer.

As a further check on the beryllium content, the idocrase of the specimen of analysis No. 3 was analyzed spectrographically by Dr. Lester Strock. The average of three analyses is 1.1 per cent BeO. The difference between the BeO reported in the chemical and spectrographic analyses may represent an error, or it may correspond to real differences in the material analyzed. Optical examination shows color zones that may be different chemically but which show almost no difference in refractive index.

TABLE 1. ANALYSES OF IDOCRASE FROM FRANKLIN, NEW JERSEY

	1	2	3
SiO_2	34.25	34.83	36.61
Al_2O_3	9.70	12.98	16.67
Fe_2O_3	—	5.69	3.31
FeO	trace	—	—
MnO	4.84	.24	3.28
MgO	3.17	2.91	2.87
CaO	33.15	33.84	33.64
BeO	9.20	3.95	1.56
Na_2O	—	.86	.17
K_2O	—	.08	—
CuO	—	—	.26
ZnO	4.86	—	.14
H_2O	1.31	.86	.68
F	—	3.07	.91
	100.48	99.31	100.10
Less $0=F_2$		1.29	.38
	100.48	98.02	99.72

1. Analyst, L. H. Bauer; 2. Analyst, F. H. Gonyer, 1941; 3. Analyst, F. H. Gonyer, 1951.

The formula given by Warren and Modell (1931) for idocrase is $Ca_{10}Al_4(Mg,Fe)_2Si_9O_{34}(OH)_4$. It is difficult to determine where the beryllium should be placed in the formula. It is possible that it substitutes for the divalent metals or for the aluminum. However, the analyses do not help to identify either of these two mechanisms.

Examination of the three analyses of Table 1 show striking differences not only in BeO but also in Al_2O_3, Fe_2O_3, MnO, ZnO and F. It seems highly unlikely that the analysts working on identical material would

TABLE 2. OPTICAL PROPERTIES OF BERYLLIAN IDOCRASE

Locality	Per Cent BeO	*n*O	*n*E	G	
1. Great Slave Lake	1.07	1.712	1.708		
2. Iron Mtn., New Mexico	1.09	1.718	1.711	3.3+	
3. Franklin, N. J.	9.20	1.712	1.700	3.385	
4. Franklin, N. J.	3.95	1.716	1.710	3.380	±.002
5. Franklin, N. J.	1.56	1.714	1.709	3.375	

Indices determined by: 1. V. B. Meen, 2. J. J. Glass, 3. H. Berman, 4 and 5. C. S. Hurlbut, Jr.

arrive at such dissimilar results for so many elements. It is more probable that the idocrase specimens collected by Mr. Bauer and thought to be the same were actually different and the difference is reflected in the analyses.

From Table 2 it appears that there is no correlation between the percentage of BeO and the refractive indices and that the difference in index is probably due to variation in the other elements.

The dimensions of the unit cell of the Franklin idocrase (crystals of analysis No. 3) determined by Weissenberg photographs are: $a_0 = 15.59$ Å, $c_0 = 11.81$. These dimensions are in fair agreement with $a_0 = 15.63$ kX, $c_0 = 11.83$ given by Warren and Modell (1931) for idocrase from Sanford, Maine; and $a_0 = 15.63$ kX, $c_0 = 11.93$ given by Kakané (1933) for idocrase from Miho, Japan.

Conclusion. From a consideration of the chemical and spectrographic analyses of the Franklin idocrase, one must conclude that either the original analysis was in error in reporting too high a percentage of BeO or that the specimen on which the analysis was made was unique.*

References

1. Glass, J. J., Jahns, R. H., and Stevens, R. E., Helvite and danalite from New Mexico and the helivite group: *Am. Mineral.*, **29**, 163–191 (1944).
2. Meen, V. B., Vesuvianite from Great Slave Lake Region, Canada: *Univ. Toronto Stud., Geol. Series*, **42**, 69–74 (1939).
3. Palache, C., and Bauer, L. H., On the occurrence of beryllium in the zinc deposits at Franklin, N. J.: *Am. Mineral.*, **15**, 30–33 (1930).
4. Silbermintz and Roschkowa, Zur Frage des Vorkommens von Beryllium in Vesuvianen: *Centr. Min., Abt. A*, 249–253 (1933).
5. Takané, Kalsutoski, *X*-ray analysis of vesuvianite from Miho and an ideal formula of the mineral: *Proc. of the Imperial Academy*, **9**, No. 1, 9–12 (1933).

DEMONSTRATION POLARISCOPE

Cornelius S. Hurlbut, Jr., *Harvard University, Cambridge, Massachusetts.*

In teaching optical crystallography, frequently it is necessary to demonstrate and explain certain optical phenomena seen through the polarizing microscope. In a large class this can be very time consuming if the in-

* After the manuscript of this note was sent to the Editor of *The American Mineralogist*, the mineral collection of Mr. Bauer was purchased by the National Museum and Harvard University. There were several specimens labeled "Be-vesuvianite" and a tube of powdered material labeled "Be-vesuvianite—analysed." Some of the powdered mineral was sent to Dr. W. T. Schaller of the U. S. Geological Survey. A spectrographic analysis made at the Geological Survey by Mr. Harry Dies gave 0.17 per cent BeO. From this analysis of the original material, one must conclude that the percentage of BeO reported in Mr. Bauer's analysis is in error.

FIG. 1. Demonstration Polariscope showing interference figure of muscovite.

structor must proceed from one student to the next giving separate explanations to each individual. A further drawback with this method is that the student and instructor are not observing the phenomenon at the same time. The *demonstration polariscope* makes it possible to carry out explanations to a class of 10 to 15 students at one time.

The instrument illustrated in Fig. 1 is 7″ long, $4\frac{1}{4}$″ wide and $7\frac{1}{2}$″ high and is constructed from sheet metal. Two 4-inch-square polarizers in crossed position are used, one at the top of the instrument and the other four inches below. Just above the lower polarizer is a rotating stage with a three-inch opening covered by ground glass. Illumination is provided by a 60-watt lamp at the bottom of the instrument. Crystals placed on the stage can be viewed by looking directly down through the upper polarizer. However, for demonstrating to a group, a mirror can be swung into position at 45° as shown in Fig. 1.

Winchell* has called attention to the use of a similar arrangement of

* Winchell, H., Demonstration of interference figures: *Am. Mineral.*, **32**, 588–589 (1947).

polarizers for the demonstration of interference figures using polished spheres of various crystals. He states that such a sphere held in the hand between the polarizers can be rotated and the student can "observe the position of the uniaxial or biaxial figure, and determine by experiment the effect of crystal orientation on the interference figure." Such experiments can be carried out with the *demonstration polariscope*. In addition thin plates can be placed on the rotating stage, and interference colors, extinction angles, twinning and other phenomena can be observed.

One of the chief virtues of the *demonstration polariscope* is that interference figures can be obtained on cleavage plates or on oriented sections of minerals. Between the stage and upper polarizer is a frame carrying a polished glass sphere 3 inches in diameter (a clear plastic sphere is equally suitable). The frame is mounted on tracks and can be pushed to the back of the instrument when not in use. With a properly oriented mineral slice and the sphere in position, an interference figure can be seen to completely fill the sphere as in Fig. 1.

The interference figures appear much the same as they would using a plate of the mineral of the same thickness with a microscope. For example, by using successively thicker cleavage plates of muscovite, one can see a sharpening of the isogyres and an increase in the number of isochromatic bands. By rotating a biaxial acute bisectrix figure to the 45° position, one can show how the optic sign is obtained with a quarter wave plate or red of the first order by placing these plates over the crystal section. Because the interference figure is seen on the surface of the sphere rather than in a plane, the emergence of both optic axes in a centered acute bisectrix figure can be seen at the same time in a crystal that has a 2V as large as 75°.

UNUSUAL FORMS OF HALLOYSITE*

K. S. Birrell, M. Fieldes, and K. I. Williamson, *Department of Scientific and Industrial Research, Wellington, New Zealand.*

Kaolin type clay mineral is a common constituent of the clay of volcanic ash soils of advanced weathering stage. Electron micrographs of such clays usually show much of the kaolin to have the characteristic cylindrical form of halloysite described by Bates (1). *X*-ray diffraction patterns of the glycerol clay show basal spacings mainly between 7.2 and 7.4 Å, indicating that the form of kaolin is mainly metahalloysite, with only minor amounts of the 11 Å spacing of glycerol halloysite corresponding to hydrated halloysite.

In the course of an investigation of the clay fraction of a subsoil derived from volcanic ash at New Plymouth, it was found that the clay,

* Soil Bureau Publication No. 61.

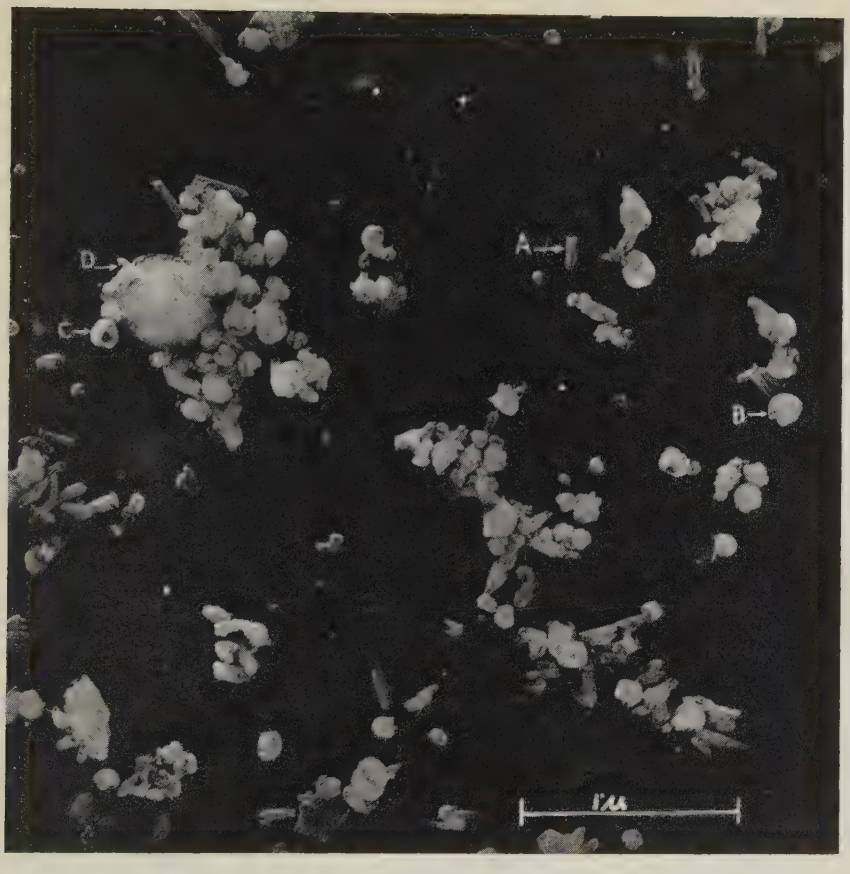

FIG. 1. Electron micrograph of clay from subsoil derived from volcanic ash, New Plymouth, New Zealand: *A*. Normal tubular hydrated-halloysite particle. *B*. Hydrated halloysite particle in form of a distorted spherical shell. *C*. Hydrated halloysite particle in toroidal form. *D*. Amorphous mass of allophane present as a minor constituent of the clay.

which comprised 46 per cent of the subsoil, had the x-ray diffraction pattern of hydrated halloysite with an intense basal reflection of the glycerol clay at approximately 11 Å.

Figure 1 is an electron micrograph of this clay. About half the particles are normal tubular halloysite of average length about 0.2 micron. Most of the remainder are round particles ranging from 0.05 to 0.2 micron in diameter. Of these some appear to be hollow, rather distorted spherical shells, while others are apparently incomplete toroids as though formed from cylindrical halloysite particles rolled up so that their ends almost meet. The details of their structure are better seen in transparencies than in a print but nevertheless, the holes in the centres of some particles can be seen even in the print.

Particles with holes similar to those in the New Plymouth clay are shown in electronmicrographs by Davis *et al.* (3) of a sample stated to be serpentine. Serpentine is the magnesium analogue of kaolin and this particular serpentine contained mainly tubes and rods, but also a few particles having a "life-saver" appearance considered by those authors to be tubular particles seen in cross-section. In the case of the hydrated halloysite sample described here the holes apparent through many of the particles were at first thought to be due to tubes seen end-on but close examination appears to indicate that the holes are either centres of toroidal shaped particles or more transparent zones of incomplete spherical shells.

The clay of less than 2 micron equivalent diameter had a cation exchange capacity of 22 milliequivalents per 100 g., SiO_2:Al_2O_3 molecular ratio of 2.09, Fe_2O_3 content of 5.1 per cent, and surface area by the *B E T* method of 137 sq. metres per gram.

Nomenclature used here for forms of halloysite is that of MacEwan (2).

References

1. Bates, T. F., Hildrbrand, F. A., and Swineford, A. (1950), Morphology and structure of endillite and halloysite: *Am. Mineral.*, **35**, 463–484.
2. MacEwan, D. M. C. (1947), Halloysite nomenclature: *Mineral. Mag.*, **28**, 36–44.
3. Davis, D. W. et al. (1950, Electron micrographs of reference clay minerals: *Preliminary Report No.* 6. *American Petroleum Institute Project* **49**, *Reference Clay Minerals.*

VAPOR PRESSURE GLYCOLATION OF ORIENTED CLAY MINERALS*

George Brunton, *Shell Development Co., Houston, Texas.*

The process of increasing the (00*l*) spacings of expanded clay minerals to facilitate their identification was introduced by Bradley (1945), MacEwan (1946, 1948), and others. They demonstrated that numerous organic substances would enter the expanded clay lattices along the (001) plane between the 2.1 sheets, replacing the water. The organic molecule is generally larger than the water it replaces and the result is that the *d* spacings of the (00*l*) reflection series are increased. The resulting increase in *d* spacings is easily recognized, and the presence of expanded clays can be demonstrated even in complex clay mixtures.

It has been the practice in the past to use ethylene glycol as the organic liquid because it is cheap, easily obtainable, and water-soluble, and because the large molecules expand the (001) spacing to approximately 17 Å for pure montmorillonites with divalent cations. Samples were prepared by mixing the clays with liquid glycol.

* Publication No. 43, Exploration and Production Research Division, Shell Development Co., Houston, Texas.

The use of x-ray geiger counter goniometers has increased in recent years for routine clay mineral identification. When this technique is used it is desirable to sediment a thin layer of minus-two-micron-size clay on a glass slide to obtain a maximum orientation of the individual clay plates. The orientation accentuates the (00l) reflections.

The same oriented slides are glycolated to identify expanded 2.1 clays in mixtures, but direct mechanical wetting of the slide with glycol

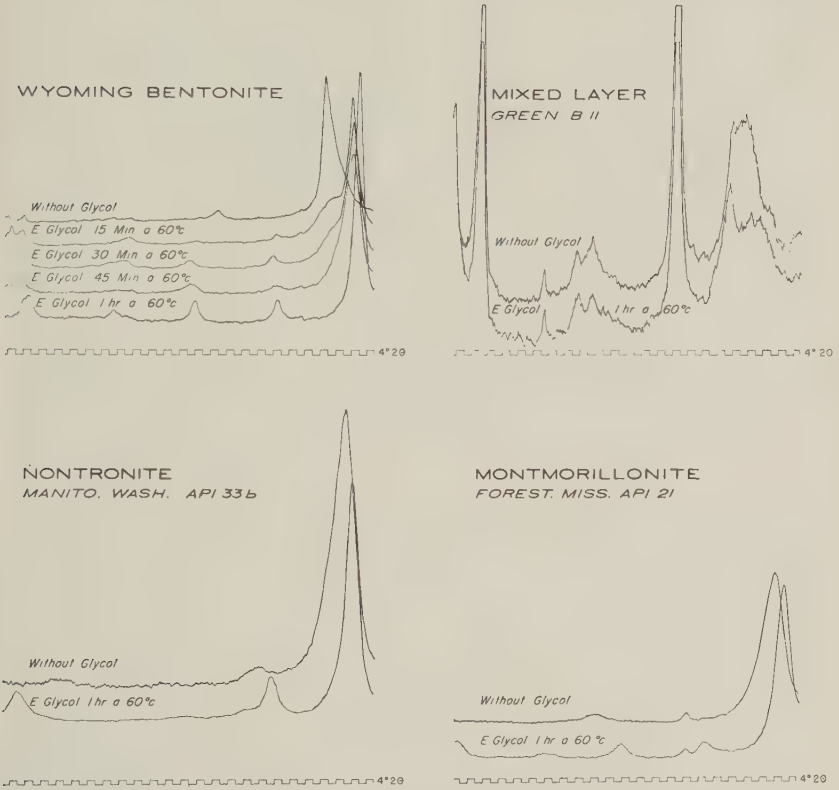

Fig. 1

often destroys the orientation, and the glycolation becomes ineffective. A simple technique for glycolating dry oriented samples has been developed which makes use of the vapor pressure of ethylene glycol at low temperatures. The vapor pressure of ethylene glycol is 39 mm. at 120° C. The glass slide on which an oriented layer of clay has been deposited is suspended in a closed vessel over a heated bath of ethylene glycol for a short time. The montmorillonite in the sample glycolates without a change in orientation and without the sample becoming wet.

It has been found that most samples glycolate satisfactorily within one hour over a bath at 60° C. For routine work an aluminum dessicator partially filled with ethylene glycol, to below the sample holder, has proved satisfactory as a glycolation vessel. A partially filled beaker containing an inverted petri dish, or some other arrangement to hold the sample above the glycol, and covered with an inverted watch glass serves equally as well. Figure one illustrates the effect of glycolation on the x-ray spectrometer traces at 60° C. of four dry oriented montmorillonite samples. The Wyoming bentonite sample was glycolated for $\frac{1}{4}$, $\frac{1}{2}$, $\frac{3}{4}$, and one hour to show the progressive shifts in the ($00l$) reflections. The other three samples were glycolated for one hour.

References

Bradley, W. F. (1945), Diagnostic criteria for clay minerals: *Am. Mineral.*, **30,** 704–713.

MacEwan, D. M. C. (1946), The identification and estimation of the montmorillonite group of minerals, with special reference to soil clays: *J. Soc. Chem. Ind.*, **65,** 298–305.

MacEwan, D. M. C. (1948), Complexes of clays with organic compounds: *J. Trans. Faraday Soc.*, **44,** 349–367.

A POINT COUNTER BASED ON THE LEITZ MECHANICAL STAGE

F. Chayes, *Geophysical Laboratory, Carnegie Institution of Washington, Washington, D. C.*

A point counter based on the stock model of the Leitz mechanical stage, which can be fitted to any Leitz petrographic microscope without retapping the table, may be of interest to many readers of this journal. The instrument was designed and built by the Baltimore Instrument Company[1] at my suggestion.

The rebuilt stage is shown in Fig. 1; numbers in parentheses in the following paragraph refer to the illustration. The stop mechanism consists of a large knob (1) in which 24 holes have been recessed from below. The stop pin (2) which engages these holes is pressed upward by a spring housed in the pin holder (3) which is fastened to the base of the stage. Rotation of the knob (1) brings successive holes into register over the pin. The stop mechanism functions admirably; point locations are firm and sure and, except at the highest magnification, the passage from point to point is accomplished without perceptible loss of focus. When the instrument is in use as a point counter the lock screws (4) are left loose. If it is to be used as a conventional mechanical stage the lock screws are pushed

[1] Interested readers should address inquiries to the Baltimore Instrument Company, 716–718 West Redwood Street, Baltimore 1, Md. The company is prepared to rebuild new stages, which it carries in stock. At the time of this writing it was also willing to adapt used stages, providing they are in good condition.

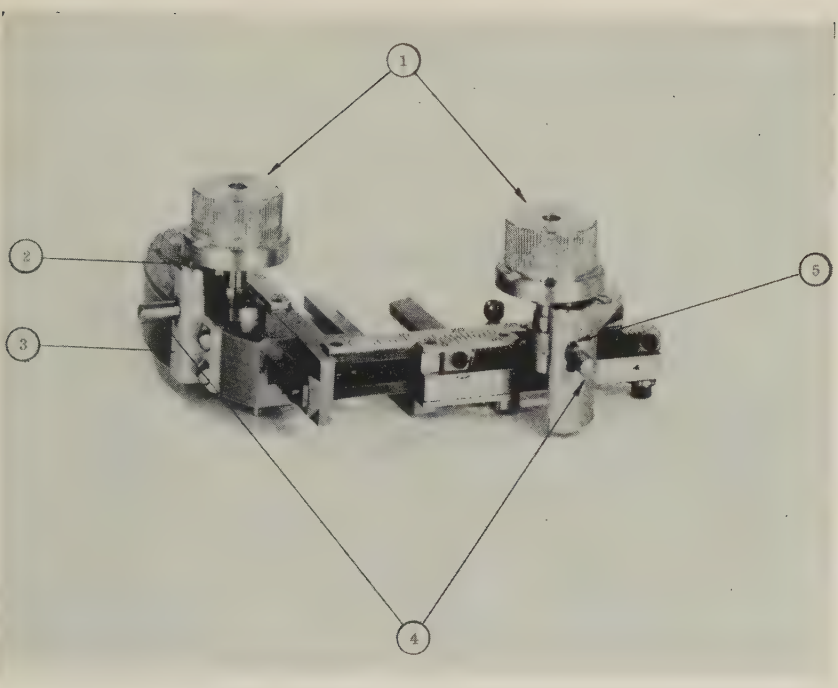

FIG. 1. Leitz mechanical stage adapted for point counter.

to the bottoms of the elongate slots (5) in which they ride and are hand tightened. This disengages the stop pins from the control knobs and restores the normal function of the stage.

The stage shown in Fig. 1 is an old and thoroughly used one. Tension on the slide proved unsatisfactory, the thin section every now and then sitting still while the stage was in motion; the same difficulty has been reported to me by other users of the Leitz stage. It is easily remedied by fastening thin strips of cellophane tape along the faces of the metal runners which hold the slide. The cellophane seems to hold the slide in position much more firmly than the polished metal.

The travel of the Leitz mechanical stage is only 25 mm. along either direction, and for some purposes this is inadequate. With a strip of rack obtained from the company we have been able to extend the travel on our instrument so that full traversing of the area underlying a 24×40 mm. coverslip can be accomplished as a matter of routine.

Manuscript received March 4, 1954

BOOK REVIEWS

A NEW PERIODIC TABLE OF THE ELEMENTS BASED ON THE STRUCTURE OF THE ATOM, by S. I. Tomkeieff. Chapman & Hall, Ltd., London, 1954. 30 pages ($13\frac{1}{4} \times 12\frac{1}{4}$ inches), 2 plates, 7 figures. Price 10 s. net.

So many modifications of the periodic table have appeared in recent years that a worthwhile one is likely to be lost in the maze of those that merit little or no attention. The novel arrangement proposed by Tomkeieff lends itself uncommonly well to the graphic representation of certain properties of the elements and of their simple compounds and to comparison of compositions of naturally occurring substances. It should therefore be of interest to geochemists, mineralogists, and teachers and students of subjects dealing with distribution of the elements and with properties of the elements and simple compounds.

The book begins with a brief history of the periodic system and continues with a more detailed discussion of the relation between atomic structure and the periodic system. A 15-page table of the elements gives atomic numbers and weights, mass numbers and relative abundances of isotopes, number and structure of shells, type of atom, group and period, valency, color, state, date of discovery, and derivation of the name of each element. An additional column giving the atomic and ionic radii, insofar as they are known, would have enhanced the usefulness of the table considerably.

The three principal types of the periodic table—rectilinear, helical, and spiral—are discussed briefly, and the advantages of the one chosen by Tomkeieff (the oval-shaped distorted spiral) are outlined:

(1) It gives a marked separation between the long and short periods.

(2) Spacing is more or less even between the symbols for the elements.

(3) The fourth group of the last short period is well separated from the eighth group of the first long period.

(4) Carbon and silicon, two geochemically important elements, are centrally located.

Tomkeieff's scheme also has to a marked degree the more general advantages of a spiral arrangement:

(1) It can be used to demonstrate the structure of the atom and the building up of the periodic system.

(2) Surfaces representing the distribution of numerical values of the properties of the elements and of their simple compounds can be contoured conveniently and continuously. Figure 5 is such a "map," representing the specific gravity of the elements in their solid states; Fig. 6, the hardness of 20 minerals belonging to the type of simple oxides. These diagrams illustrate the relations very clearly and can serve as an aid to memory and to help predict properties of compounds.

(3) Similar contouring can represent the chemical composition of various natural aggregate bodies. Figure 7 shows the average composition of meteorites in this way.

The two plates in the back of the book are duplicates of the cone-shaped periodic chart. One is bound in, but the other, in color, is purposely separate so that it can be cut out, pasted on thin cardboard, and rolled into a truncated cone, about 12 in. high and $3\frac{3}{4}$ in. across the base, to make a handy 3-dimensional model of the periodic system.

The presentation is concerned principally with the construction and general relationships of the table and barely touches on the representation of properties of elements and compounds. A subsequent volume will elaborate on this use and multiply the examples given.

Earl Ingerson,
U. S. Geological Survey, Washington 25, D. C.

ANLEITUNG ZU OPTISCHEN UNTERSUCHUNGEN MIT DEM POLARISATIONSMIKROSKOP, by MAX BEREK, (1953) Rinne-Berek: herausgegeben von C. H. CLAUSSEN, A. DRIESEN, UND S. RÖSCH. E. Schweizerbart'sche Verlagsbuchhandlung, Stuttgart. xiii+366 pages, 285 figures, 21 tables, and 108 formulae. DM29.—.

Aimed at a wide audience, this text provides probably the most comprehensive introduction to the use of the polarizing microscope yet published. A listing below of the major subject headings serves to give only a slight hint of the amazing wealth of useful information contained in this book.

Part I

A. Introduction to the fundamentals of wave optics (pp. 1–15).
B. Methods of producing plane polarized light (pp. 16–25).
C. Recognition of polarized light (polarizer and analyser) (pp. 26–28).
D. The polarizing microscope (pp. 29–63).
E. Preparation of sections for observation in transmitted light (pp. 63–65).
F. Introduction to the fundamentals of orthoscopic observations in transmitted light (pp. 65–83).
G. Relations of optical phenomena to the structure of materials (pp. 84–145).
H. Simple measurements with the polarizing microscope in orthoscopic view (pp. 146–190).

Part II

A. The stereographic projection (pp. 191–196).
B. The indicatrix and its relation to crystal morphology (pp. 196–213).
C. The conoscopic interference figure (pp. 213–234).
D. The diagnostics of the indicatrix in transmitted light (including a discussion of the universal stage—G.J.N.) (pp. 234–293).
E. Observations and measurements in perpendicular reflected light (pp. 294–331).
F. Observations and measurements in inclined reflected light (pp. 332–346).
G. Exercises for optical investigations (pp. 347–355).

The table of contents and the 10-page index are remarkably complete and useful. Illustrations leave little to be desired; all pictured instruments are those manufactured by Leitz. Not a single reference to the literature is given, although author credit is given on appropriate illustrations. Considering the broad survey of the subject that is offered by this book, the lack of any bibliography must be noted as an extremely serious fault. Errors both of fact and of typography are few, if at all present. Typically, the covers are insecurely attached.

Much of the material covered in this book is either new to texts on the polarizing microscope or poorly if at all covered in other texts. Such include remarks on fine adjustments and tests of the optical system, a section on strain patterns in isotropic media and their study by polarized light, a well-conceived discussion of the actual appearance under the microscope of crystals, crystallites, spherulites, and the like, disturbing optical phenomena such as the pseudo-uniaxial intereference figure obtained from isotropic subjects, and many others. As a whole the discussions, many of which are brief, are remarkably well conceived and highly informative. Relative treatment of the different subjects is quite uneven. Some subjects are given practical treatment, whereas others—e.g., reflected light optics—are treated largely on a theoretical basis. Yet others, like the discussion of stereographic projections in its being devoted almost entirely to the Wulff net, are so one-sided as to be of little help. Despite the wide coverage, a few surprising omissions occur, among which polarization figures from opaque minerals and Chayes' point counter technique for modal analyses seem especially unfortunate.

The book should be unusually valuable to the student for its large collection of special

hints on the use and adjustment of the instrument, for carefully detailed instructions in interpretation of the optical measurements made on crystals in section, and for its explanation of the many bothersome and seemingly inconsequential features seen in the routine study of a thin-section.

Like all texts, this one, as unusually informative as it is, fails to provide all that any one student may desire in his pursuit of the subject. In this light and in view of the large number of textbooks on optical mineralogy now available, it is perhaps not amiss to give one man's opinion of what constitutes the best, namely the following:

(1) The book here under review—for scope of coverage, for detailed and practical instruction in the use of the polarizing microscope, and for a good insight into what a remarkably useful tool the polarizing microscope can be.

(2) Conrad Burri (1950) *Das Polarisationsmikroskop*, Verlag Birkhäuser, Basel—for an exhaustive treatment, slanted practically, of the mathematical-physical bases and techniques of optical mineralogy, for its thorough instruction in the use of accessories most frequently employed by the petrographer, and for an adequate bibliography.

(3) Kurt Michel (1950) *Die Grundlagen der Theorie des Mikroskops*, Wissenschaftliche Verlagsgesellschaft M. B. H., Stuttgart—for an exceptionally authoritative, theoretically modern, and complete treatment and application to optical instruments of optical physics. This book is an invaluable addition to the library of any microscopist.

(4) Hans Schneiderhöhn (1952) *Erzmikroskopisches Praktikum*, E. Schweizerbart'sche Verlagsbuchhandlung, Stuttgart—for a full treatment of perpendicular reflected light optics and a useful bibliography.

Yet to be added to this list is a non-existent annotated bibliography of optical mineralogy, an addition which would be most valuable for its use in pointing to the existence of an amazing variety of applications to which the polarizing microscope can be fruitfully employed in geologic investigations. It might not be amiss also at this time to suggest that more effort be given to translation of existing texts, as may be necessary and desirable.

GEORGE J. NEUERBURG,
U. S. Geological Survey, North Hollywood, California

A GLOSSARY OF CLAY TRADE NAMES, compiled by ROBERT H. S. ROBERTSON and issued by the *Clay Minerals Group of the Mineralogical Society of Great Britain and Ireland*, 36 pages, price 4S, 1954.

The Committee of the Clay Minerals Group of the Mineralogical Society of Great Britain and Ireland has published this glossary of trade names of commercial clays with an appeal to all who read it, or who have information on clay trade names, to send their additions and corrections to the compiler. This first edition is an excellent beginning, which can be improved if all who have information will cooperate to make the revision more complete and serviceable. It is the aim of the next edition to include the trade name or number, the synonyms, chemical analysis, mineralogical composition, uses of the clay, the locality of its occurrence, the supplier, and references to the literature. Special forms have been devised and will be sent to those willing to fill them in and may be secured from the Hon. Secretary Dr. R. C. Mackenzie, Macaulay Institute of Soil Research, Craigiebuckler, Aberdeen, Scotland.

In addition to the Clay Trade Names given in this glossary Appendix I gives a short list of trade names that might be mistaken as referring to clays and Appendix II gives a list of Trade Names used for vermiculite.

VICTOR T. ALLEN,
Institute of Technology, Saint Louis University, Saint Louis, Missouri

X-RAY DIFFRACTION PROCEDURES FOR POLYCRYSTALLINE AND AMORPHOUS MATERIALS, by HAROLD KLUG AND LEROY E. ALEXANDER. John Wiley and Sons, New York, 1954. vii+716 pages, 324 figs. Price $15.00.

This book is a very welcome addition to the literature on x-ray methods. Its scope is indicated by the chapter headings and lengths: Elementary crystallography—(55 pages); Production and properties of x-rays—(55); Fundamental principles of x-ray diffraction—(51); Powder photograph techniques—(23); Spectrometric powder techniques—(83); Interpretation of powder diffraction data—(71); Qualitative and quantitative analysis of crystalline powders—(50); Precision determination of lattice constants from powder photographs—(52); Crystallite size determination from line broadening—(48); Further applications of poly-crystalline diffraction—(47); Diffraction studies on non-crystalline materials—(48); Small angle scattering—(31). An appendix includes a suggested layout for a diffraction laboratory and a discussion of the handling and processing of x-ray film. together with several pages of useful tables. Both an author and a subject index are included, and at the end of each chapter is a list of pertinent books. Over 550 references are given as footnotes throughout the book.

The material is clearly presented, with many examples, and is adequately illustrated with numerous figures and photographs. The reviewer has found very little to criticize.

In the introductory chapter on crystallography, a few of the figures are poorly drawn or oriented, such as Fig. 1–27(8), and especially Fig. 1–6*A*, which gives the very opposite concept to that which the authors are trying to present, namely, that in a distorted crystal the angles are unchanged. It is unfortunate that the authors have helped propagate an all too common error when discussing the relationship of Miller indices to zone symbols. They incorrectly state "Actually, zone symbols *uvw* are simply Miller Indices of the plane normal to the zone axis." This statement applies only to the cubic system, and to certain special zones of the hexagonal, tetragonal and orthorhombic systems. In all other cases the relationship is not a simple one. It can be very concisely stated as "Miller Indices are coordinates in the reciprocal lattice, while zone symbols are coordinates in the direct lattice."

For indexing cubic powder photographs, the rather cumbersome reciprocal lattice and the $\sin^2\theta$ methods are described, while the very simple and convenient slide rule and logarithmic scale methods of Davey are not mentioned.

In discussing the equation of a plane *hkl*, there is developed (1–12) the standard formula for a plane through the origin, $hx+ky+lz=0$. It would seem to be pedagogically sound to have introduced at this point the explanation of the all important use of this formula, not as that of a plane through the origin, but in the form $hx+ky+lz=?$ This occurs in the geometrical structure factor, and gives the position of any atom in the unit cell with respect to any plane *hkl*.

However, these are very minor defects. Either for self study, as a text or as a reference, this book will prove to be of great value. It is written by men who not only know the theory of x-ray diffraction, but who have had plenty of practice.

LEWIS S. RAMSDELL,
University of Michigan, Ann Arbor, Michigan

ROCKS AND MINERAL DEPOSITS, by PAUL NIGGLI, English translation by Robert L. Parker. 559 pages, 331 figures, 73 tables. W. H. Freeman and Co., San Francisco, 1954. $12.00.

The original version, in German, of this book was reviewed in *The American Mineralogist*, **34,** 128–129 (1949). The translation, in general, faithfully follows the European edition, and thus the book remains a work on the principles of geochemistry, crystal chemistry, physical chemistry and classification that are pertinent to the formation of rocks and

mineral deposits. Some new material, particularly in the sections dealing with crystal chemistry and classification, has been added. Some parts have been omitted or shortened; the most conspicuous being the section on geophysics that appeared in the original version. In scope and content the book remains, however, as broad as before. The translation is uniformly good throughout; some usages not generally acceptable to American geologists and mineralogists (wolframates, zincblende) appear here and there. There are still retained, however, most of the difficulties of the European edition, for example the complex notations for the formulae of minerals; the emphasis on the personally developed Niggli systems of graphic representation and calculation; the extraordinary preoccupation with detailed classification and standardization of materials, properties and processes; and the inordinate use of new, obscure and confusing terms, such as lepidide, chymogenic, pseudomorphoid, crystalloplast, magnophyric, merismite, mediiphyric and phlebite.

Most of the illustrations have been transferred without change with retention of their German words. For these, translations appear beneath the figures. In most cases this is satisfactory, but for those that contain much terminology, it is an awkward arrangement. A few figures are set entirely with English words. Most of the examples cited in text, tables and figures are from localities outside of North America, although some American examples are presented. The degree of geographic identification of the localities is irregular; many are carefully located as to countries; for others the placement is incomplete; and some examples are not located at all—an irritating detail.

The book will serve well to introduce the ideas of the late Professor Niggli to those American mineralogists and geologists who lacked the patience (or courage) to struggle with the German version. Despite the extraordinary amount of included material, the wide scope and the carefully outlined presentation, the book cannot be considered monographic because of its personalized viewpoint. Nevertheless, it is the only successful modern integration of the basic principles and laws of mineral and rock genesis.

E. Wm. Heinrich,
University of Michigan, Ann Arbor, Michigan

PETROGRAPHY, AN INTRODUCTION TO THE STUDY OF ROCKS IN THIN SECTIONS, by Howell Williams, Francis J. Turner, and Charles M. Gilbert. 416 pages, 133 figures. W. H. Freeman and Co., San Francisco, Calif. 1954. $6.50.

There has long been a pressing need for a modern English textbook in elementary petrography. Petrography, by Williams, Turner and Gilbert, in the main fills this gap in the list of earth science textbooks. The book is divided into three parts with separate author responsibility: Part One, Igneous Rocks (Williams); Part Two, Metamorphic Rocks (Turner); and Part Three, Sedimentary Rocks (Gilbert).

Part I begins with a discussion of the origin of igneous rocks, magmatic evolution (crystal differentiation, assimilation and mingling of magmas) and associations. This summary is concise and excellent; the approach to the question of granitization is judicial and the viewpoint is temperate throughout. Next follow descriptions of igneous textures, a section which is logically organized and complete, yet introduces to the student relatively few unnecessary or awkward terms. Some of doubtful significance for the beginning student might be hydatogenic, merocrystalline and diktylaxitic. Problems of igneous rock nomenclature and classification—ever controversial subjects—are next considered. In their preface (page vi) the authors state " . . . we have striven . . . to reduce the list (of rock names) as much as possible." However, for the igneous group this striving seems to have been somewhat faint hearted. Admittedly the decapitation point on varietal names is difficult to establish practically, but should a newcomer to petrography be confronted with such local and special names as georudite, ciminite, kulaite, orvietite, sommaite, ankara-

mite, kaiwekite, madupite, cedricite and others similar? This seems hardly calculated to increase his interest in systematic igneous petrography. Some illustrations also are captioned with varietal names, without their more general petrographic equivalent being stated.

Under classification a brief summary is presented of the various bases that have been and are being used—SiO_2 content, Si saturation, Al saturation, normative minerals, mode of occurrence, textures and mineralogy (color index, quartz, feldspars). The usage adopted includes the separation into igneous clans, a first subdivision on texture and further subdivision chiefly on mineralogy, i.e. mainly on the presence of quartz as an essential mineral and the nature of the feldspars. In some cases, however, color index is employed in addition, which may lead to some confusion on the part of the student. Gabbros and diorites are separated on the basis of plagioclase composition, in general, but in some cases the authors override this criterion and employ color index instead. This is unfortunate, for although color index is described on page 50, the authors do not detail how color indices are determined, nor do they indicate which of several outlined color index classifications they are using.

The descriptions of the various igneous rock types follow. Both general descriptions and many fine detailed examples are given, with commendable emphasis on those from North American localities. Systematic petrographic descriptions have too long been accustomed to habitual reference to the "classic" European localities and have shamefully neglected many more recently better studied localities in this country and elsewhere abroad. The systematic descriptions begin with the gabbro clan, jump back to the ultramafic clan and then proceed to increasingly siliceous rocks. Fine-grained types precede coarse-grained types. From the genetic viewpoint this may be of interest, but is it as practical for teaching petrography to the beginning student? Certainly coarse-grained rocks are easier to identify than their fine-grained or glassy equivalents. Some petrographers might also feel that because of their relative mineralogical simplicity granites represent an easier initial group than do the mafic and ultramafic rocks. If the arrangement is to be genetically significant why group lamprophyres in the same chapter with peridotites? In fact the genetic basis for a wholesale grouping of lamprophyres may be questioned. Other petrographers will doubtless wish to disagree on the value of the use of adamellite for quartz monzonite, of the neglect of tonalite and of the use of rhyodacite for quartz latite and of trachyandesite for latite. A number of statements in the descriptive sections also invite questions: (p. 123) "Phenocrysts of quartz, of the α or β variety, may be present . . . "; (p. 132, with regard to graphic granites) " . . . their composition approximates closely to that of a eutectic mixture of quartz and feldspar"; and (pp. 135 and 136) the implication that secondary muscovite and lithium muscovites in granites are necessarily pneumatolytic and that some andalusite and sillimanite in granites are pneumatolytic because of their association with topaz and tourmaline. The discussion of pegmatites is wisely restricted to granitic types, but on p. 148 eudialite, which is characteristic of feldspathoidal types, is listed as an accessory. Also new evidence as to the nature of the feldspar in rhomb porphyries requires their reclassification.

In Part II, on metamorphic rocks, a much larger discussion is devoted to origin than in the first part. Indeed some sections are heavily weighted with petrogeny rather than petrography, despite the authors' intentions, as stated in the preface, that the book is to deal more with the rocks than with the processes of their formation. Part of this emphasis is due, doubtless, to the preoccupation with the facies classification of metamorphic rocks, which may be a difficult subject for the beginning student in petrology to assimilate and the categories of which do not lend themselves at all readily to grouping by *mineralogical* assemblages, with which, after all, the student must first deal, either in hand specimen or

in thin section. Certainly it is not always possible to assign a rock to a specific facies prior to studying its petrography in detail. For example, marbles and calcareous schists of various grades are more conveniently studied as a unit, rather than under a separation that places some marble descriptions in a chapter with high-grade schists, amphibolites, granulites and eclogites and others with hornfelses. Many significant metamorphic rocks or rock groups are not described or merely mentioned—hematite and magnetite schists, optalites, epidosites, pyrophyllite schists, and even quartzites. Yet the doubtful metamorphic rock, olivinite, rates half a page.

The subdivisions in Part II are: Metamorphism, its petrographic criteria and its products—conditions, types, textures, facies and classification; hornfelses and spotted slates; cataclasites, mylonites and phyllonites; slates, phyllites and schists of low metamorphic grade; and high-grade schists, amphibolites, granulites and eclogites.

Sedimentary rocks, Part III, is subdivided into origin; composition and texture; sandstones; argillaceous rocks; calcareous rocks; and miscellaneous sedimentary rocks. The section on metamorphic rocks was placed before that on sedimentary rocks, apparently in order to emphasize similarities between some igneous and metamorphic environments. It seems doubtful that such placing is of more value to the student than the arrangement which permits him a general understanding of sedimentary petrography *prior* to his beginning metamorphic petrography.

Sandstones are subdivided into two classes on the degree of sorting: a well sorted type, or arenite, and a poorly sorted type, or wacke, a term proposed by Fischer in 1933. It seems unlikely that many American petrographers will adopt this latter term and some students, in not giving it the German pronunciation, may be more inclined to use it as an adjective rather than as a noun.

The descriptions of the various sandstone types are excellent and extraordinarily complete, much more so than in any modern textbook available to the reviewer. In contrast the section on clays and shales is conspicuously but perhaps rightly abbreviated, for microscopic methods form a subordinate technique for the study of these materials. No descriptions are given of bauxite or diaspore clays. Again, the section on the carbonate rocks is well organized and is given with fine detail, although chalk, travertine and some other types are not presented. The last chapter, miscellaneous sedimentary rocks, discusses siliceous sediments, iron-rich sediments, phosphatic sediments, and anhydrite and gypsum, all briefly.

From the viewpoint of the quality and completeness of the petrographic descriptions, the section on igneous rocks probably ranks first, followed by that on sedimentary rocks, in which much new descriptive material appears, and last by that on metamorphic rocks, in which the emphasis is more genetic. No photomicrographs appear, the illustrations consisting chiefly of excellent drawings of rocks in thin section. Nearly all of these illustrations, which constitute one of the most conspicuously successful features of the book, are by Williams. There is no doubt that the book is well conceived, well organized and well executed, particularly for a first edition, and that it will have a widespread success commensurate with its high quality.

E. Wm. Heinrich,
University of Michigan, Ann Arbor, Michigan

KLOCKMANN'S LEHRBUCH DER MINERALOGIE, by Paul Ramdohr. 14th edition, revised, 1954. 669 pages, 687 figures, one plate, numerous tables. Ferdinand Enke Verlag, 3 Hasenbergsteige, (14a) Stuttgart—W., Germany. Price, paper cover DM 65.00; bound in linen DM 69.00.

This German textbook, now revised for the fourth time by Paul Ramdohr, Professor of

Mineralogy at Heidelberg University, has become, through its 14 editions and 60 years of existence, one of the best known and most widely distributed of all fundamental works in mineralogy and crystallography at the elementary and intermediate level. The new edition continues in the patterns of the early ones, following a conservative, traditional approach in exposition, yet copious in information and modern in fact. Part I, General Mineralogie, deals with systematic crystallography, crystal structure including an introduction to the use of x-rays, physical properties of minerals, mineral and crystal chemistry and mineral formation, occurrence and paragenesis. It concludes with a list of 93 famous mineral localities, briefly described, and a short section on economic mineralogy. Part II, of 360 pages, is the systematic description of mineral species, grouped according to nine classes: elements; sulfides; haloid salts; oxides and hydroxides; nitrates, carbonates, borates (oxygen salts with O in 3-fold coordination); sulfates, chromates, molybdates and tungstates (oxygen salts with O in 4-fold coordination); phosphates, arsenates, vanadates; silicates; and organic compounds. Not only are principal species described, but many rare minerals are treated briefly.

The new edition not merely maintains the high standards of its predecessors but represents a further increase in quality. To those who seek an excellent text or general reference book in fundamental mineralogy, in German, this book is highly recommended.

E. Wm. Heinrich,
University of Michigan, Ann Arbor, Michigan

THE ORIGIN OF METAMORPHIC AND METASOMATIC ROCKS, by Hans Ramberg. xvii+317 pages, 130 figures, 20 tables. The University of Chicago Press, 5750 Ellis Ave., Chicago 37, Ill. 1952. $10.

The Origin of Metamorphic and Metasomatic Rocks is in the author's words, "A treatise on recrystallization and replacement in the earth's crust." It is an attempt to apply the principles of thermodynamics and crystal chemistry to an explanation of metamorphism and metasomatism. It takes as its basic assumption that ion migration directly through crystal structures or within intergranular films is the dominant process in the reconstitution of metamorphic rocks and formation of some igneous rocks. With this premise constantly in mind Ramberg has skillfully woven a background of physicochemical theory for silicate reactions in the solid state.

About 30 pages are devoted to the thermodynamics of metamorphic processes, followed by another 30-page chapter detailing the equilibrium diagrams of metamorphic minerals, some of which are deduced from observations based on their paragenetic relations in metamorphic rocks. A discussion of crystal kinetics follows, in which are described the mechanisms whereby new equilibria can be achieved by recrystallization in rocks as the result of their reactions to a changed environment. In this section the principles of solid state diffusion are enunciated and the available quantitative data on diffusion rates are listed.

Next follow presentations of the facies principle and of the mechanism of metasomatic transfer of matter through rocks. Various causes of metamorphic differentiation are suggested and described. The last part of the book considers metasomatism in nearly unmetamorphosed and low-grade sediments and in regionally metamorphosed complexes. Granites à la Ramberg result from the gravity controlled upward migration of light ions and the downward streaming of heavy ions. Furthermore, "The growth of pegmatites in regionally metamorphosed areas is just a phase of 'granitization' . . . " (p. 248).

The book is somewhat irregular in its organization, but Ramberg presents his ideas energetically and with distinction. Doubtless the controversial theses presented will please

a few, irritate many and infuriate still others. It should be required reading for all geologists interested in problems of metamorphism.

E. Wm. Heinrich,
University of Michigan, Ann Arbor, Michigan

THE THIN-SECTION MINERALOGY OF CERAMIC MATERIALS (2nd Edition). by G. R. Rigby. 231 pp., 10 Plates, 14 Figures, 27 Tables, 2 Appendices, 3 Indexes. The British Ceramic Research Association, Queens Road, Penkhull, Stoke-On-Trent. Staffordshire, England. 1953. £ 1. 12. 6d.

The first edition of this book was reviewed in *The American Mineralogist*, **38**, 146–147 (1953). The major changes in the second edition are the inclusion of descriptions of 50 new "minerals," extension of the section, "Raw materials used in ceramics," description of the preparation of polished sections and the inclusion of 40 photomicrographs of commonly occurring ceramic "minerals."

The book is divided into six parts: I—The preparation of sections; II—The identification of mineral phases; III—Optical properties of minerals found in ceramic materials, slags, glasses, and sinters; IV—Determinative tables; V—Photographs of minerals under the microscope; and VI—Appendices. Part II is an abbreviated version of the principles and practices of optical crystallography; part III continues to be the most valuable contribution that the book provides. However some of the usages employed and data cited for the "true" minerals are incorrect or inadequate; for example, the use of octagons for octahedra (p. 93); the non-identification of fluorite cleavage; the inference that cronstedite, amesite and chamosite are clay minerals; the confused intermingling of petrographic and mineralogical names; the lack of mention of the existence of high-temperature plagioclase; the use of obscure and rejected mineral varietal names (turgite, kyanophilite); and the inclusion of rhodonite and wollastonite as pyroxenes. Despite the improvements of this second edition, further refinements are possible. Doubtless the book would be benefited by careful checking of the mineralogical information by a non-ceramic mineralogist. However, the book remains the foremost collection of the properties of the minerals of ceramic raw materials and the "minerals" of ceramic products.

E. Wm. Heinrich,
University of Michigan, Ann Arbor, Michigan

NEW MINERAL NAMES

Ghassoulite

GEORGES MILLOT, La Ghassoulite, pole magnesien de la serie des Montmorillonites. *Compt. rendu*, **238**, 257–259 (1954).

Material from Ksabi province, eastern Morocco, was analyzed in 1843 by Damour who found SiO_2 55, Al_2O_3 1.2, Fe_2O_3 1.4, MgO 2.8 (evidently a misprint for 28 M.F.), CaO 1.01, K_2O 0.52, H_2O 10.35, sand 1.5; sum 98.98%. (Damour and later workers referred the material to sepiolite). *X*-ray study shows this to be a member of the montmorillonite group with a basal spacing of 15 Å. After treatment with glycerol, the spacings were (in Å) 17.5 very strong, 8.8 medium, 5.85 weak, 4.48 weak, and 3.55 weak. The analysis gives the formula $(Ca_{0.07}K_{0.05})(Mg_{2.86}Fe_{0.07})(Si_{3.76}Al_{0.09})O_{10}(OH)_2$ or $Mg_3Si_4O_{10}(OH)_2$, an end member of the montmorillonite group, saponite having part of the Mg replaced by Al. The name is from the Moroccan term "ghassoul" meaning a clay used in laundering.

DISCUSSION: The material is obviously identical with stevensite, see Faust and Murata, *Am. Mineral.*, **38**, 973–987 (1953), and the name ghassoulite is therefore unnecessary.

MICHAEL FLEISCHER

Cardenite

D. M. C. MACEWAN, "Cardenite," a trioctahedral montmorillonoid derived from biotite. *Clay Minerals Bull.*, Vol. **2**, No. 11, pp. 120–126 (1954).

Mitchell and Muir in 1937 observed that certain Scottish soils had a very high cation exchange capacity relative to the amount of clay minerals present. Further work by Mitchell, Muir, and Hart showed that the high cation exchange capacity, 91 milliequivalents/100 g. was due to "weathered biotite." This material was dark brown, biaxial negative with γ 1.598. Analysis (by Muir) of NH_4-saturated material gave SiO_2 39.00, Al_2O_3 15.54, Fe_2O_3 11.46, FeO 2.33, MgO 12.76, CaO 1.36, K_2O 0.29, Na_2O 0.68, MnO 0.21, TiO_2 0.03, loss on ignition 17.33; sum 100.99%, cation exchange capacity 84 m.eq./100 g.

X-ray study by MacEwan showed the presence of a little fresh biotite and some material of vermiculitic or hydrobiotitic nature; the bulk of the material was definitely a member of the montmorillonite group. *X*-ray powder data are given; the strongest line is at 10.7 Å; glycerol treatment gives a strong reflection at 17.8 Å. The NH_4-saturated material gave a spacing of 12 Å in contact with excess H_2O; the Ca-saturated material gave 15 Å under similar conditions.

Recalculation of the analysis above gives $(Al_{0.89}Fe_{1.37}'''Fe_{0.30}''Mg_{3.00}Ca_{0.24})(Si_{6.17}Al_{1.83})O_{20}(OH)_4+M_{0.401}$ where $M=NH_4$. The mineral is decomposed easily by even mild acid treatment, as, for example, by normal oxalic acid in the cold. It is believed that biotite altered first to hydrobiotite or vermiculite and then further to cardenite.

The name is for the locality, Carden Wood, Aberdeenshire, Scotland.

M. F.

Corrensite

FRIEDRICH LIPPMANN, Über einen Keuperton von Zaisersweiher bei Maulbronn Heidelberg. *Beitr. Mineral. Petrog.*, **4**, 130–134 (1954).

The name corrensite is given to a clay mineral that is especially abundant in the finest fraction ($<0.6\mu$) of a red Keuper clay. *X*-ray and *D.T.A.* data are given. The material is characterized by giving *x*-ray spacings at 28 Å and 14 Å that remain when the sample is heated to 500° (chlorite group) and by giving spacings of 16 Å and 32–33 Å after treatment with glycerol. Similar material had previously been described by Honeyborne, *Clay Min-*

erals Bull., **1**, No. 5, 150–157 (1951), and by Stephen and MacEwan, *Ibid.*, 157–162, and *Geotechnique*, **2**, 82 (1950).

The name is for Prof. Carl W. Correns, 1893–, Director of the Sedimentary Petrography Institute, Göttingen University.

M. F.

Ulvöspinel

Fredrik Mogensen, A ferro-ortho-titanate ore from Södra Ulvön. *Geol. Fören. Förk.*, **68**, 578–588 (1946).

Paul Ramdohr, Ulvöspinel and its significance in titaniferous iron ores. *Econ. Geol.*, **48**, 677–688 (1953).

The name ulvöspinel (for the locality, Ulvö Islands, Ångermanland archipelago, northern Sweden) is given to the spinel $TiFe_2O_4$(a_0=8.74 Å). Ramdohr shows it to be a common constituent of tinaniferous magnetites, generally as very fine exsolution lamellae, parallel to (100) of magnetite.

M. F.

It is with deep regret that we record the death of Dr. Charles Palache, professor emeritus of mineralogy and crystallography of Harvard University and Honorary President of The Mineralogical Society of America. Dr. Palache suffered a stroke and died at his home in Charlottesville, Virginia, on Dec. 5, 1954. He was 84 years old. He was a member of the National Academy of Sciences, recipient of the first Roebling Medal in 1937 and served as President of the Mineralogical Society in 1921 and as President of the Geological Society of America in 1937.

Frank H. Riddle, vice-president of the Champion Spark Plug Company of Detroit, Michigan, has been named the 1955 recipient of the Albert Victor Bleininger Award. The award is the highest honor conferred in this country for distinguished achievement in the field of ceramics and is given annually by the Pittsburgh Section.